Department of Forest Products Technology

Cellulose based bio-interfaces for immunodiagnostic applications

Hannes Orelma

Aalto University

DOCTORAL DISSERTATIONS

Aalto University publication series
DOCTORAL DISSERTATIONS 138/2012

Cellulose based bio-interfaces for immunodiagnostic applications

Hannes Orelma

Doctoral dissertation for the degree of Doctor of Science in Technology to be presented with due permission of the School of Chemical Technology for public examination and debate in Auditorium Puu2 at the Aalto University School of Chemical Technology (Espoo, Finland) on the 9th of November 2012 at 12 noon.

Aalto University
School of Chemical Technology
Department of Forest Products Technology
Forest Products Surface Chemistry

Supervising professor
Professor Janne Laine

Thesis advisor
Dr. Ilari Filpponen

Preliminary examiners
Professor Kevin Edgar, Virginia Polytechnic Institute and State University, USA
Professor Gil Garnier, Monash University, Australia

Opponent
Professor Robert Pelton, McMaster University, Canada

Aalto University publication series
DOCTORAL DISSERTATIONS 138/2012

ISBN 978-952-60-4835-2 (printed)
ISBN 978-952-60-4836-9 (pdf)
ISSN-L 1799-4934
ISSN 1799-4934 (printed)
ISSN 1799-4942 (pdf)
http://urn.fi/URN:ISBN:978-952-60-4836-9

Unigrafia Oy
Helsinki 2012

Finland

441 697
Printed matter

Aalto University

Abstract

Aalto University, P.O. Box 11000, FI-00076 Aalto www.aalto.fi

Author
Hannes Orelma

Name of the doctoral dissertation
Cellulose based bio-interfaces for immunodiagnostic applications

Publisher School of Chemical Technology

Unit Department of Forest Products Technology

Series Aalto University publication series DOCTORAL DISSERTATIONS 138/2012

Field of research Forest Products Chemistry

Manuscript submitted 5 June 2012 **Date of the defence** 9 November 2012

Permission to publish granted (date) 25 September 2012 **Language** English

☐ **Monograph** ☒ **Article dissertation (summary + original articles)**

Abstract

In this work, the interactions between various proteins and modified cellulose surfaces were investigated. The work focused on the development of immobilization methods for the covalent attachment of specific immunological antibodies (proteins) onto cellulose substrate. The immobilization methods were explored using cellulose model surfaces and surface sensitive techniques, such as quartz crystal microbalance with dissipation monitoring (QCM-D) and surface plasmon resonance (SPR).

The highest adsorption of globular proteins on unmodified cellulose surfaces occurred at their respective isoelectric points, suggesting a non-electrostatic adsorption mechanism. An increased surface charge at the cellulose substrate was found to enhance the adsorption of all the proteins investigated. This indicated the presence of attractive electrostatic interactions and the adsorption was found to be mainly irreversible. In addition, the effect of oligosaccharide regions of proteins on their adsorption on cellulose was examined with one glycoprotein, avidin. The adsorption of avidin on cellulose was driven by a combination of electrostatic and non-electrostatic forces, and the adsorption was mainly irreversible. Moreover, the oligosaccharide regions of avidin decreased its adsorption strength to cellulose.

In this work, several strategies for covalent immobilization of antibodies onto functionalized cellulose matrices were developed. The novel biointerfaces were capable of sensing antigens both selectively and quantitatively. The use of traditional conjugation chemistries typically leads to a random conformation of immobilized antibodies on the surfaces which in turn may decrease the ability of immobilized antibodies to bind antigens due to the sterical hindrances. Therefore, in this work, the antibodies were immobilized onto cellulose in more oriented manner using avidin-biotin linkage. This approach resulted in over two-fold higher antigen response when compared to those of the traditional conjugation chemistry. In the last part of this work, a biointerface was prepared on a water-resistant nanofibrillar cellulose (NFC) film. The NFC film was made amine reactive by using sequential TEMPO-mediated oxidation and EDC/NHS activation. Activated NFC-films were observed to bind antibodies covalently, and the antibodies could be deposited using standard inkjet printing techniques. The developed NFC-based biointerfaces are expected to open new venues for using cellulose in immunodiagnostic applications.

Keywords Cellulose, antibodies, immobilization, immunodiagnostic

ISBN (printed) 978-952-60-4835-2 **ISBN (pdf)** 978-952-60-4836-9

ISSN-L 1799-4934 **ISSN (printed)** 1799-4934 **ISSN (pdf)** 1799-4942

Location of publisher Espoo **Location of printing** Helsinki **Year** 2012

Pages 150 **urn** http://urn.fi/URN:ISBN:978-952-60-4836-9

Aalto-yliopisto

Tiivistelmä

Aalto-yliopisto, PL 11000, 00076 Aalto www.aalto.fi

Tekijä
Hannes Orelma

Väitöskirjan nimi
Selluloosapohjaiset biointerfaasit immunodiagnostisiin aplikaatioihin

Julkaisija Kemian tekniikan korkeakoulu

Yksikkö Puunjalostustekniikan laitos

Sarja Aalto University publication series DOCTORAL DISSERTATIONS 138/2012

Tutkimusala Puunjalostuksen kemia

Käsikirjoituksen pvm 05.06.2012 **Väitöspäivä** 09.11.2012

Julkaisuluvan myöntämispäivä 25.09.2012 **Kieli** Englanti

☐ **Monografia** ☒ **Yhdistelmäväitöskirja (yhteenveto-osa + erillisartikkelit)**

Tiivistelmä

Työssä tutkittiin proteiinien vuorovaikutusta pintamuokattujen selluloosamateriaalien kanssa hyödynnettäväksi immunodiagnostisissa sovelluksissa. Erityisesti työssä tutkittiin immunologisten vasta-aineiden kiinnittämistä pysyvästi selluloosapintoihin, ja kiinnitettyjen vasta-aineiden aktiivisuutta tunnistaa antigeenejä, vasta-aineille spesifisiä proteiineja. Edellä mainittujen proteiinien adsorptiota selluloosamateriaaleihin tutkittiin käyttäen pintaherkkiä menetelmiä, kuten kvartsikidevaakaa (QCM-D) ja pintaplasmoniresonanssi-instrumenttia (SPR) selluloosamallipintojen kanssa.

Tutkitut proteiinit sitoutuivat modifioimattomiin selluloosapintoihin parhaiten niiden isoelektrisissä pisteissä, mikä osoittaa adsorption tapahtuvan pääasiassa muiden kuin sähköisten vuorovaikutusvoimien välityksellä. Selluloosapinnan kasvanut varaus kasvatti kaikkien tutkittujen proteiinien adsorptiota modifioiduille selluloosapinnoille. Tutkimuksessa selvitettiin myös yhden glykoproteiinin, avidiinin, adsorptiota muokatuille selluloosapinnoille, sekä avidiinin proteiinikuoren oligosakkaridiketjujen vaikutusta adsorptiomekanismeihin. Avidinin adsorptio selluloosapinnalla tapahtui sekä sähköisten ja ei-sähköisten vuorovaikutusten välityksellä ja sitoutuminen oli pysyvää. Tutkimuksessa havaittiin myös oligosakkaridiketjujen vähentävän avidinin adsorptiota selluloosapinnalle.

Työssä kehitettiin menetelmiä sitoa vasta-aineita selluloosapintoihin vesifaasissa hyödyntäen ionisia polysakkarideja (karboksymetyyliselluloosa ja kitosaani), jotka adsorboituvat irreversiibelisti selluloosapintoihin. Tutkimuksissa havaittiin, että adsorboimalla tutkittuja ionisia polysakkarideja selluloosapintoihin, voidaan vasta-aineita sitoa selluloosapintaan kovalenttisten sidosten välityksellä. Kehitetyillä biointerfaasilla pystyttiin detektoimaan antigeenejä spesifisesti. Vasta-aineen konformaatio kiinteällä pinnalla vaikuttaa sen kykyyn sitoa tunnistettavaa antigeeniä. Perinteisessä kovalenttisessa immobilisaatiossa vasta-aineen konformaatiota ei pystytä hallitsemaan. Työssä tutkittiin menetelmää kiinnittää vasta-aineita selluloosapintoihin avidini-biotiinisidoksen avulla. Avidini-biotiinisidoksen avulla biointerfaasin kyky tunnistaa antigeenejä saatiin kaksinkertaistettua. Tutkimuksen viimeisessä vaiheessa kehitettiin biointerfaasi hyödyntäen nanoselluloosafilmejä, joiden pinnat modifioitiin käyttäen TEMPO-hapetusta ja EDC/NHS-aktivointia. Tutkitun aktivoidun nanoselluloosakalvon havaittiin sitovan vasta-aineita kovalenttisesti, ja niiden kiinnitys demonstroitiin mustesuihkutulostusta hyödyntäen. Kehitetty biointefaasi tarjoaa lujan ja kestävän alustan tulevaisuuden immunodiagnostisille sovelluksille.

Avainsanat Selluloosa, vasta-aine, immobilisointi, immunodiagnostiikka

ISBN (painettu) 978-952-60-4835-2 **ISBN (pdf)** 978-952-60-4836-9

ISSN-L 1799-4934 **ISSN (painettu)** 1799-4934 **ISSN (pdf)** 1799-4942

Julkaisupaikka Espoo **Painopaikka** Espoo **Vuosi** 2012

Sivumäärä 150 **urn** http://urn.fi/URN:ISBN:978-952-60-4836-9

Preface

This work was carried out in the Department of Forest Products Technology at Aalto University, School of Science and Technology, during the years of 2008 – 2012. The work was performed as a part of the BioActive paper I and II projects funded by the National Agency for Technology and Innovation (TEKES) with industrial partners.

I am grateful to my supervisor Professor Janne Laine for giving me the opportunity to work under his supervision. My instructors, Ilari Filpponen, Leena-Sisko Johansson, and Susanna Holappa are thanked for supporting and guiding my research and scientific writing during my studies. Professor Orlando Rojas is thanked for giving me the opportunity to visit in his surface nanomaterial research group at North Carolina State University (NCSU), USA, and guiding my research and writing work.

I am thankful for my co-authors Tuija Teerinen, Professor Monika Österberg, and Terhi Saarinen, for giving the opportunity to work with you. I am thankful to Docent Eero Kontturi for guiding me in the scientific world of cellulose. Tuomas Hänninen is thanked for introducing the TEMPO-oxidation chemistry to me and soulful discussions in work and elsewhere. I am also grateful to Karoliina Junka for fruitful discussions and sharing a room with me.

I want to thank all the past and present colleagues of my research group. Special thanks go to Niko Aarne, Tiina Nypelö, Laura Taajamaa, Paula Eronen, Elli Niinivaara, Petri Myllytie, Susanna Ahola, Tero Taipale, Katri Kontturi, Ania Olszewska, Ola Sundsman, Miro Suchy, and Timo Pääkkönen. The members in the colloids and interface group in NCSU are thanked for supporting me during my visit at NCSU. Special thanks go for Justin Zoppe, Soledad Peresin, Ingrid Hoeger, Carlos I-III, Nafisa Islam, and Julio Arboleda. The technical staff, Risu, Rita, Anu, Marja, and Aila, is thanked for assistance in practicalities in laboratories. Riitta Hynynen is thanked for helping me in many practicalities. Joe Campbell is thanked for performing XPS-tests, and reading and correcting my manuscripts.

The members of TEPS are acknowledged for keeping me in touch with the normal life. My parents, brother, relatives, and friends are thanked for supporting me during my doctoral studies.

Finally, my deepest thanks go for my wife Petra and son Eelis, for understanding and supporting me during this work.

Helsinki, October 15th, 2012

Hannes Orelma

List of publications

This thesis is mainly based on the results presented in four publications which are referred as Roman numerals in the text. Some additional data related to the work is also discussed.

Paper I Orelma H., Filpponen I., Johansson L.-S., Laine J., and Rojas O. (2011) Modification of Cellulose Films by Adsorption of CMC and Chitosan for Controlled Attachment of Biomolecules, *Biomacromolecules,* 12 (12), 4311 - 4318.

Paper II Orelma H., Teerinen T., Johansson L.-S., Holappa S., and Laine J. (2012) CMC-modified cellulose biointerface for antibody conjugation. *Biomacromolecules,* 13 (3), 1051 - 1058.

Paper III Orelma H., Filpponen I., Johansson L.-S., and Laine J. (2012) Generic Method for Attaching Biomolecules via Avidin-Biotin Complexes Immobilized on Films of Regenerated and Nanofibrillar Cellulose. *Biomacromolecules*, 13 (9), 2802 - 2810.

Paper IV Orelma H., Filpponen I., Österberg M., Johansson L.-S., and Laine J. (2012) Surface functionalized nanofibrillar cellulose (NFC) film as a platform for immunoassays and diagnostics. *Biointerphases*, 7 (61), 1 - 12.

Author's contribution to the appended joint publications:

I-IV Hannes Orelma was responsible for the experimental design, performed the main part of the experimental work, analysed the corresponding results, and wrote the manuscripts.

Other publications that are not included in this thesis but to which the author has contributed:

Paper V Saarinen T., Orelma, H., Grönqvist, S., Andberg, M., Holappa, S., Laine, J. (2009) Adsorption of different laccases on cellulose and lignin surfaces, *BioResources,* 4 (1), 94 - 110.

Paper VI Marjamaa, K., Orelma, H., Andberg, M., Holappa, S., Laine, J., Kruus, K. (2012) Adsorption and catalytic action of Trichoderma reesei cellulases on cellulose model surfaces revealed by QCM-D, *Biotechnology and bioengineering*, Submitted.

Paper VII Virtanen H., Orelma, H., Erho, T., Smolander, M. (2012) Development of printable bioactive paper containing laccase. *Process biochemistry*, 47 (10), 1496 - 1502.

List of abbreviations

AFM	atomic force microscopy
BSA	bovine serum albumin
CMC	carboxymethyl cellulose
DS	degree of substitution
DP	degree of polymerization
EDC	1-ethyl-3-[3-dimethylaminopropyl]carbodiimide hydrochloride
hIgG	human Immunoglobulin G
LS	Langmuir-Schaeffer
MFC	microfibrillar cellulose
Mw	molecular weight
NFC	nanofibrillar cellulose
NHS	n-hydroxysuccinimide
RMS	root mean square
SPR	surface plasmon resonance
TEMPO	2,2,6,6-tetramethylpiperidine-1-oxyl free radical
TMSC	trimethylsilyl cellulose
QCM-D	quartz crystal microbalance with dissipation
XPS	X-ray photoelectron spectroscopy

Table of contents

1 Introduction and outline of the study

Studies on the preparation of biointerfaces on cellulosic materials are presented in this thesis. Cellulose is an abundant and renewable material in the biosphere, and its chemistry and material properties are rather well characterized. It belongs to a group of carbon neutral materials, and therefore it can be used to compensate for the use of fossil based materials. The most important sources of cellulose are woods and plants. However, in the Nordic countries, the wood based materials have been the major cellulose source due to the large forest regions available. The dissolved cellulose based materials have traditionally been utilized in immunodiagnostic applications (Elias 2000). Recently, the utilization of natural cellulose fibers, and its substructures (nanofibrils), on diagnostical applications have gained more attention (Pelton 2009). Compared to the homogenously dissolved cellulose, natural wood fibers are heterogeneous substrates containing several constituents. Therefore, analysis of the surface interactions with natural fiber materials could be beneficial for leading to a better understanding of the limits and possibilities when natural fiber based materials are utilized in immunodiagnostic applications.

Cellulose is rather stable and unreactive material that contains only a limited selection of free conjugation sites. Traditionally, the immobilization of antibodies on cellulose has been carried out using two main immobilization methods: direct adsorption and covalent conjugation. The direct adsorption is the simplest route to attach antibodies to cellulose, but its disadvantages, such as irreversible binding and reduced activity of antibodies, have led to a demand for more sophisticated conjugation chemistries (Rusmini, Zhong & Feijen 2007). Cellulosic materials contain a large number of hydroxyl groups that can contribute to the covalent conjugation of antibodies in non-polar solvents. The conjugation reactions in aqueous media require surface functionalization strategies for introducing suitable conjugation sites on cellulose, which can contribute to the formation of covalent linkages.

The aim of this thesis was to prepare and evaluate several different routes for antibody immobilization on cellulosic supports. All the work was carried out in aqueous solutions using chemistries with low toxicity. In **Paper I**, the effect of the surface charge of cellulose surfaces on protein adsorption was investigated. This was carried out using the surface plasmon resonance (SPR) technique with surface tailored cellulose model surfaces. The presence of electrostatic interactions was observed in the adsorption of proteins on hydrophilic surfaces. In **Paper II**, an immobilization strategy to covalently conjugate anti-

hemoglobin on cellulose using carboxymethyl cellulose (CMC) acting as a linker molecule was investigated. The covalent coupling reaction between antibody and CMC-modified cellulose was analyzed by combining the quartz crystal microbalance with dissipation (QCM-D) and SPR techniques. The specificity and detection limits of the prepared anti-hemoglobin biointerface were analyzed. In **Paper III**, a strategy to use avidin-biotin linkages for orienting the antibodies conformation on cellulose surfaces was investigated. The immobilization of avidin on carboxylated cellulose, and the ability of the immobilized avidin to detect biotinylated proteins were investigated by using QCM-D, atomic force microscopy (AFM), and X-ray photoelectron spectroscopy (XPS). Specific binding of biotinylated molecules on avidin modified cellulose was investigated with biotinylated bovine serum albumin (BSA) and anti-human immunoglobulin G (anti-hIgG). The influence of the oriented conjugation chemistry on the detection of antigens was investigated on nanofibrillated cellulose (NFC) surfaces by using QCM-D. In **Paper IV**, the methods developed in **Papers I – III** were applied to immobilize antibodies on NFC-films. TEMPO-oxidation chemistry was used to introduce carboxyl groups toposelectively on NFC-films, which in the later stage were converted to amine reactive esters. The carboxylation reaction was verified using conductometric titration and contact angle measurements (CAM). The amine reactivity of the activated NFC-films was characterized using fluorescence-stained anti-human IgG. The inkjet printing technique was utilized for depositing antibodies on activated NFC-films.

In general, this work presents several routes to immobilize antibodies on cellulosic materials in a controllable way. This knowledge could be useful in preparing more sophisticated immunodiagnostic tests based on the natural fiber support materials.

2 Background

2.1 Cellulosic supports in immunodiagnostic applications

Immunodiagnostic assays, also referred as to immunoassays, are quantitative or qualitative tests that utilize antibodies to measure the presence of soluble analytes, antigens, in complex sample fluids. The antibodies, obtained by either isolation of human body fluids or growing them in the host animals, are conjugated onto solid supports. The basic requirements for all diagnostic assays are similar; low detection limit, high analyte selectivity, small sample preparation, and high cost-effectiveness. Hence, the optimized support materials and specific conjugation chemistries define the accuracy and usability of the assay in the clinical testing. Traditionally, immunodiagnostic assays are based on the use of synthetic polymeric materials produced mainly from oil. Recently, sustainable renewable support materials such as natural cellulosic fibers have gained significant attention.

2.1.1 Immunodiagnostic assays and traditional support materials

The preliminary studies of immunodiagnostic testing were carried out in the later 1950s by Yalow and Berson with radioactively-labeled peptide hormone insulin (Yalow, Berson 1959). This was first time when a rapid diagnostic test was utilized to qualitatively measure the soluble analytes. Soon after that it was observed that there is a significant health risk with the radio-labeled antibodies of radio-immunodiagnostic assays (RIA). The enzyme linked immunosorbent assay (ELISA) was developed in the early 1970´s by Engvall and Perlmann (1971). The ELISA test is a sandwich type assay that employs enzyme-labeled secondary antibodies to sense the bound analyte on primary antigens (Figure 1). The intensity of the enzymatic color reaction can be used to qualitatively determine the concentration of the measured analyte. This test type is still, over three decades later, the most used method to routinely screen for several human diseases (Lequin 2005). The disadvantage of the ELISA test is the demand of multiple measurement steps and expensive laboratory equipment. Therefore, this test type has largely been used only in laboratories.

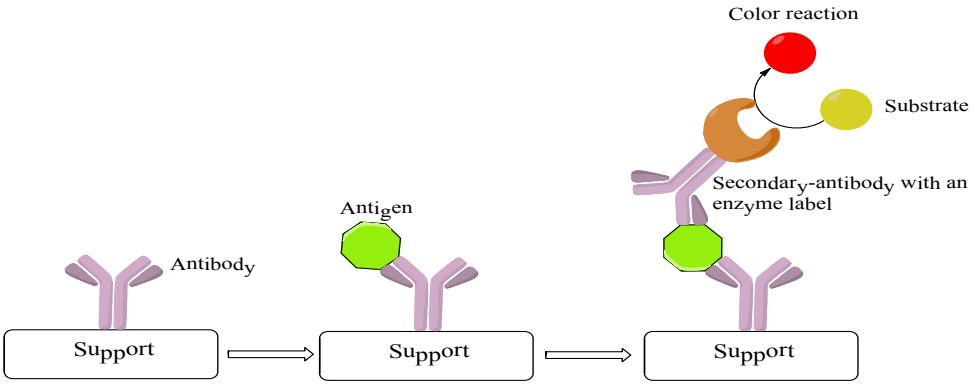

Figure 1. Enzyme labeled immunosorbent assay (ELISA). Antigens are bound onto a solid support via conjugated primary antibodies. The binding of the antigen is exposed using enzyme labeled secondary-antibodies that causes a visible color reaction when the substrate material of the enzyme is applied in the test.

The ELISA and radiolabeled immunoassay (RIA) methods need multiple measurement steps, which are sometimes too complicated in commercial use. Therefore, an immunodiagnostic test, which could simultaneously sense the analytes and illustrate the result of the test using a visible color reaction in a testing time of minutes, was developed. This semi-qualitative assay, referred as a lateral flow test, was presented in the early 1980´s (Hawkes, Niday & Gordon 1982)(Smits et al. 2001). In the lateral flow test, a porous membrane is employed to cause a laminar flow for a liquid that drives the soluble sample liquid through the membrane due to the presence of capillary forces (Figure 2). The laminar flow phenomenon can be obtained only by using porous matrixes. Therefore, laminar flow tests are typically based on the use of porous cellulosic materials such as nitrocellulose and paper. Lateral flow tests are intensively used in several commercial rapid diagnostic applications such as medical, food, and water analyses (Yager et al. 2006)(Posthuma-Trumpie, Korf & van Amerongen 2009). For urine testing, where the volumes of samples are higher, dipstick tests have also been used (Hawkes, Niday & Gordon 1982). This test type is identical with the laminar flow test but it does not contain any sample pad. The dipstick tests are used in the routine testing various constituents from human urine such as human chorionic gonadotropin (HCG), which is known as a pregnancy test (Deville et al. 2004).

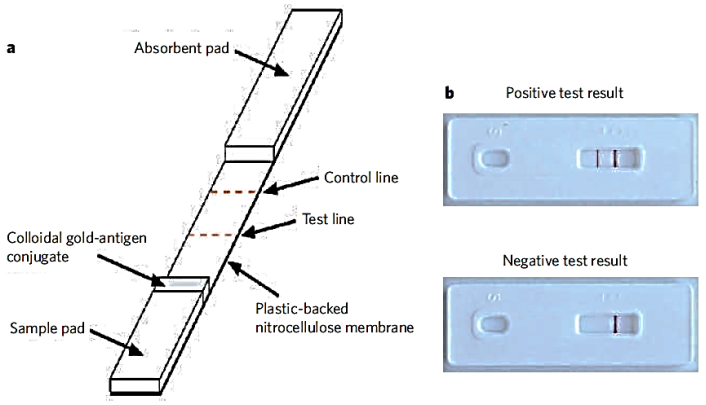

Figure 2. Typical lateral flow test. (a) A sample liquid with a soluble analyte is applied into the sample pad where the liquid flows through the membrane. The analyte in liquid first reacts with gold nanoparticle stained secondary antibodies, and then the conjugate flows through the migration membrane where it is caught in the test line by primary antibodies. (b) The visible mark in the test line is caused by gathering of nanoparticles in the small area. The validity of the test is verified with a control line, where both reacted and unreacted antibodies are caught. (Adapted from (Yager et al. 2006)).

The basic requirement for stable immunodiagnostic assays is that the supporting material does not cross-interact with analytes. Traditionally, the solid supports in the ELISA and RIA assays have widely been based on synthetic polymeric materials. In that case, the cross-reactivity between analytes and the plastic supports have been blocked by adsorbing proteins such as bovine serum albumin (BSA). The protein fills the "holes" on the surface, preventing the non-specific binding of antigens (Kenna, Major & Williams 1985)(Sverre-Henning 1997). Similar treatment steps have also been used for the semi-synthetic nitrocellulose membranes in laminar flow tests. Otherwise, the anionic charge of nitrocellulose electrostatically binds proteins, causing a false response (Spinola, Cannon 1985). Additional, clear disadvantages of nitrocellulose based matrices are their brittle nature and their high flammability. By the virtue of those properties, renewable totally natural fiber-based materials could be a competing platform to be used as a supporting material in rapid diagnostic assays.

2.1.2 Natural fiber based supports in immunodiagnostic applications

Natural cellulose fiber-based materials exhibit interesting characteristics, such as their hydrophilic nature, high stability, low toxicity, and high industrial availability (Pelton

2009). Therefore, the development of natural fiber-based immunodiagnostic assays has attracted significant attention. The first paper-based "diagnostic test" for the detection of glucose in urine was demonstrated in the late 1950´s by Free and coworkers (Free et al. 1957). This pioneering test was based on the use of immobilized glucose oxidase enzymes, which catalyzed the reduction of glucose to D-glucono-δ-lactone. The use of the capillary flow properties of porous paper in immunodiagnostic testing was first demonstrated by Zuk and coworkers (Zuk et al. 1985). This test was an enzyme immunochromatographic test, where the antigen binding in the paper strip was visualized by an external substrate addition step. The complete paper-based laminar flow test for immunodiagnostic analysis has been demonstrated in several reports (Abe, Suzuki & Citterio 2008)(Fenton et al. 2009)(Lappalainen et al. 2010). Moreover, in these studies non-contact dispersing techniques were used to manufacture these low-cost diagnostic paper assays (Figure 3). The multicomponent paper based laminar flow test, manufactured by inkjet printing of filter paper with hydrophobic polymer walls, has also been demonstrated (Bruzewicz, Reches & Whitesides 2008). Splitting of the laminar flow to separate flow channels allows analysis of multiple analytes simultaneously. In addition, fluid channeling in paper has been applied to the size-based extraction of molecules from complex mixtures (Osborn et al. 2010). A multicomponent paper-based microfluidic test on the testing of glucose and BSA simultaneously from urine has been demonstrated (Martinez et al. 2010). The use of a paper matrix in the routine ELISA-testing has also been represented (Cheng et al. 2010). In this case, the paper-based support was prepared on a chemically treated paper using photolithography with UV-light. The use of rapid immunodiagnostic testing for screening for the quality of foods can be found in the review paper by Krska and Molinelli (Krska, Molinelli 2009). The examples presented above show the growing potential for immunodiagnostic tests using natural cellulosic fiber based materials. However, the knowledge of surface interactions and immobilization reactions on the wood fiber surfaces is presently imperfect. Many of those papers were targeted to demonstrate the action of prepared test without focusing on the detailed analysis of conjugation and adsorption reactions. Hence, a deeper understanding of interfacial reactions could be beneficial when more effective and sophisticated immunodiagnostic tests are developed.

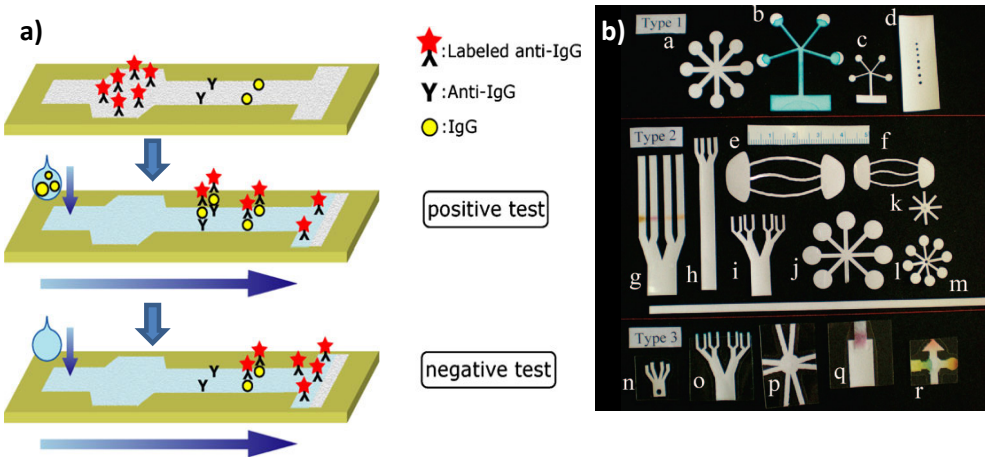

Figure 3. The reaction scheme of a paper-based laminar flow assay on the detection of human immunoglobulin G (a). Examples of the possible shapes of lateral flow assays performed by two-dimensional scission (b). (Figures are obtained from (Abe, Suzuki & Citterio 2008) and (Fenton et al. 2009), respectively).

2.1.3 Chemistry of natural cellulosic materials

Cellulose, nature's unique biopolymer, was reported for the first time in the 1833 by Payen and Persoz (Payen, Persoz 1833). Since then the scientific interest to unravel the detailed structure and chemistry of cellulose has constantly continued. But even today, the actual, comprehensive chemistry of cellulose is under debate. Cellulose is a linear syndiotactic polymer composed of D-anhydroglucopyranose units via β-(1-4) linkages (Figure 4). It has been proposed that the repeating unit of cellulose is the dimer cellobiose (two D-anhydroglucopyranose units linked together), composing an isotactic linear polymer (Klemm 1998). Cellulose is a polydisperse material that is comprised of a set of polymer chains with varying chain lengths (Sjöström 1993). The length of cellulose is defined as a number of D-anhydroglucopyranose units linked together (degree of polymerization (DP)). The average DP varies in natural cellulosic materials from 500 up to 12000 (Table 1). Cellulose is insoluble in water when the DP is over 6 (Nehls et al. 1994) by virtue of its remarkable affinity to form hydrogen bonds. The hydrogen bonding of cellulose chains takes place between the hydrogen of the OH-group in the sixth position and oxygen of the hydroxyl group in the third position of another chain (Klemm 1998). In addition, those hydrogen bonds cause the rigid nature of cellulose chains, which together with its low solubility in water leads to a strong tendency to build ordered structures (crystalline regions).

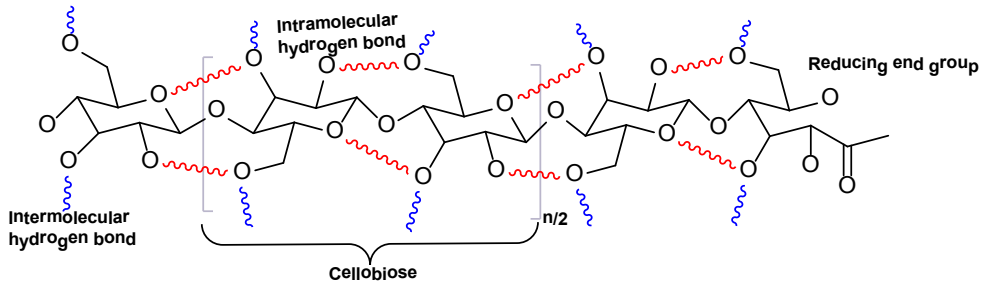

Figure 4. Structure of a cellulose chain with intra- and intermolecular hydrogen bonding patterns. In this model, hydrogen atoms are not indicated.

Table 1. Typical DP ranges of various cellulose materials. (Adapted from (Klemm 1998)).

Material	Range of DP
Native cotton	Up to 12000
Scoured and bleached cotton linters	600 – 800
Wood pulp (dissolving pulp)	600 – 1200
Man-made cellulose filaments and fibers	250 – 500
Cellulose powder prepared by partial hydrolysis and mechanical disintegration	100 – 200

Depending on the source of cellulose, native cellulose has been found to exhibit two different parallel crystalline structures (Cellulose Iα and Iβ) (Atalla, Vanderhart 1984). Cellulose Iα is the dominant crystalline structure for native bacterial and valonia cellulose, whereas cellulose Iβ dominates in the higher plants such as wood and cotton. The crystallization of cellulose accumulates cellulose chains together creating an elementary fibril (Figure 5) composed of a 6x6 cellulose I lattice (Cosgrove 2005). Due to the rigid nature and the hydrogen bonding ability of cellulose, the elementary fibrils self-assemble into fibrillar bundles called microfibrils that contain both crystalline and amorphous regions (O'Sullivan 1997). The most used model to illustrate this structural heterogeneity is the Fringed fibril model (Hearle 1958). In this model, the crystalline regions of cellulose are linked together by amorphous regions without any semi-crystalline regions. However, the validity of this model is under scientific debate. When a cellulosic material is in contact with water, water penetrates the amorphous regions of cellulose, breaking down the hydrogen bonding patterns and causing the swelling of the cellulosic matrix (Müller et al. 2000). On the other hand, the tight packing of cellulose chains in the crystalline regions

prevents the penetration of water into the microfibrils. The crystalline structure can be separated using non-polar solvent systems (Dawsey, McCormick 1990), such as lithium chloride/dimethylacetamide (LiCl/DMAc), which breaks the intermolecular hydrogen bonding patters between the cellulose chains. The dissolved cellulose can be recrystallized in an aqueous solvent system leading to twisting of the cellulose chains to the anti-parallel cellulose II conformation (Fink, Philipp 1985). This cellulose II lattice is also referred as regenerated cellulose, and it is widely used in various applications on, e.g., non-woven cellulose fibers, fabrics, and cellulosic membranes.

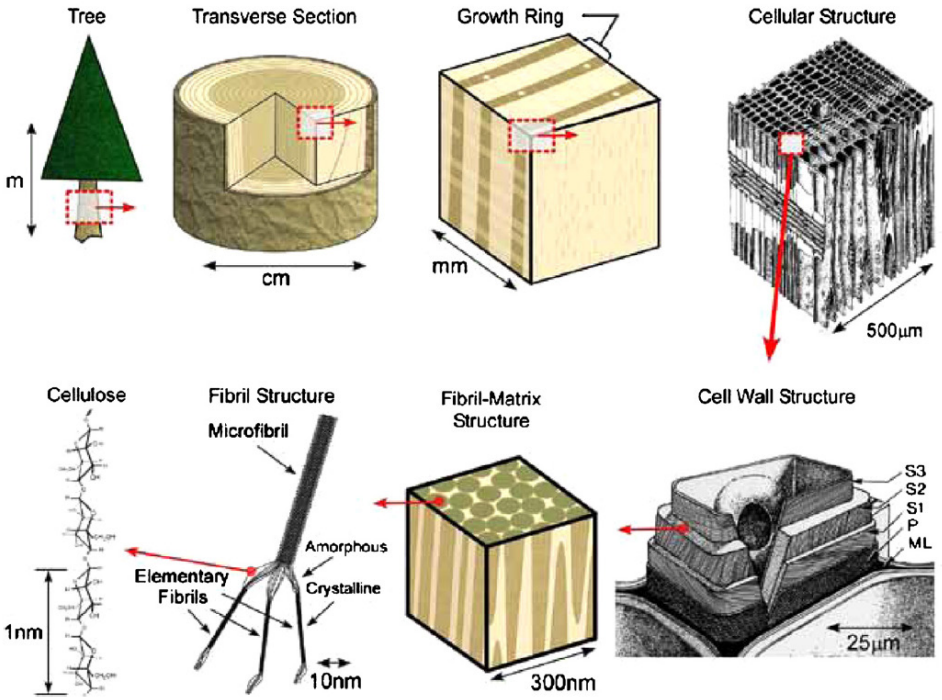

Figure 5. Schematic representation of the hierarchical structure of wood tissue. (Adapted from (Postek et al. 2011)).

Wood tissue, which generally speaking is the most environmental friendly cellulose source and is largely available, is composed of hollow wood fibers (Figure 5) that are glued together by lignin and pectin. The structure of wood fibers is composed of different cell wall layers — middle lamellae (ML), primary cell wall (P), and secondary cell walls (S) 1 – 3. These cell wall layers are chemically diverse, and the chemical compositions between these layers differ (Sjöström 1993). Cellulose locates mainly in the secondary cell wall layers S1, S2, and S3, packed in cellulose microfibrils. The S2-layer is the most important cell wall layer in a wood fiber by virtue of its thickness and high cellulose content (Krässig 1993).

Therefore, this layer has the most influence on the material properties of cellulosic end products. The middle lamellae glues fibers together, and it is mainly composed of lignin and pectin. A flexible primary wall layer is sandwiched between the S1 and the middle lamellae. It is composed mainly of amorphous hemicelluloses and lignin, but also a small amount of cellulose microfibrils in random orientations has been found (Sjöström 1993).

Hemicelluloses are a diverse group of water soluble branched heteropolymers, composed of various monosaccharides with a low degree of polymerization (DP of 50 - 300). The high solubility of hemicelluloses in water is caused mainly by both the branched structure and the presence of charged side groups. The chemical composition of hemicelluloses in different plant species varies (Sjöström 1993). In generally, hemicelluloses that are present in hardwood fibers are glucuronoxylan and glucomannans, whereas softwood species contain mainly galactoglucomannans and arabinoglucuronoxylan (Table 2). The role of hemicellulose in wood cell wall layers is to fill the voids, provide coupling to lignin, and regulate the structure of cell walls (Atalla et al. 1993). Lignin, in all wood tissues, has a three dimensional amorphous random network; the lignin precursors, p-coumaryl alcohol (hardwoods), coniferyl alcohol (softwoods), and sinapyl alcohol (hardwood), are connected via radical polymerization reactions. The extent of lignin in different plant species varies significantly, but it has similar functions in all wood species — glue individual wood fibrils together, provide compression strength, and protect plants against pathogens (Boerjan, Ralp & Baucher 2003).

Table 2. The major hemicellulose components in softwood (SW) and hardwood (HW). (Adapted from (Sjöström 1993)).

Wood	Hemicellulose type	Amount (% on wood)	Composition			DP
			Units	Molar ratios	Linkage	
SW	Galacto-glucomannan	5-8	β-D-Man*p* β-D-Glc*p* α-D-Gal*p* Acetyl	3 1 1 1	1 → 4 1 → 4 1 → 6	100
	(Galacto)-glucomannan	10-15	β-D-Man*p* β-D-Glc*p* α-D-Gal*p* Acetyl	4 1 0.1 1	1 → 4 1 → 4 1 → 6	100
	Arabino-glucuronoxylan	7-10	β-D-Xyl*p* 4–O–Me–α-D-Glc*pA* α-L-Araf	10 2 1.3	1 → 4 1 → 2 1 → 3	100
HW	Glucuronoxylan	15-30	β-D-Xyl*p* 4–O–Me–α-D-Glc*pA* Acetyl	10 1 7	1 → 4 1 → 2	200
	Glucomannan	2-5	β-D-Man*p* β-D-Glc*p*	1-2 1	1→ 4 1→ 4	200

The surface chemistry of cellulosic fibers and microfibrils is important since all chemical reactions take place in the interface between a surface and bulk media. When natural cellulose-based materials are utilized in applications where the high cellulose content is needed, only chemical pulping with multiple bleaching steps can provide high quality cellulosic fibers. The chemical disintegration, pulp cooking, selectively dissolves lignin, mainly from middle lamella that separates the wood fibers (Sjöström 1993)(Duchesne, Daniel 2000). However, in pulp cooking a part of lignin and hemicellulose from the secondary wall layers is also removed, which produces small pores on the fiber surface (Maloney, Paulapuro 1999). After removal of lignin from a softwood (Norway Spruce) in the KRAFT-process, which is the most used industrial delignification process, it has been observed that cellulose microfibrils are visible on the fiber surface (Figure 6), and the microfibrils are uncovered or only covered with a few molecular layers of hemicelluloses (Duchesne et al. 2001). The average pore size on the fiber surfaces is approximately 20 nm measured by AFM (Fahlen, Salmen 2005). The lignin content on softwood fibers after KRAFT-process with bleaching steps have been measured by XPS to be about 0.5 % or lower (Laine, Stenius 1994)(Risén, Hultén & Paulsson 2004). Those results demonstrate that the surfaces of delignified wood fibers after delignification steps have a cellulosic structure. But

there are a small amount of hemicelluloses present, introducing a slight negative charge for wood fibers.

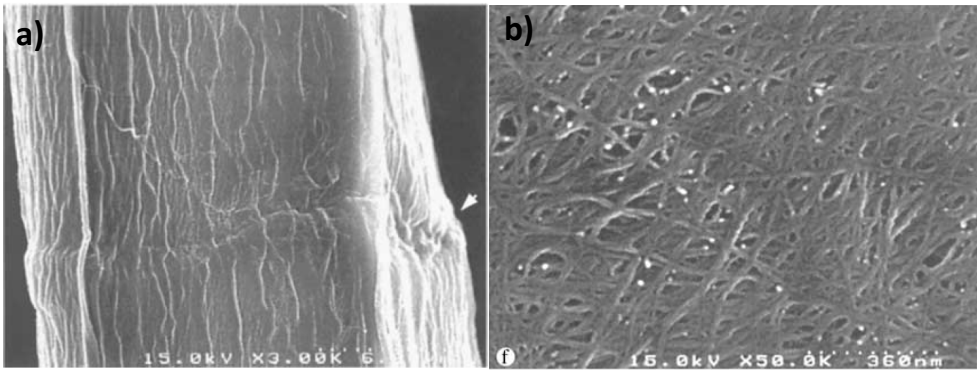

Figure 6. FE-SEM micrograph of the exterior surface of a delignified softwood kraft fiber (hemicellulose content 10%) with low magnification (a) and high magnification (b). (Adapted from (Duchesne et al. 2001)).

2.1.4 Microfibrillar cellulose (MFC)

Microfibrils of delignified wood fibers can be disintegrated by using mechanical disintegration (Turbak, Snyder & Sandberg 1983) together with chemical treatments such as enzymatic (Pääkkö et al. 2007), 2,2,6,6,-tetramethylpipelidine-1-oxyl radical mediated oxidation (TEMPO-oxidation) (Saito, Isogai 2004), or carboxymethylation (Wagberg et al. 2008). The enzymatic and chemical methods are pre-treatments, which are used to ease the mechanical disintegration of cellulose nanofibrils. Pure mechanical disintegration of cellulosic microfibrils produces thick microfibril bundles, not only individual microfibrils, and the energy input needed is high. Moreover, pure mechanical disintegration is a rough method that always alters the physical properties of the cellulose microfibrils, observed as the lowered DP values of MFC. Enzymatic pre-treatment has been found to ease mechanical disintegration (Pääkkö et al. 2007). This method is based on the finding that cellulase enzymes can catalyze the hydrolysis of bonds between cellulose microfibrils, which lower the energy demand needed from mechanical disintegration. The enzymatic methods do not alter the surface chemistry of cellulose microfibrils, and thus the chemical properties of microfibrils produced are similar to the raw material. The chemical pre-treatment methods have also been found to lower the energy inputs in the production of cellulose nanofibrils. TEMPO-oxidation and carboxymethylation are the most used methods, which

are based on the introduction of anionic functional groups to the surfaces of cellulose microfibrils. The anionic charge causes electrostatic repulsion between cellulose microfibrils that drastically ease mechanical disintegration (Saito et al. 2007). Carboxylated cellulose microfibrils, produced using the prescribed methods, are found to carry a high surface charge that stabilizes them in aqueous suspensions (Wagberg et al. 2008)(Saito, Isogai 2004). In general, all cellulose microfibrils prepared from natural fiber materials have a slight anionic surface charge by virtue of a small amount of hemicellulose on the fibril surfaces (Fall et al. 2011).

Cellulose microfibrils have very interesting characteristics, such as high aspect ratio (100 - 150), high strength properties, and low toxicity towards to living organisms. In aqueous suspensions, cellulose microfibrils are found to form a network that behaves like a pseudoplastic gel due to the high hydrogen bonding and entanglement of cellulose microfibrils (Herrick et al. 1983). This microfibrillar cellulose (MFC) gel has been employed to cast strong translucent cellulose films (Henriksson et al. 2008)(Syverud, Stenius 2009)(Aulin, Gällstedt & Lindström 2010)(Fujisawa et al. 2011). The properties of the NFC-films are mainly adopted from the raw material used, and thus, a homogenous cellulose microfibrillar gel has high transparency (Nogi et al. 2009)(Fujisawa et al. 2011)(Aulin, Gällstedt & Lindström 2010). NFC-films have good strength and oxygen barrier properties only in dry atmosphere. But, due to the hydrophilic nature of cellulose, those properties are significantly disturbed in the wet state. However, NFC-films, cast from mechanical disintegrated MFC (low charged MFC) have been observed to exhibit such a low water uptake that they have rather good strength properties also in high humidity conditions (Spence et al. 2010). The hydrophobicity of NFC-films can be improved using various grafting and surface functionalization chemistries (Siró, Plackett 2010). But then, almost every time, the surface properties of cellulosic microfibrils are altered causing a loosely bound fibrillar network that reduces the strength properties of the NFC-film. The potential applications for cast NFC-films are food and pharmaceutical packaging materials, where the high oxygen barrier properties with low toxicity are beneficial. However, the inherent characteristics of cellulosic nanomaterials might also be utilized in medical and diagnostic applications.

2.1.5 Cellulose model surfaces

Cellulosic fibers always have a complex surface structure due to their varying characteristics e.g. roughness, porosity, and chemical composition that make the analysis of the adsorption and conjugation of proteins to be a challenging task to study. To fundamentally

study adsorption phenomena on cellulosic fibers, cellulose thin films can be utilized. These model surfaces exhibit similar chemistry as the native cellulose fibers. Moreover, these ultrathin model cellulose surfaces enable in-situ studies with surface sensitive methods e.g. Quartz Crystal Microbalance with Dissipation monitoring (QCM-D), Surface Plasmon Resonance (SPR), Atomic Force Microscopy (AFM), and X-Ray Photoelectron Spectroscopy (XPS). The first cellulose model surfaces were reported in 1972 (Agnihotri, Giles 1972). There, cadoxen(tri(ethylenediamine)cadmium hydroxide was successfully employed to cast a cellulosic monolayer on water. The development of cellulose model surfaces has continued for several decades, and various cellulose thin films has been introduced, e.g., regenerated cellulose, nanofibrillated cellulose, nanocrystalline cellulose, and cellulose bilayer model surfaces with various characteristics (Kontturi, Tammelin & Österberg 2006). In this chapter, only the model cellulose surfaces, which were utilized in this work, are discussed in detail i.e. the regenerated cellulose films with low and high crystallinity, and nanofibrillar cellulose films.

Cellulose model surfaces are usually prepared using spin coating or Langmuir-Schaefer (LS) techniques. Both methods are scientifically well established, and allow deposition of ultrathin cellulose layers with thicknesses varying from 5 to 100 nm. Normally, about a 15 nm thick cellulose film has been found to be enough to evenly cover the supporting material (Kontturi, Tammelin & Österberg 2006). In prescribed methods, the cellulosic material is first either dissolved or dispersed in a liquid medium before deposition on the solid support. The mostly used solvent systems to dissolve cellulose are dimethylacetamide with lithium chloride (DMAc-LiCl) (Dawsey, McCormick 1990) and N-methylmorpholine-N-oxide (NMMO) (Rosenau et al. 2001). The deposition of dissolved cellulose can be carried out either directly or by first derivatizing the cellulose using, as an example, hexamethyldisilazane (Cooper, Sandberg & Hinck 1981) to produce a cellulose derivative soluble in organic solvents. The Langmuir-Schaefer method (LS) is based on the preparation of a hydrophobic monolayer on a water surface whose properties can be controlled by adjusting the surface tension (Langmuir, Schaefer 1938). Theoretically, when the hydrophobic support is in the contact with the monolayer, this monolayer layer is transferred onto the surface of the support. In general, the deposited monolayer is not uniform and often several dips are needed to insure the uniformity of the film. Cellulose II surfaces from trimethylsilylated cellulose (TMSC) using the LB-method has been demonstrated earlier by Schaub and co-workers (Schaub et al. 1993). The TMSC-surfaces can be converted into cellulose form with an HCl-vapor treatment that causes a vapor-phase transition from TMSC to cellulose. LS-deposited cellulose II films have been investigated in detail by Tammelin and co-workers (Tammelin et al. 2006). The degree of crystallinity of deposited

cellulose II films prepared by the LS-method was found to be 60 %, and the roughness of the film was approximately 0.5 nm (Figure 7a) (Aulin et al. 2009). Regenerated cellulose surfaces prepared from TMSC can also been deposited on silica supports by using the spin-coating technique (Geffroy et al. 2000). The spin-coated cellulose surfaces are highly amorphous, and their roughnesses is approximately 3 nm (Figure 7b) (Kontturi, Thune & Niemantsverdriet 2003). The most recent approach to produce cellulose model surfaces is to use mechanically disintegrated native cellulose I nanofibrils (Ahola et al. 2008b). These NFC-model cellulose (Figure 7c) surfaces adopt the chemistry and morphology of native wood fibrils (cellulose I with a small amount of hemicellulose, depending on the source of pulp NFC prepared from). The roughness of those NFC-model surfaces has found to be approximately 3.2 nm (Ahola et al. 2008b).

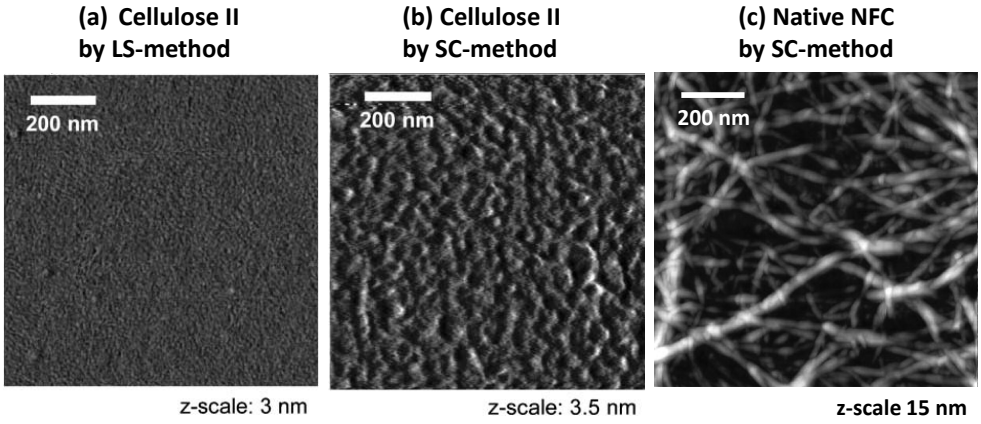

Figure 7. AFM images of: (a) a partially crystalline cellulose II surface deposited from TMSC by Langmuir-Schaefer method, (b) a fully amorphous cellulose surface deposited from TMSC by the spin-coating method, and (c) a nanofibrillar cellulose surface prepared by the spin-coating method. (Images (a) and (b) were adapted from (Kontturi, Tammelin & Österberg 2006), and image (c) adapted from (Ahola et al. 2008b)).

2.2 Sensing antibodies

Antibodies (Ab), also referred to as immunoglobulins (Igs), are the host proteins of the human immune system. Antibodies have a specific affinity to bind antigenic determinants, foreign molecules, through specific amino acid sequences. Commercial antibodies are produced in living mammals or isolated from human blood following tight ethical guidelines. Antibodies can be divided into two different subgroups, monoclonal antibodies

(mAb) and polyclonal antibodies (pAb), according to their specificity to bind antigenic determinants. Polyclonal antibodies are collected directly from serum, whereas the production of monoclonal antibodies requires multiple production and purification steps. Polyclonal antibodies are a collection of heterogeneous mixtures of antibodies with varying affinities, but also a small amount of several other Ig classes is present. Thus polyclonal antibodies may cross-react with antigens other than the target antigen, whereas monoclonal antibodies contain only a single Ig-class with negligible non-specific cross-reactivity.

2.2.1 The chemistry of antibodies

Immunoglobulins (Igs) are glycoproteins, which are composed of one or more identical Y-shaped units. Immunoglobulins (Igs) can be separated into five major subclasses (IgG, IgA, IgM, IgD, and IgE) on the basis of their physical, chemical, and immunological properties (Figure 8). The IgG (γ-heavy chain), IgD (δ-heavy chain), and IgE (ε-heavy chain) are Y-shaped antibodies composed of four polypeptide chains (two light chains and two heavy chains). IgA (α-heavy chain) is a dimer and IgM (μ-heavy chain) is typically a pentamer. Approximately 75 % of human serum immunoglobulin belongs to the IgG-class (Hamilton 1987), and this type is the most used antibody subclass. In this thesis, only the IgG-type antibodies were exploited, and thus this sub-type is discussed in more detailed here. IgG has four subclasses IgG>IgG2>IgG3>IgG4, classified mainly on the length of the heavy chains (Hamilton 1987). However, the antigenic binding point of these IgG subclasses are equivalent, and thus their antigen binding ability is almost a constant. The Y-shaped immunoglobulin G units are comprised of two identical heavy chains (Mw of each~50,000) and two identical light chains (Mw of each~25,000) linked together through both sulfur bridges and non-covalent interactions between polypeptide chains (Madigan, Martinko & Brock 2009). Moreover, the individual polypeptide chains are composed of various numbers of amino acids (22 common amino acids) through the peptide (amide) bonds, and each light and heavy chain has been analyzed to contain approximately 220 and 440 amino acids, respectively (Amit et al. 1986). The amino terminal ends of the polypeptide chains have considerable variation in amino acid composition. Therefore, they are refer to variable (V) regions, whereas the constant (C) regions have rather constant amino acid composition. The composition of the variable regions of heavy and light chains determines which antigens can be detected. The antigens, in turn, are specific for a type of antibody. The protein and polysaccharide content of the IgG class has been found to be 82-96 % and 4-18 %, respectively (Peakman et al. 2009).

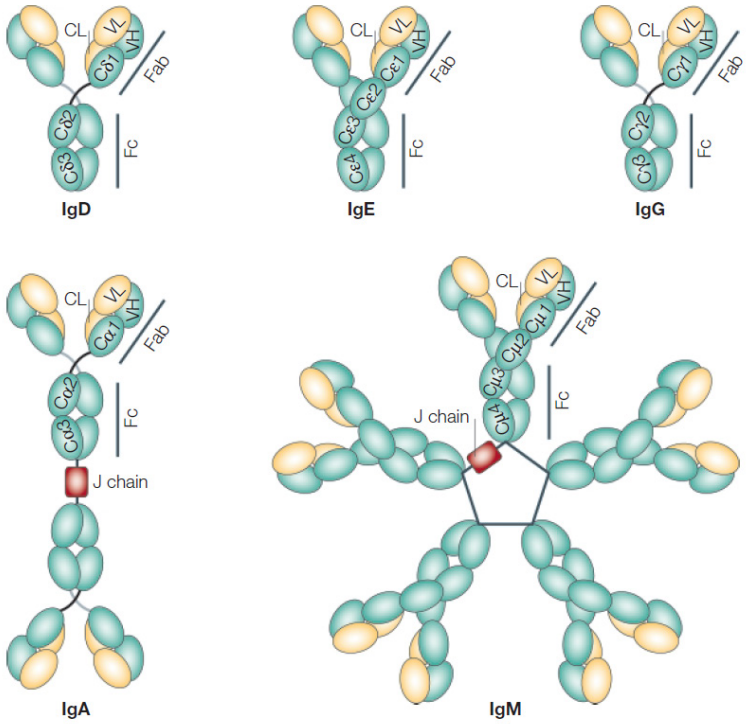

Figure 8. Schematic illustrations of structures of five major Immunoglobulin classes. All classes have similar V_H and V_L domains that bind antigen. In the illustration, light chains are green, heavy chains are blue, and circles denote the sites of glycosylation. (Adapted from (Rojas, Apodaca 2002)).

Immunoglobulin G antibodies have the similar substructure of all proteins — the primary structure (an amino acid sequence of a polypeptide chain), secondary (twisting and folding of a polypeptide chain, α-helix or β-sheet folding), tertiary (three dimensional structure composed of two polypeptide chains), and quaternary structure (three dimensional structure composed of many polypeptide chains) (Branden, Tooze cop. 1999). The heavy and light chains interact together with non-covalent interactions between side-chain functionalities (residues) and sulfur bridges, defining the three dimensional folding of an IgG in water (Figure 9a). In an aqueous environment, the hydrophobic amino acid residues tend to be oriented inside in the structure of an antibody, whereas ionic amino acid residues (hydrophilic) are oriented in bulk water (Thanki, Thornton & Goodfellow 1988). Due to the ionic (hydrophilic) side chain functionalities, the conformation of an immunoglobulin molecule alters as a function of the properties of the solvent. Low ionic strength conditions stabilize the structure of a protein, whereas higher salt concentrations lead to precipitation due to the reduced stability and denaturation of proteins (salting out) (Ara-

kawa, Timasheff 1984). Each antibody has a specific pH where its surface net charge is zero (sum of negative and positive charges), i.e. the point of isoelectricity (pI) (Patrickios, Yamasaki 1995). Below the pI, positively charged amino acid residues dominate, leading to positive net charge. Conversely, above the pI, the antibody has a negative net charge due to the domination of ionized anionic amino acid residues.

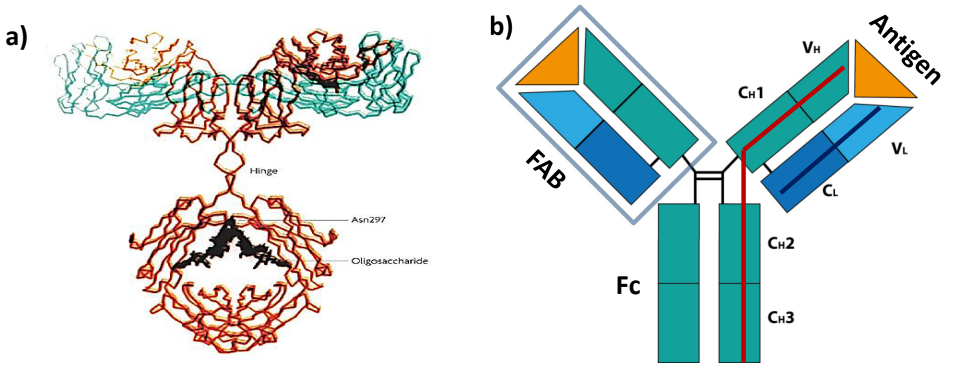

Figure 9. Three dimensional illustration of folding of a human IgG (Adapted from (Jefferis 2009)) (a). Two dimensional schematic illustration of the structure of the basic Y-shaped unit composed of two identical heavy chains (red line) and two identical light chains (black line) by sulfuric bridges (b). The constant domains (C_H1, C_H2, and C_H3) are identical in all IgG antibodies. The fragment antigen-binding (FAB) is a part of antibody that can separated by digestion of the hinge region.

Antigens binding to antibodies take place through the variable V_H and V_L regions of fragment-antigen binding (FAB fragments) (Figure 9b). The specific point on the core of an antigen which reacts with the FAB-fragment is called as an epitope. The antigen-antibody interaction is always highly specific due to the variations in the amino acid sequences of V_H and V_L regions, which are specific for the type of the antibody (Peakman et al. 2009)(Davies, Sheriff & Padlan 1988). X-ray crystallographic studies have shown that antibody-antigen interactions are caused mainly by van der Waals interactions, formation of hydrogen bonds, and to a lesser extent the formation of salt-bridges (Braden, Poljak 1995). Therefore, the binding of antigen to antibody is reversible, allowing the regeneration of the antigen-antibody bond in suitable conditions (mainly at low pH and high ionic strength). The strength of this binding, also referred as to an affinity, is the sum of the attractive and repulsive forces, which can be analyzed using indirect methods by obtain the affinity constant (Friguet et al. 1985). Recently, atomic force microscopy has also been exploited for direct analysis of the strength of the antigen-antibody interaction (Allen et al. 1997). The affinity is not the only characteristic that defines antigen binding to antibodies.

The specificity, the ability of an individual antibody FAB fragment to react with only one antigenic determinant, is also important. In general, antibodies specificity varies significantly between different species. IgGs can also react through the Fc-regions with a variety of host effector molecules. In the human immune system antibody molecules serve as an immunologic bridge in the recognition of foreign pathogens and other species responsible for triggering the host response system (Canfield, Morrison 1991).

2.2.2 Conjugation sites on antibodies

The covalent conjugation of antibodies onto solid surfaces takes place through the residues of amino acids. Hence, residues that can orientate on the outside of the IgG are more accessible for the covalent linking reactions (Rusmini, Zhong & Feijen 2007)(Jameson, Wong 2009). Polar (hydrophilic) amino acid residues have a higher affinity to orientate out into the aqueous media, whereas non-polar (hydrophobic) amino acid residues are hidden in the protein structure (Manavalan, Ponnuswamy 1978). Amino acids with ionizable residues (Figure 10) are significant from the conjugational point of view because covalent conjugation reactions take place through those accessible side functionalities. Aspartic acid and glutamic acid are carboxyl-containing amino acids that have a negative charge. The theoretical pKa of aspartic (Asp) and glutamic (Glu) acids are 3.7-4.0 and 4.2-4.5, respectively. When these groups are ionized and they can act as a nucleophile in addition reactions. Cysteine (Cys) is only amino acid that contains a sulfhydryl group, which is ionized at high pH (pKa of 7.7 – 9.1); however, cysteine has a high hydrophobicity, and hence, it is usually partially inaccessible for conjugation reactions (Hermanson 2008). Lysine (Lys) and arginine (Arg) are amine containing amino acids, and they are protonated at acidic and neutral pH (pKa of 9.3 – 9.5 and 12-12.4, respectively). Histidine (His) has an imidazole ring that is protonated at alkaline pH (pKa of 6.7 – 7.1). Tyrosine (Tyr) and tryptophan (Tryp) are aromatic ring-containing amino acids that are normally located inside an IgG, and therefore their accessibility in water is low (Hermanson 2008).

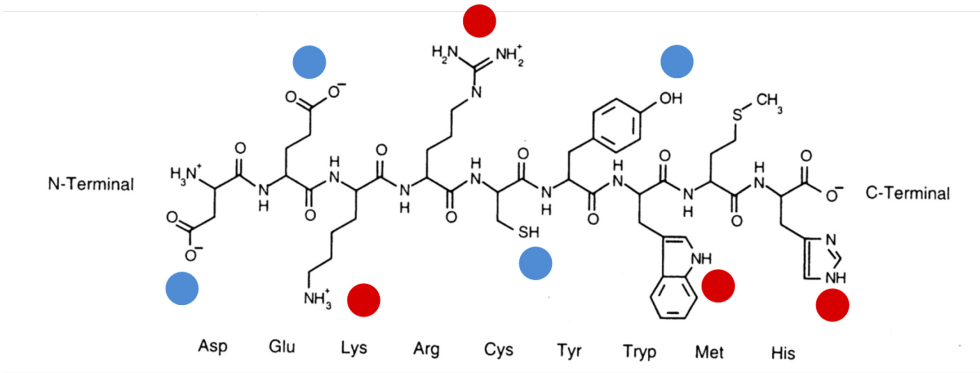

Figure 10. Protein chain, composed of the most reactive amino acids. Blue circles represent an amino acid with an anionic residue, whereas red circles represent amino acids with a cationic residue. (Adapted from (Hermanson 2008)).

Solvent accessibility calculations are used to estimate the reactivity of different amino acids in conjugation reactions (Bordo, Argos 1991). Lysine and arginine were found to be most accessible amine containing amino acids. From the anionic amino acids, aspartic and glutamic acids were found to have the highest accessibility. An amino acid with high solvent accessibility could however also has a steric hindrance that restricts the covalent conjugation reaction (Smith, Withka & Regan 1994). Immunoglobulin G also contains oligosaccharides, mainly composed of galactose and mannose, which exist in the C_H2 regions of a Fc-fragment (Krapp et al. 2003)(Mizuochi et al. 1982). Those carbohydrate chains are located in the exterior of an FC-fragment, and hence should be easily accessible. However, an oxidative treatment is usually needed to open those moieties, enabling the covalent conjugation reactions. These carbohydrate regions are important since, through those units, an oriented immobilization of IgG can be obtained on solid matrices (Lu, Smyth & O'Kennedy 1996).

2.3 Immobilization of sensing antibodies on cellulosic supports

Natural cellulosic fiber surfaces contain mainly cellulose with a small amount of residual hemicellulose (Sjöström 1993.). Hence, the major functional groups that are largely available for the covalent conjugation (chemisorption) of antibodies are hydroxyls. The hydroxyl groups are difficult to utilize in covalent conjugation reactions in an aqueous environment due to the cross-reactions of activation chemicals with water. Moreover, non-aqueous hydroxyl reactive chemistries are toxic, and solvent exchange is needed to remove

the residual substances. Therefore, the direct adsorption is the only realistic approach to bind antibodies to native cellulosic materials in an aqueous solution. However, cellulosic surfaces can be modified to introduce new functional groups on the cellulosic fiber surfaces (Klemm, Philipp & Heinze 1998). Given functional groups can then be utilized in the covalent linking of antibodies to cellulose even in water. Normally, chemical conjugation leads to random orientation of antibodies, where their biological activity to bind antigenic determinants is reduced. Therefore, immobilization strategies to secure oriented binding of antibodies on solid have been developed. In the following chapter, the most common immobilization strategies are discussed.

2.3.1 Protein adsorption on cellulosic materials

Direct adsorption is the easiest route to immobilize proteins onto solid surfaces. However, the protein adsorption does not allow any orientation of the active sites of a protein to the liquid medium, hence, causing a randomly oriented immobilization. The adsorption process on solid surfaces is always complex due to the presence of various interactions such as dehydration forces, Van der Waals forces, electrostatic (overlap of electrical double layers), hydrophobic, and hydrogen bonding (Norde 1996)(Nakanishi, Sakiyama & Imamura 2001). Therefore, many proteins adsorb irreversibly on several different types of surfaces. After the initial binding step, proteins typically go through a structural rearrangement (Figure 11), where the hydrophobic amino acids can interact with the surface causing permanent docking (Haynes, Norde 1994). Hence, it is difficult to predict exactly how a protein adsorption phenomenon takes place. However, some general rules for adsorbing globular proteins on a solid surface have been observed. It has been reported that many proteins adsorb more on hydrophobic surfaces than on hydrophilic surfaces due to the presence of hydrophobic forces (Prime, Whitesides 1991)(Lee, Kim 1974). On the other hand, the protein adsorption on hydrophilic surfaces takes place only if the electrostatic interactions are present, due to the lack of dehydration forces, then the adsorption is irreversible only if proteins go through a structural rearrangement (Arai, Norde 1990)(Norde 1996)(Prime, Whitesides 1993). The protein´s “softness” is an important factor indicating how easily structural rearrangements of a protein can take place. The structure of a soft protein does not prevent structural deformations, and thus adsorption is largely irreversible. Globular proteins, including blood serum proteins, are classified to belong into the group of hard proteins, meaning that they have only a limited ability to make structural arrangements. Structural rearrangements have also found to be related to biochemical

activity of proteins. Adsorbed proteins that have gone through remarkable structural arrangements are to lose their biochemical activities (Norde, Zoungrana 1998)(Sethuraman, Belfort 2005). On the other hand, at least a part of biochemical activity is present when hard proteins are adhered to surfaces.

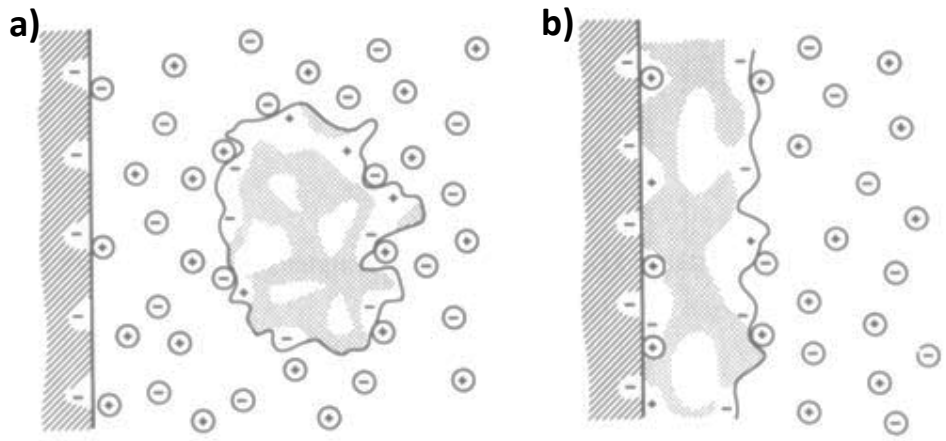

Figure 11. Schematic representation of a protein molecule and a sorbent surface before (a) and after adsorption (b). Shaded areas represent hydrophobic regions. (Adapted from (Norde 1996)).

Surfaces of cellulosic materials always have a hydrophilic nature due to the presence of polar hydroxyl groups, which can contribute to hydrogen bonding with proteins or the binding of water to the surface. Cellulosic surfaces are typically far from the smoothness and flatness of metallic or synthetic polymer surfaces. The knowledge of protein adsorption on cellulosic materials have largely been achieved with regenerated cellulosic materials in chromatographic applications (Hage 1999). It has been observed earlier that increased anionic surface charge increases the adsorption of cationically charged proteins on cellulose, but in that case the adsorption was irreversible to a large extent (Peterson, Sober 1956). Recently, on-line adsorption measurement tools have been utilized in the analysis of adsorption where the heterogeneity of the cellulosic materials can be taken into account. However, those analyses have intensively focused on the analysis of the adsorption of cellulose specific enzymes on cellulosic surfaces (Turon, Rojas & Deinhammer 2008)(Ahola et al. 2008c)(Saarinen et al. 2009). Detailed analysis of the adsorption of immunoglobulins and other serum proteins on natural cellulose has not earlier been reported.

2.3.2 Chemical conjugation of antibodies on cellulose

Covalent linking reactions take place through the nucleophilic and electrophilic groups that can contribute to the formation of covalent bonds. A nucleophile is any atom that contains an unshared pair of electrons or an excess of electrons available to donate an electron pair to an electrophile (Ritchie 1972). The relative order of the nucleophilicity of the major groups in biological materials can be summarizes as follows: $R\text{-}S^- > R\text{-}NH_2 > R\text{-}COO^- = R\text{-}O^- >> \text{-}OH$ (Hermanson 2008). The external surfaces of cellulosic materials contain a significant amount of hydroxyl groups, which can be exploited as conjugation sites for the immobilization of proteins. On the other hand, amine groups are abundant functional groups in the exterior areas of proteins (Bordo, Argos 1991). The covalent conjugation of proteins to cellulose through the hydroxyl groups can be carried out using various chemistries such as carbonyldiimidazole (CDI) (Stöllner, Scheller & Warsinke 2002), epoxide (Uy, Wold 1977), and periodate oxidation (Van Leemputies, Horisberger 1974). However, these hydroxyl reactive chemistries always need at least one activation step in a non-polar solvent. The use of carboxyl reactive chemistries on the covalent immobilization of proteins and other molecules to cellulose has been demonstrated in the literature (Arola et al. 2012, Filpponen, Argyropoulos 2010). Covalent bonding through the carboxyl group does not take place spontaneously in water, due to the low nucleophilicity of carboxyls in water (Hermanson 2008). Therefore, an activator is needed to achieve bond formation. The most used linker chemistries to achieve bond formation through the carboxyl group are CDI (Fernandez-Lafuente et al. 1993) and 1-ethyl-3-(3-dimethylaminopropyl)carbodiimide (EDC) (Grabarek, Gergely 1990). However, only EDC is a water soluble activator, and hence it has been widely utilized on the conjugation of proteins. EDC reacts with a carboxyl anion forming an active *O*-acylisourea intermediate that is easily displaced by a nucleophilic attack by the amine containing molecule (Figure 12). The *O*-acylisourea intermediate is unstable in aqueous solutions, and therefore, if the intermediate does not react in seconds with amine containing molecules, the N-unsubstituted urea will be released into the medium (Nakajima, Ikada 1995)(Gilles, Hudson & Borders Jr. 1990). This hydrolysis failure can be prevented by adding N-hydroxyl succinimide (NHS) in the reaction mixture, which stabilizes the amine-reactive intermediate by converting it to an amine-reactive NHS-ester intermediate (Staros, Wright & Swingle 1986). This amine reactive NHS-ester intermediate is semi-stable in water, and the yield of amide bond formation is significantly increased. In this work the EDC/NHS chemistry was employed to link proteins to cellulose.

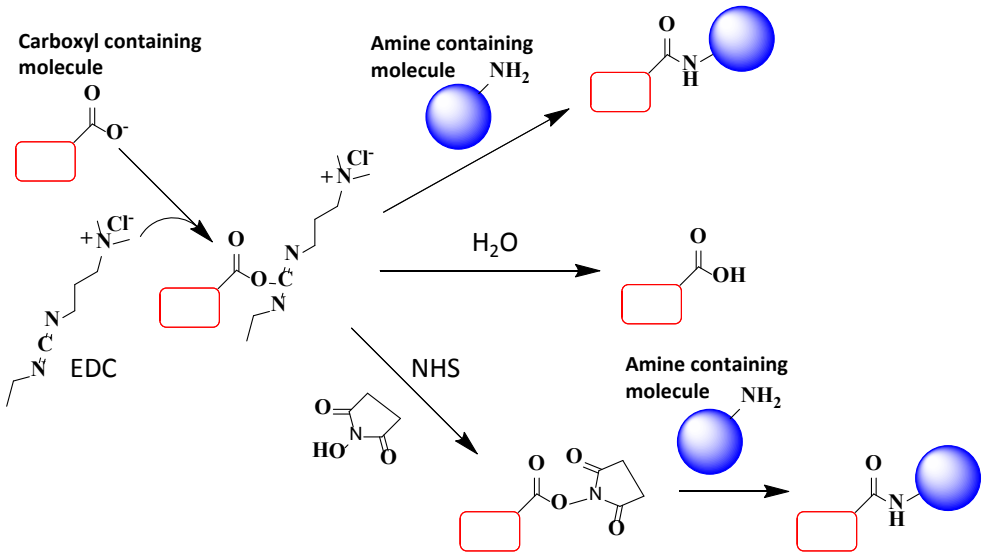

Figure 12. Reaction scheme for covalent conjugation of a carboxylate containing molecule with an amine containing molecule via EDC/NHS activation. Alternative reaction pathways are also represented in this illustration.

Chemical conjugation reactions do not orient the proteins´ conformation at support surfaces, but they form a random orientation of antibodies, where the antibodies FAB-fragments ability to bind antigenic determinants is reduced (Rao, Anderson & Bachas 1998). The conformation of conjugated proteins can be controlled using several different chemistries such as immobilization of liberated FAB-fragments via sulfuric bonds (Lu et al. 1995), immobilization with carboxypeptidase through carboxyl residues at a C-termini of antibodies (You, Lin & Lowe 1995), immobilization with protein-A (Gersten, Marchalonis 1978), conjugation with Avidin (Guesdon, Ternynck & Avrameas 1979), and immobilization through the oxidized carbohydrate moieties of antibodies (O'Shannessy, Hoffman 1987). In this study we have employed the avidin-biotin linkage method to orient the conformation of proteins on cellulose. Avidin is a quaternary biotin binding protein that has been utilized to orient immobilization of various biotinylated antibodies on solid surfaces (Rusmini, Zhong & Feijen 2007)(Green 1975)(Pei, Yang & Wang 2001). Avidin has a disadvantage to bind non-specifically also other molecules than biotin through its polysaccharide regions and cationic charge (Hiller et al. 1987). It has been demonstrated that the specificity of avidin can be enhanced by deglycosylation chemistries, which do not influence the biotin binding properties of avidin (Bayer et al. 1995). Moreover, several avidin modifications have been introduced in the literature such as reversible avidins (Laitinen et al. 2003)(Wu, Wong 2005)(Aslan et al. 2005), bifunctional avidins with two different bio-

tin binding pockets (Nordlund et al. 2004)(Riihimaki et al. 2011), bifunctional avidin that binds biotin covalently (Leppiniemi et al. 2011), and avidin modification with high thermal stability (denaturation temperature over 90°C) (Nordlund et al. 2003).

2.3.3 Functionalization of cellulosic materials

The aim of the surface functionalization of cellulose is to introduce new functional groups (conjugation sites) on cellulose, which can contribute to covalent conjugation reactions. The cellulosic surface always contains –OH groups (hydroxyls), which enable a possibility to chemically convert hydroxyls groups of the anhydroglucopyranose units to various functional groups using functionalization and grafting chemistries (Klemm et al. 1997)(Roy et al. 2009)(Bhattacharya, Misra 2004). The chemistries most used for functionalization of native cellulose are carboxymethylation, TEMPO-mediated oxidation, and amination. These chemistries are not surface sensitive, and due to the chemicals penetration through the cell wall of wood fibers, the substructures of wood fibers are also permanently altered. Carboxymethylation converts the –OH groups of cellulose to carboxymethyl form (Walecka 1956)(Klemm, Philipp & Heinze 1998). A disadvantage of the carboxymethylation treatment is that the carboxymethylation reaction can be carried out only in non-aqueous solvent systems. Therefore, aqueous based 2,2,6,6,-tetramethylpipelidine-1-oxyl radical mediated oxidation (TEMPO-oxidation) has gained more attention (De Nooy, Besemer & Van Bekkum 1995). The TEMPO-radical selectively oxidizes –OH groups of the C6-carbons of cellulose to aldehyde form (Figure 13), which are then subsequently converted to carboxyls by an oxidant (Isogai, Kato 1998). The amination reactions of cellulose can also be carried out in aqueous solution using, e.g., ethylene imine or 2-aminoethyl sulfate (Klemm, Philipp & Heinze 1998). The great disadvantage of amination chemistries is their high toxicity for human DNA and the environment.

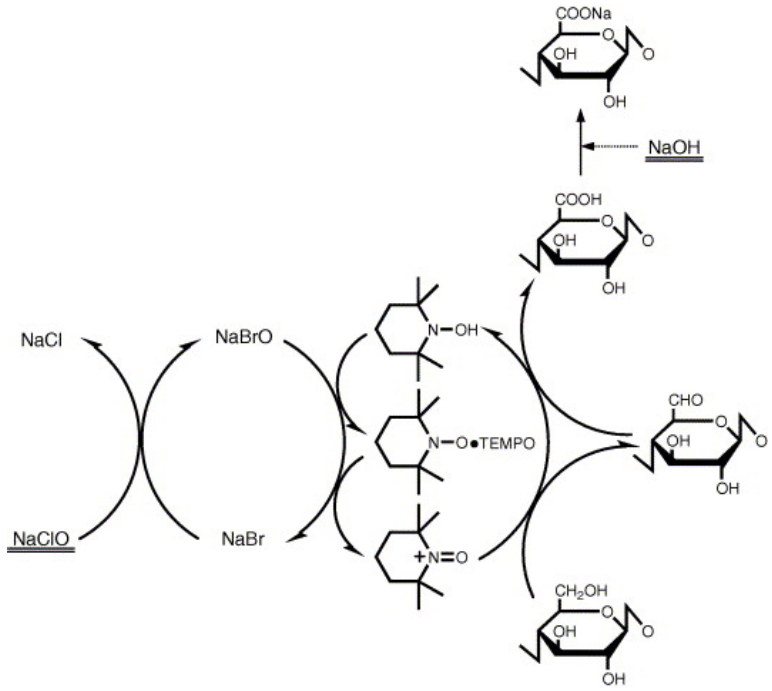

Figure 13. Proposed mechanism of the TEMPO-mediated oxidation of cellulose. (Adapted from (Saito et al. 2006)).

The functionalization of cellulose using polymer adsorption is a non-destructive (soft) method for introducing new conjugation sites on cellulosic materials. The adsorption of polymers can be reversible or irreversible based on the type of bonds formed. Reversible adsorption takes place when bonding takes place through electrostatic interactions only. On the other hand, non-electrostatic interactions lead to irreversible adsorption of polymers. Cationic polyelectrolytes have found to adsorb on negatively charged cellulosic materials, but in that case the adsorption is largely reversible (Wågberg 2000)(Lindstrom, Wågberg 1983). The adsorption of polyelectrolytes is controlled by numerous factors such as ionic strength, charge density, molecular weight, and medium. Moreover, cationic polyelectrolytes do not normally contain suitable conjugation sites to anchor materials for covalent conjugation.

Various polysaccharides, including water soluble hemicelluloses and cellulose derivatives, have a natural affinity to adsorb irreversibly on cellulose (Ishimaru, Lindström 1984). The mechanisms behind this non-ionic attachment have been partly unraveled, but it has been proposed that the cellulose-like backbone is the most dominant factor when polysaccharides adhere to cellulose (Mishima et al. 1998). The adsorption of cellulose-like

ionic polysaccharides, such as CMC and chitosan (Figure 14), on cellulosic materials has been demonstrated in the literature (Laine et al. 2000)(Nordgren et al. 2009)(Myllytie, Salmi & Laine 2009). These polysaccharides carry suitable functional groups that can be utilized in covalent conjugation of proteins to cellulose. Chitosan is a water soluble ionic polysaccharide that carries amine groups. Amine groups are protonated at acidic pH which promotes chitosan solubility in water (Majeti N.V 2000). The cationic nature of chitosan leads to its binding to cellulose in an extended conformation, and the adsorption has been speculated to be driven by combinations of electrostatic and non-electrostatic interactions (Myllytie, Salmi & Laine 2009). Anionically charged carboxymethyl cellulose (CMC) has also been found to adsorb on cellulose instead of the expected electrostatic repulsion towards cellulose. However, an electrolyte is needed to diminish the repulsive electrostatic interactions, allowing CMC to adhere irreversibly on cellulose. Several factors such as pH, ionic strength, temperature, concentration, and molecular weight, have been found to influence the adsorption of CMC on cellulose (Kästner et al. 1997)(Laine et al. 2000). In general, the molecular weight and DS of CMC and the ionic strength of the solution are the dominating factors for the CMC adsorption. In this work, chitosan and CMC were utilized in the functionalization of cellulosic surfaces for subsequent covalent conjugations of antibodies to cellulose. The polysaccharides used are commercial products, non-toxic, and widely used in various applications, properties that are beneficial where low toxic immunoassays concepts are concerned.

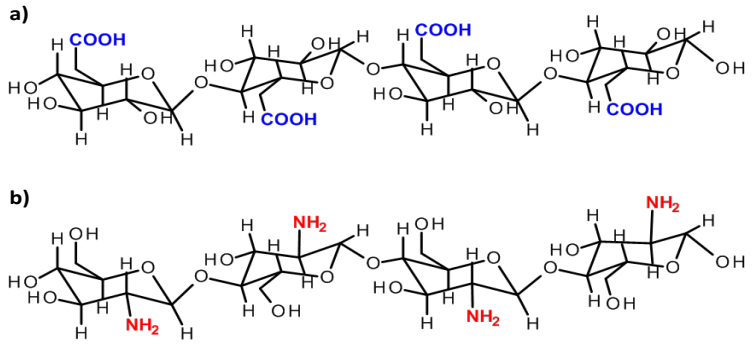

Figure 14. Structures of carboxymethyl cellulose (CMC) (a) and deacetylated chitosan (b).

3 Experimental

The materials and methods used in the experiments included in this thesis are described in detail in the attached Papers I-IV. The main cellulosic materials, proteins, and antibodies used in this work are presented in the Materials section. The main characterization methods used in this work are discussed in the Methods section. This chapter provides a general background for the experiments presented in the Results and Discussion.

3.1 Materials

3.1.1 Cellulose model surfaces and NFC-films

Trimethylsilyl cellulose (TMSC), used in Papers I-III, was prepared by silylation of microcrystalline cellulose powder from spruce with hexamethyl disilazane according to Cooper, Sandberg & Hinck (1981) and Greber, Paschinger (1981). The detailed description of the synthesis of TMSC that was used in this work has been presented by Tammelin et al. (2006). The conversion of TMSC to cellulose form by desilylation was carried out according to Schaub et al. (1993), and performed following the procedure presented by Kontturi, Thune & Niemantsverdriet (2003). In papers I and II, TMSC was deposited on gold covered QCM-D (Q-Sense AB, Sweden) and SPR (paper I, Bionavis Oy, Finland and Paper II, GE Healthcare, Sweden) wafers using a polystyrene anchor layer. Langmuir-Schaefer (LS) deposition was carried out according to the procedure represented by Tammelin et al. (2006). In paper III, TMSC was spin-coated on silica covered QCM-D crystals (Q-Sense AB, Sweden) with a WS-650SX-6NPP spin coater (Laurell Technologies, USA) following a procedure presented by Kontturi, Thune & Niemantsverdriet (2003). An area per charge of 460 nm^2 for TMSC-based cellulose surfaces has been reported (Österberg 2000).

The nanofibrillar cellulose surfaces that were used in Papers III and IV were prepared from unmodified hardwood (birch) pulp. The carbohydrate composition of the pulp used was 73 % glucose, 26 % xylan and 1 % mannose (Eronen et al. 2011b). The charge of the pulp used was 65 µeq/g (Eronen et al 2011a). The hardwood pulp was first washed into sodium form according to Swerin, Ödberg & lindström (1990), and subsequently extensively fluidized by a Microfluidics M-110 (Microfluidics Intl. Corp, Newton, MA, USA). A more detailed description of the fluidization process and conditions can be found in Tai-

pale et al. (2010). The NFC-model cellulose films were prepared on silica covered QCM-D crystals (Q-Sense AB, Sweden) according to Ahola et al. (2008b). The bundles of NFC were first removed with mechanical stirring with an ultrasonic microtip for 10 min with a 25 % amplitude setting, and then centrifuged at 10400 rpm for 45 min. The supernatant, individualized cellulose nanofibrils, of the centrifuged NFC-solution was spin-coated on silica covered QCM-D crystals with a WS-650SX-6NPP spin-coater (Laurell Technologies, USA).

The unmodified NFC-gel, prepared as described above, was used to cast NFC-films (Paper IV) without any pretreatment steps. The NFC-gel was filtered onto a 20 μm polyamide filter membrane using 2.5 bar pressure to remove the excess water. The deposited films were rolled five times with a smooth metal rolling pin to tighten the structure of the film. The casted NFC-films were dried between clean plotting boards under external pressing. The thickness of the films was approximately 150 μm.

3.1.2 Antibodies and other proteins

Protein adsorption on cellulose (Paper I) was analysed using polyclonal human immunoglobulin G (human IgG) and bovine serum albumin (BSA) obtained from Sigma-Aldrich (USA). The conjugation of antibodies on CMC modified cellulose in Paper II was analysed using monoclonal anti-hemoglobin IgG obtained from Medix Biochemica (Finland). The conjugation of proteins on cellulose in oriented fashion (Paper III) was investigated using avidin, neutravidin, and biotinylated bovine serum albumin (biotin-BSA) ordered from Pierce (Rockland, IL, USA). Biotinylated anti-human IgG was obtained from Sigma-Aldrich (USA). The attachment of antibodies on NFC-films (Paper IV) was analyzed using anti-human immunoglobulin G antibody (anti-hIgG) and human immunoglobulin G (hIgG) obtained from Sigma-Aldrich (Finland). The fluorescence staining of antibodies were carried out with dansyl chloride and fluorescein isothiocyanate (FITC). The detailed description of staining procedures is presented in Paper IV. The attachment of anti-human IgG on activate NFC-films was carried out using a commercial EPSON R800 piezoelectric inkjet printer with a CD-printing tray without any modifications. The clean inkjet cartridges were obtained from MIS associates, USA. All antibodies and proteins used in this thesis were used without any purification steps.

All other chemicals used in Papers I-IV were analytical grade if not otherwise specified, and used without any purification steps. All water used was deionized and further purified

with a Millipore Synergy UV unit (MilliQ-water). All buffer solutions were prepared from analytical grade laboratory chemicals using MilliQ-water.

3.1.3 Polysaccharides and chemicals for surface functionalization

The functionalization of cellulose surfaces in Papers I and III was carried out using carboxymethyl cellulose (CMC, Mw 250 000, DS 0.7) ordered from Sigma-Aldrich (Finland). In paper II, carboxymethyl cellulose (CMC, Finnfix WRM, Mw 250 000, DS 0.6) was obtained from CP Kelco. All CMC used in this thesis was first dissolved in MilliQ water and purified with 12 – 14 kDa spectrapor dialysis membrane tubes (Spectrumlabs, CA, USA). The dialyzed CMC was dried to solid form using freeze drying. In Paper I cellulose modification was also carried out using chitosan (Mw 50 000 – 190 000, deacetylation degree 75 – 85 %) obtained from Sigma-Aldrich (USA), and was used without any purification steps. The adsorption of aqueous solutions of CMC and chitosan on cellulose was carried out using salt-containing buffer solutions. After surface modifications, all surfaces were rinsed with an appropriate buffer solution to remove loosely adsorbed polysaccharides. In Papers II and IV, the alkaline TEMPO-mediated oxidation was utilized to introduce carboxyl groups on the NFC-films. The TEMPO-oxidation was performed using mixture of 0.13 mmol 2,2,6,6,-tetramethylpipelidine-1-oxyl radical (TEMPO), 4.7 mmol NaBr, and 5.65 mmol NaClO at pH 10 according to (Isogai, Kato 1998). The oxidation reaction was stopped by both ethanol addition and MilliQ-water rinsing.

3.1.4 Conjugation chemicals

The covalent conjugation of proteins on surface modified cellulose surfaces was carried out in Papers II – IV using EDC/NHS conjugation chemistry. The CMC modified cellulose surfaces (Papers II and III) and TEMPO-oxidized NFC-films (Paper IV) were treated with a mixed solution of 0.1 M 1-ethyl-3-[3-dimethylaminopropyl]carbodiimide hydrochloride (EDC) and 0.4 M N-hydroxysuccinimide (NHS) obtained from Sigma-Aldrich (Finland). After EDC/NHS treatment the surfaces were rinsed with an aqueous buffer solution to prevent self-crosslinking of the conjugated protein. The conjugated antibodies and (neutr)avidin were adsorbed on NHS-ester-cellulose surfaces from the appropriate aqueous buffer solution. The unused NHS-esters were removed by ethanolamine (Sigma-Aldrich, USA) treatment, and in papers II, III, and IV the non-specific protein binding was

blocked using S*uperblock* blocking agent obtained from Pierce (Rockland, IL, USA). *Superblock* is a protein solution that fills the free spaces between the antibodies thus preventing the non-specific binding of antigens on the surface of a biointerface. More detailed description of the conjugation conditions and activation times are described in Papers II-IV.

3.2 Methods

The main experimental methods used in this thesis were QCM-D, SPR, AFM, and XPS. The main studies were carried out using cellulose model surfaces prepared with the Langmuir-Schaefer technique or the spin coating technique. The detailed principles of these methods are described here. Details of other methods are presented in Papers I–IV and references presented here.

3.2.1 Model cellulose film preparation techniques

Langmuir-Schaefer deposition (LS) was used to deposit regenerated cellulose II surfaces on QCM-D and SPR wafers (Papers I and II). The fundamental studies of the properties of a water insoluble monolayer at a water-air interface were carried out by Langmuir (1917). A water insoluble material is spread on a water surface, and by using external barriers, an evenly spread monolayer can be produced. The transferring of a monolayer from a water-air interface onto a solid substrate was first demonstrated by Blodgett (1935), but there, the transferring of monolayer layers was carried out by sinking the substrate in a bath, causing deposition on both sides of a substrate. Later, the horizontal dipping procedure, Langmuir-Schaefer deposition (LS), was developed to attach monolayers selectively only one surface of a substrate (Langmuir, Schaefer 1938). This LS-deposition method was used in this thesis. Trimethylsilyl cellulose dissolved in chloroform was added to a water surface (Figure 15), which after evaporation creates a uniform TMSC-layer. The properties of the TMSC-monolayer were controlled by keeping the surface pressure of the bath constant at 15 mN/m during the dipping cycles. The hydrophobic TMSC was transferred onto polystyrene covered QCM-D and SPR wafers. Theoretically, a bilayer of TMSC is transferred on each dipping cycle. The uniformity of the TMSC-layer on the wafer was insured by dipping 30 TMSC-monolayers onto each wafer surface. The TMSC on a wafer was con-

verted to cellulose form using an HCl-vapor treatment according to Kontturi, Thune & Niemantsverdriet (2003). The description of preparation of cellulose model surfaces using the LS-method has been presented in detail in Tammelin et al. (2006).

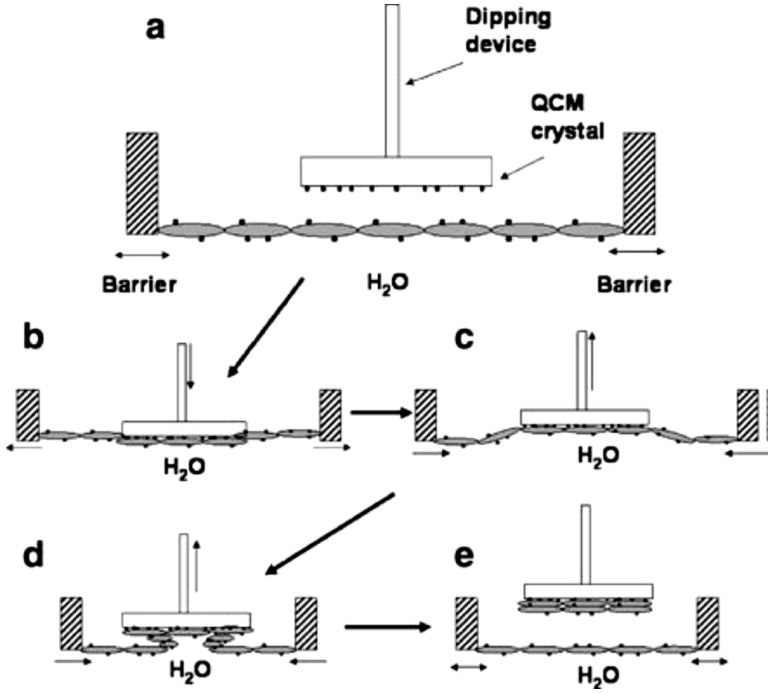

Figure 15. Schematic representation of Langmuir-Schaefer deposition to transfer a TMSC-layer onto a hydrophobic surface. The horizontal arrows indicate the movement of the barriers. The grey ovals represent TMSC molecules, and the black spots represent the hydrophobic part of TMSC and a solid surface. (Adapted from (Tammelin et al. 2006)).

The spin-coating technique was employed in this work to prepare ultrathin cellulose II and NFC-cellulose surfaces on QCM-D crystal surfaces. The spin-coating technique is based on the spread of dissolved or dispersed materials in volatile solvents on solid surfaces by high speed spinning (Figure 16). The properties of the ultra-thin films are controlled by several parameters e.g. spinning acceleration, spinning speed, solvent properties, and concentration of the liquid (Hall, Underhill & Torkelson 1998). In the spin-coating technique used to prepared regenerated cellulose II model surfaces (Paper III), TMSC was first dissolved in toluene and applied on a silica covered QCM-D crystal. The solvent was then evaporated by spinning the crystal with a spinning speed of 3000 rpm according to Kontturi, Thune & Niemantsverdriet (2003). The TMSC layer on the crystal surface was then converted to cellulose form with an HCl-vapor treatment. In Paper IV the spin-coating technique was utilized for preparing nanofibrillar cellulose (NFC) model surfaces.

The finest fraction of a centrifuged aqueous NFC solution (supernatant) was spin-coated onto PEI-coated QCM-D crystals with a spinning speed of 3000 rpm. The attachment of cellulose nanofibrils to the PEI-coated crystals was secured by placing the crystals into an oven with a temperature of 80 °C for 30 min. The preparation of NFC-model surfaces on PEI-coated QCM-D crystals is presented in detail in Ahola et al. (2008b).

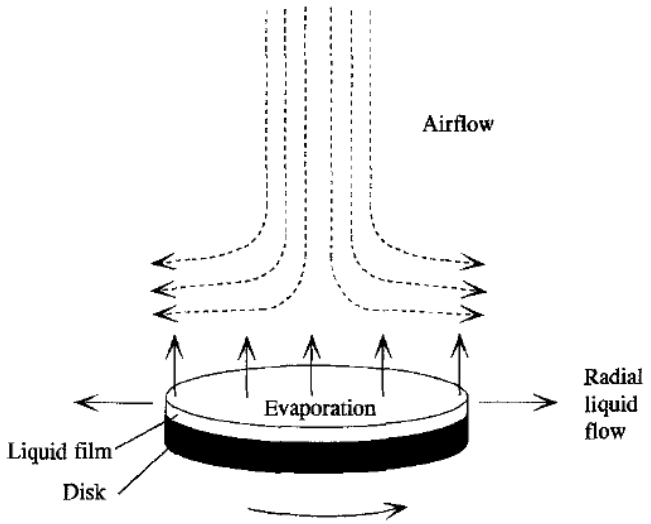

Figure 16. Schematic representation of spin-coating an ultra-thin material layer onto a solid substrate. (Adapted from (Van Hardeveld et al. 1995).

3.2.2 Surface Plasmon Resonance (SPR)

The surface plasmon resonance (SPR) technique was employed to analyze adsorption and conjugation of proteins and polysaccharides on cellulose. The SPR method is an optical technique that has gained a lot of attention in surface and drug research. The SPR technique is based on a physical phenomenon called surface plasmon resonance (SPR) (Schasfoort, Tudos & Gedig 2008). The SPR phenomenon was observed for the first time by Wood (1902), but the complete explanation of the observed phenomenon was only presented over six decades later by Kretchmann and Reather (1968). The SPR phenomenon takes place when a thin semitransparent metal film (typical gold or silver) is placed on a prism, and a monochromatic p-polarized light beam is directed to pass the prism. When the beam is reflected off from the metal film under conditions of total internal reflection (Figure 17), the photons of a light beam interact with free electrons (plasmons) of the met-

al film causing a surface plasmon resonance wave (SPR-wave) propagating through the metal film. This coupling between the photons and the plasmons consumes energy that can be observed as a dip on the intensity of the reflected light. The angle when the dip in intensity is observed is referred to as the SPR-angle. The SPR-wave can penetrate a liquid medium above the metal film about 200 nm before it decays. The SPR-angle is highly sensitive to any changes in the refractive index (RI) on the sensor surface. Therefore, it can be utilized in the analysis of adsorption of molecules on the sensor surface. More information of this method can be found in detail in the review articles of Pattnaik (2005) and Homola, Yee & Gauglitz (1999).

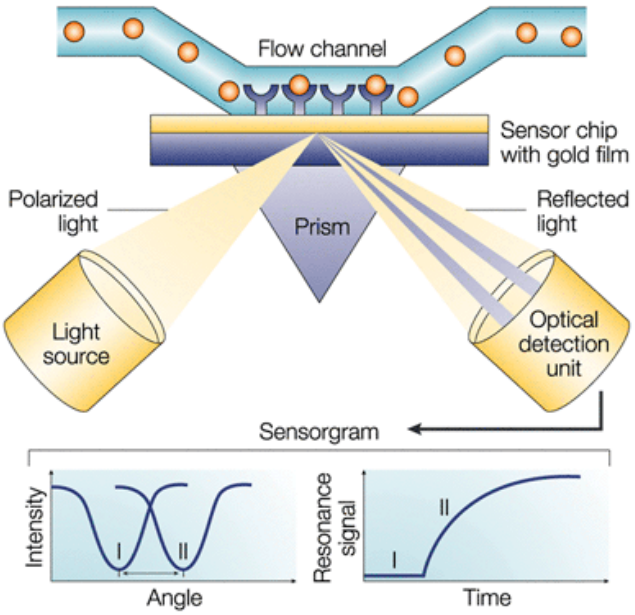

Figure 17. Schematic representation of the working principle of the surface plasmon resonance technique used in this work. The adsorbed molecules on the gold surface alter the refractive index of the surface, which is sensed as a change of SPR-angle. (Adapted from (Cooper 2002)).

The surface coverage of adsorbed molecules, $\Delta m_{SPR,}$ is linearly proportional to a change in the resonance units (1000 RU corresponds to angle change of 0.1 °) according to the equation 3.1.

$$\Delta m_{SPR} = C_{SPR} \Delta RU \qquad (3.1),$$

where C_{SPR} is the proportion constant for the adsorbed molecules, and ΔRU is a change in resonance units. For most proteins, the approximation of 1 RU corresponding to 0.1

ng/mm² can be used (Stenberg et al. 1991). For polysaccharides, only a limited number of proportion constants have been presented in the literature. However, another model for the estimation of surface coverage on the sensor surface has been presented by Jung et al. (1998). The surface coverage can be calculated by first calculating the thickness of the adsorbed layer, d, according to equation 3.2.

$$d = \frac{l_d}{2} \frac{\Delta_{SPR}}{m(n_a - n_0)} \quad (3.2),$$

where l_d is a characteristic evanescent electromagnetic field decay length and can be estimated to be 0.37 of the wavelength of the laser, Δ_{SPR} is a change in the SPR angle, m is a sensitivity factor for the sensor obtained by calibrating the SPR, n_o is the refractive index of the bulk medium (1.334 RIU for buffers), and n_a is the refractive index of the adsorbed molecules. Then, the surface coverage, Δm_{SPR}, can easily be calculated according to the equation 3.3.

$$\Delta m_{SPR} = d * \rho \quad (3.3),$$

where d is the thickness of the adsorbed layer (calculated by equation (3.2)), and ρ is the specific volume of the adsorbed molecules. The refractive indices and the specific volumes for various substances can be found in the literature.

The SPR measurements were carried out with a SPR Model Navi 200 (Oy BioNavis Ltd, Finland) in Paper I, and a Biacore 1000 instrument (GE Healthcare, Sweden) in paper II. Before experiments, the cellulose model films were stabilized by driving a buffer solution through the measurement chambers until a stable baseline was acquired. All experiments were duplicated at least once to get accurate results. A mass sensitivity of a SPR used in this work was 0.15 mdeg that corresponds to a mass change of 0.1 ng/cm².The details of the experiments and the modeling parameters with the equations used can be found in the Papers I and II.

3.2.3 Quartz Crystal Microbalance with Dissipation (QCM-D)

The QCM-D technique was used to characterize adsorption of proteins and polysaccharides on cellulose model surfaces. This method is widely used in surface research because of its unique property to follow mass adsorption on solid surfaces while simultaneously obtained information on the viscoelastic properties of the adsorbed layer. The QCM-D uses an oscillating quartz crystal, on which changes in frequency and dissipation are

measured (Figure 18). The changes in frequency of an oscillating crystal are the result of both increased mass adsorption on the sensor surface and increased coupling of the liquid medium to the adsorbed layer, whereas the energy dissipation of the sensor surface is caused by frictional losses in the adsorbed layer. The principles of this method are described in detail by Rodahl et al. (1995).

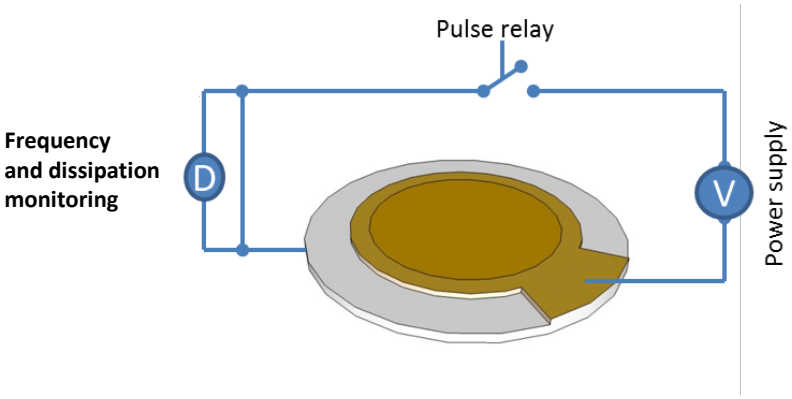

Figure 18. Operating principle of the QCM-D crystal.

The adsorbed mass per unit surface (*Δm),* for rigid adsorption layers, is proportional to the frequency change according to the Sauerbrey´s equation (3.4) (Sauerbrey 1959)(Höök et al. 1998).

$$\Delta m = -\frac{C\Delta f}{n} \qquad (3.4),$$

where *C* is the device sensitivity constant (*17.7 ng Hz*$^{-1}$ *cm*$^{-2}$ for a *5 MHz* quartz crystal), and *n* is the overtone number. This equation is only valid if the adsorbed layer is evenly distributed on the sensor surface and the adsorbed mass is small compared to mass of the crystal.

Often the adsorbed layer exhibits viscoelastic properties, and then equation 3.4 underestimates the adsorbed mass. The viscoelastic properties of the adsorbed layer in QCM-D are analyzed by the energy dissipation (*D*). The dissipation is measured in a QCM-D by cutting the driving voltage of the crystal, and recording the decaying of the amplitude as a function of time. Viscoelastic adsorption layers have higher energy dissipation due to frictional losses compared to rigid adsorption layers, observed as shorter damping times. The dissipation factor of the oscillating system is defined by

$$D = \frac{E_{diss}}{2\pi E_{stored}} \qquad (3.5),$$

where E_{diss} is the energy dissipated during one oscillation cycle, and E_{stored} is the total energy stored in the oscillating system. The principles of dissipation measurements in QCM-D have been described in detail by Höök et al. (1998).

For estimating the true sensed mass of a viscoelastic adsorption layer Johansmann´s model can be used (Johannsmann et al. 1992). This model is an extension of Sauerbrey´s model where the viscoelastic coefficients are included. This model is represented by equation 3.6.

$$\delta\hat{f} \approx -f_0 \frac{1}{\pi\sqrt{\rho_q \mu_q}}\left(f\rho d + \hat{J}(f)\frac{f^3\rho^3 d^3}{3}\right) \quad (3.6),$$

where δf is a shift in the frequency, f_o is the fundamental frequency of the crystal in air, f is the resonance frequency in contact with liquid media, d is the thickness of the film, $\hat{J}(f)$ is the shear compliance, and ρ is the density of the fluid. ρ_q and μ_q are the density and the shear modulus of quartz. If the equivalent mass, m^*, is introduced into this equation, a more convenient form of this equation is cast (equation 3.7).

$$\hat{m}^* = -\frac{\sqrt{\rho_q \mu_q}}{2f_0}\frac{\delta\hat{f}}{f} \quad (3.7),$$

where one thus obtains

$$\hat{m}^* = m_0\left(1 + \hat{J}(f)\frac{f^2\rho d^2}{3}\right) \quad (3.8).$$

The true sensed mass, m_o, in this equation can be calculated under the assumption that the $\hat{J}(f)$ is independent of the frequency in the accessible frequency range. Then, the true sensed mass (equation 3.8) can be obtained as the intercept of the equivalent mass plotted against the square of the resonance frequency (f^2).

The Voight-model (parallel spring and damper) is also applied in this thesis to estimate adsorbed masses for viscous adsorption layers ($\Delta D>0$). This iterative model uses both the change in the frequency (Δf) and the change in the dissipation (ΔD) data in the calculations. The calculations were carried out in a Q-tools data analysis program. The principles of this model are described in detail by M. V. Voinova (1999). The fitting parameters of this model are presented in Paper I.

The QCM-D experiments were carried out using a QCM-D E4 instrument (Q-Sense AB, Sweden). A mass sensitivity of a QCM-D used in this work was 0.1 Hz that corresponds to a mass change of 1.8 ng/cm^2. Constant fluid flow of 0.1 ml/min through the measurement chamber was used. Before experiments, the cellulose model films were stabilized by driv-

ing a buffer solution through the measurement chamber until a stable baseline was acquired. The changes in frequency and dissipation were followed as a function of time at the 5 MHz fundamental frequency and its 7 overtones. The details of the experiments, the modeling parameters, and equations used are presented in detail in Papers I-IV.

3.2.4 Atomic Force Microscopy imaging (AFM)

The AFM imaging technique was used in this thesis to characterize topographical and morphological changes on the cellulose surfaces and the NFC-films. Nowadays, the AFM technique is one of the most used techniques in surface science since it allows the surface characterization at nanoscale (Binnig, Quate & Gerber 1986). This Nobel prize winning method is based on a sharp tip (radius of curvature 5-10 nm) that is attached to oscillating cantilever (Figure 19). The tip scans the exterior surface of a sample, and the movements of the tip are monitored with a laser beam and a photodiode. The data of the movements are then used to produce a three dimensional map of the analyzed surface. In AFM, there are three different imaging modes used — contact, non-contact, and tapping mode, but only tapping mode is applicable for the characterization of soft materials such as cellulose, due to the smaller risk of surface damage caused by the tip (Magonov, Elings & Whangbo 1997). In this work, tapping imaging mode was applied to the surface characterization, and therefore only it is discussed here. In tapping mode, the tip is oscillating with a constant oscillation frequency, and the changes in amplitude are monitored. When the tip scans the sample surface, the oscillation frequency is kept constant by vertical movements of the cantilever, which is used to produce a three dimensional height image. The hard surfaces cause only a small or negligible change in amplitude, whereas soft and sticky surfaces reduce the amplitude of the oscillating tip significantly. This amplitude change can be used to produce a three dimensional hardness map of the sample surface. The principles of the AFM imaging techniques can be found in detail in reports of (Rugar, Hansma 1990)(Meyer 1992).

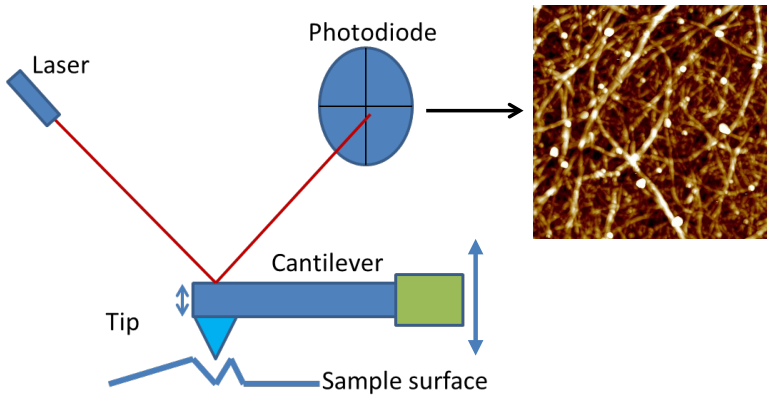

Figure 19. Working principle of the AFM technique. A sharp tip scans the sample surface. The tip movement on the surface is monitored by a laser beam that is directed to top of the cantilever, and the reflected beam is directed to a photodiode. The three dimensional map on the sample surface is obtained by recording the vertical movements of the cantilever.

The AFM experiments were carried out in this work by using a Nanoscope IIIa Multimode scanning probe microscope (Digital Instruments Inc., USA). All images were scanned in tapping mode in air using silicon cantilevers (NSC15/AIBS from MicroMash, Estonia, radius of curvature less than 10 nm, height of the tip approximately 25 nm). The AFM images scan sizes were 1 x 1 μm^2 and 5 x 5 μm^2, and no any image processing was done for the images. The experimental conditions in detail can be found in Papers I-IV.

3.2.5 Additional techniques

X-ray photoelectron spectroscopy (XPS). The changes in chemical composition of the cellulose model surfaces (Papers I-IV) and the NFC-films (Paper IV) were characterized by XPS. In this work, a Kratos analytical AXIS 165 electron spectrometer with a monochromatic Al Kα X-Ray source was used. The XPS experiments were performed on dry samples, together with an in-situ reference sample (S&S 5893 Blue ribbon 6 ashless, 100% cellulose) (Johansson, Campbell 2004), and the spectra were collected normal to the surface. The sampling area was less than one mm in diameter, and several locations on each sample was analyzed. The relative amounts of carbon, oxygen, nitrogen (protein marker), and silicon were determined from C 1s, O 1s, N 1s, and Si 2p signals from low-resolution scans. The high resolution C1s spectrum was curve fitted for further chemical analysis using pa-

rameters defined for cellulosic materials as described by Johansson, Campbell (2004). More information about to the XPS technique can be found in Moulder, Chastain (1992).

Contact angle measurements (CAM). The introduction of carboxyl groups on the NFC-films after TEMPO-mediated oxidation (Paper IV) were analyzed using a contact angle contact angle goniometer CAM 200 (KSV instruments Ltd, Helsinki, Finland). Measurements were performed at room temperature with water as a probe liquid. The droplet volume used was 6.5 µl, and the recording time was 120 sec for measuring the time dependency in changes of the contact angle. Contact angles were measured on three different spots on each sample. More information about to contact angle measurements on solid surfaces can be found in the excellent review paper of Kwok, Neumann (1999).

Conductometric titration. The increase in the charged groups (carboxyls) on the NFC-films after TEMPO-mediated oxidation (Paper IV) was analyzed using a conductometric titrator 751 GPD Titrino (Metrohm AG, Herisau, Switzerland). Dried, acid washed NFC-films (size 2.5 x 2.5 cm2) were disintegrated in MilliQ-water with a blade type homogenizer, the Polytron PT 2000 (Kinematica Inc., NY, USA). The conductometric titration was performed by adding 0.02 ml of 0.1 M NaOH at 30 sec intervals. The calculation of the amount of weak acids (carboxyls) was performed as described in the standard SCAN-CM 65:02.

Confocal laser scanning microscopy (CLSM). Macro scale topography of the NFC-films and printing of fluorescein stained anti-human IgG on the NFC-films was characterized with a Leica TCS SP2 confocal laser scanning microscope (Leica microsystems CMS GmbH, Manheim, Germany. The image was achieved using reflection image and fluorescence modes with 488 nm laser wavelengths, and image sizes of 750 x 750 µm^2. The detection wavelength ranges were 488 ± 10 nm and approximately 490-550 nm. The 3D-image was rendered from the 60 optical sections of the NFC-film using topography mode. No any sample pretreatment was done except placing the sample between two clean microscopy glasses. The roughness profile of the NFC-film was calculated using a rendered topographical 3-D image with the Leica confocal microscope software. Additional information about to CLSM technique can be found in Paddock (1999).

4 Results and discussion

The most important findings of this work are summarized in this chapter. The more detailed results can be found in the attached Papers I-IV.

4.1 Surface functionalization of cellulose

The development of a cellulose based biointerface started by first investigating suitable surface functionalization strategies to introduce conjugation sites on cellulose. These conjugation sites enable the covalent conjugation of antibodies on cellulose under aqueous conditions. The functionalization strategies analyzed were surface carboxylation with CMC adsorption, TEMPO-mediated oxidation, and amination with chitosan adsorption (Figure 20). In this section the cellulose model surfaces with QCM-D and SPR techniques were employed.

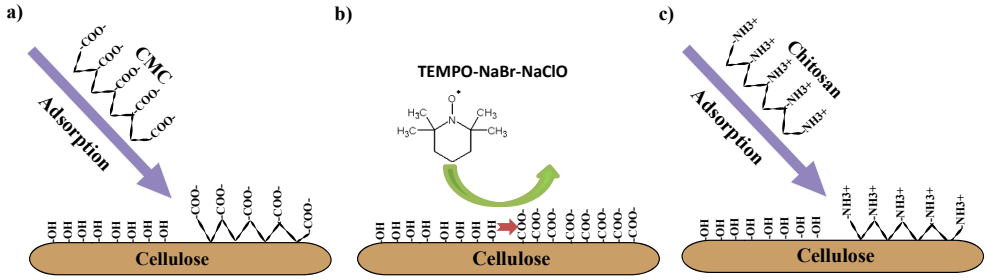

Figure 20. Schematic illustrations of functionalization of cellulose by CMC-adsorption (a), TEMPO-mediated oxidation (b), and chitosan-adsorption (c).

4.1.1 Carboxylation of cellulose by CMC adsorption

Carboxymethyl cellulose (CMC) is a cellulose derivative that contains carboxymethyl substituents. The backbone of CMC is identical with cellulose, which enables an irreversible adsorption of CMC on cellulose in salt containing solutions (Laine et al. 2000). CMC adsorption introduces carboxyl groups on cellulose, which can be utilized in the covalent conjugation of antibodies with EDC/NHS chemistry (Staros, Wright & Swingle 1986).

Moreover, CMC adsorption is a non-destructive method that does not alter the substructure of the cellulosic material. CMC adsorption on wood fiber surfaces has been employed earlier to increase the anionic surface charge of wood fibers for enhancing the strength properties of paper (Heinze, Koschella 2005)(Laine et al. 2000). Moreover, non-toxic CMC has widely been used as an additive in various food and pharmaceutical applications acting as a thickening agent or emulsifier. The adsorption of CMC on cellulose was investigated by QCM-D with regenerated cellulose surface in order to characterize the effect of the adsorption conditions of CMC on the properties of the adsorption layer. Detailed results are presented in Paper II. Figure 21a shows the effect of the salt concentration on the adsorption of CMC on cellulose, where the change in dissipation is plotted against the change in the frequency. The slope of the curve represents the rigidity of the adsorbed layer. A small slope in the ΔD-ΔF curve corresponds to rigid adsorption layer, whereas the steep slope value corresponds to viscoelastic adsorption layer. The adsorption of CMC on cellulose was irreversible in all tested conditions. Without salt, only a small amount of CMC adhered onto cellulose due to the presence of electrostatic repulsions between the CMC and cellulose. The increased salt concentration remarkably enhanced the adsorption of CMC on cellulose, and the adsorbed CMC-layer gained a more coiled surface conformation. The calculated adsorbed masses for 0.2 mg/ml CMC in 0, 10, and 100 mM $CaCl_2$ were 20, 530, and 1100 ng/cm^2 (equation 3.6), respectively. These findings were in good accordance with earlier published results (Liu et al. 2011). The presence of salt in the CMC solution has been showed to lead to a more coiled conformation of CMC due to reduced electrostatic interactions between the charged anhydroglucopyranose units of CMC (Gondo et al. 2006). Moreover, the presence of salt has been demonstrated to diminish the electrostatic repulsion between the cellulosic fibers and CMC that leads to enhanced CMC adsorption on cellulose (Laine et al. 2000). The effect of the concentration of CMC on the adsorption of CMC on cellulose is shown in Figure 21b. The adsorption of CMC on cellulose increased linearly as a function of the CMC concentration. The observed concentration effect is accordance with Fick´s law that states that the increased concentration gradient increases the rate of diffusion that increases CMC´s mass adsorption on the surface (Motchmann, Stamm 1991). The viscoelasticity of the adsorbed CMC layer increased almost linearly as a function of the adsorbed mass. It is known that the adsorbed layer becomes thicker as the polymer concentration increases due to the fact that when the surface becomes occupied with adhering polymer there is less free space for further adsorption, and the conformation of adsorbed polymer becomes more extended (Scheutjens et al. 1980). CMC desorption from the cellulose surface was small, and only slight structural arrangements of the adsorbed layer was observed during the rinsing steps. The calculated adsorbed masses (calculated by equation 3.6) for 0.02, 0.2, and 2 mg/ml CMC in 10 mM

$CaCl_2$ were 474, 500, and 834 ng/cm², respectively. These findings were good accordance with earlier published results (Liu et al. 2011).

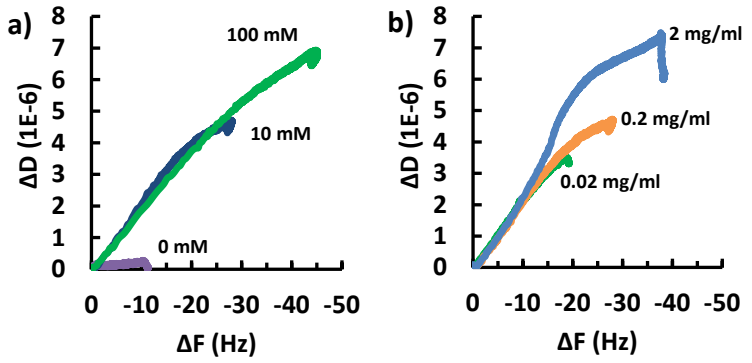

Figure 21. ΔD-ΔF plots of QCM-D for adsorption of (a) 0.2 mg/ml carboxymethyl cellulose (CMC) on cellulose at $CaCl_2$ concentrations of 0, 10, and 100 mM; (b) carboxymethyl cellulose at concentrations of 0.02, 0.2, and 2.0 mg/ml in constant salt, 10 mM $CaCl_2$. (Paper II).

The adsorbed CMC-layer couples water due to the presence of polar substituents, the carboxyls, of CMC. The coupled water of the CMC-layer was analyzed by comparing acoustic QCM-D and optical SPR measurements. The SPR technique measures the "dry mass", whereas the QCM-D technique measures both the dry mass and the coupled water. The adsorption of CMC on cellulose monitored by QCM-D and SPR are shown in Figure 22a. Most of the CMC adsorbed on cellulose in the first minutes as can be seen in the SPR and QCM-D curves. However, the adsorption curve measured in QCM-D, steadily increased as a function of time. This corresponds to conformational changes in the adsorption layer when the cellulose film becomes fully occupied with adhering CMC and there is no enough continues free space for further adsorption (Scheutjens, Fleer 1980). The water content of the adsorbed CMC layer was over 85 %, which demonstrates that the adsorbed CMC-layer on cellulose has hydrogel like properties. The water coupling values are accordance with early published data of Liu et al. (2011) and Ahola et al. (2008a). The topographical changes on the dried cellulose surface after adsorption of CMC were analysed by AFM (Figure 22b and c). Adsorbed CMC is slightly smoother than the substrate cellulose surface, but otherwise the changes were almost invisible. This demonstrates that the adsorbed CMC-layer is thin and evenly distributed on a cellulose surface. The analysed roughness profiles of the adsorbed CMC-layer correspond to findings of Liu et al. (2011).

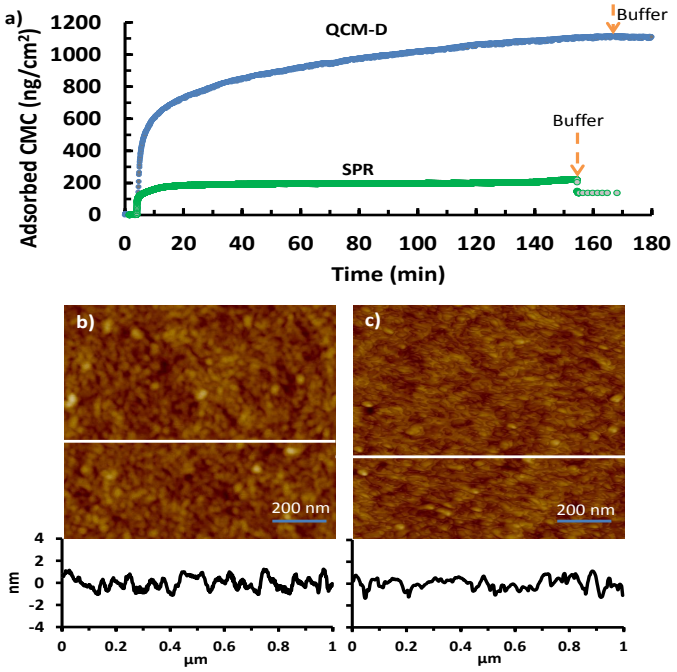

Figure 22. (a) Adsorption of 1 mg/ml carboxymethyl cellulose on cellulose in 100 mM $CaCl_2$ monitored by QCM-D and SPR. The adsorption curves are modeled using equations 3.4 and 3.1. The AFM height images for (b) unmodified and (c) CMC modified cellulose. The Z-range of the images is 10 nm. (Paper II).

4.1.2 Amination of cellulose by chitosan adsorption

All proteins contain both carboxyl and amine groups on their external surfaces. Therefore, amination of cellulose can also be utilized for the covalent conjugation of proteins to cellulose. Chitosan is an antibacterial amine containing polysaccharide that can be prepared by deacetylation of the chitin in the exoskeleton of crustaceans (Majeti N.V 2000). Adsorption of chitosan on cellulose has earlier been verified by Myllytie, Salmi & Laine (2009). Chitosan is soluble in water only at pH values under 7, when the primary amine groups of chitosan are protonated. This is a disadvantage when this polysaccharide is used in surface modifications. Chitosan adsorption on cellulose was analyzed with the QCM-D and SPR techniques. Detailed results are presented in Paper I. Figure 23a shows the irreversible adsorption of chitosan on cellulose in QCM-D. The adsorption kinetics of chitosan was similar to that of CMC. This demonstrates that both these polysaccharides have a sim-

ilar natural affinity to adsorb on cellulose. The adsorption layer of chitosan is rather viscoelastic as can be seen in the change in dissipation value. The frequency change after buffer rinsing corresponded to an adsorbed amount of 440 ng/cm^2. The chitosan modified cellulose surface was then rinsed with MilliQ-water. In those conditions, chitosan is insoluble that causes a drop in the coupled water. The positive change in frequency and negative change in dissipation correspond to layer compression and decrease of water binding. However, the buffer rinsing (pH 5) after the MilliQ-water transports the curves to almost same level than before MilliQ-rinsing. It demonstrates that the compression of the chitosan-layer due to protonation changes of the amines of chitosan was rather reversible. The adsorbed mass and the adsorption kinetic profile were similar to those presented earlier by Myllytie, Salmi & Laine (2009) and Eronen et al. (2011a).

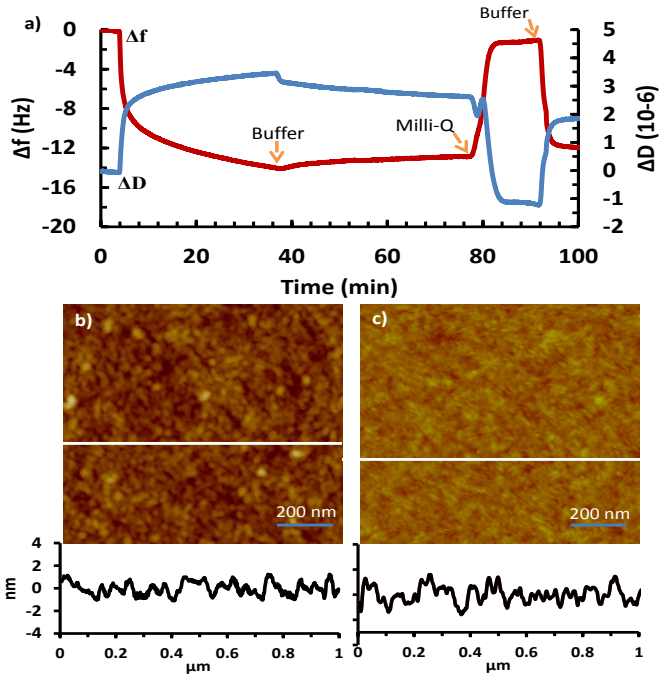

Figure 23. Change in frequency (Δf) and change in dissipation (ΔD) for adsorption of 0.5 mg/ml chitosan on cellulose at pH 5 (a). In the later stage the chitosan modified surface was rinsed with Milli-Q water (pH 7). The AFM height images for (b) unmodified and (c) chitosan modified cellulose. The Z-range of the images is 10 nm. (Paper I).

The topographical changes on dried cellulose surfaces after adsorption of chitosan were analyzed by AFM. The topographical changes after chitosan adsorption are presented in Figure 23b-c. The adsorbed chitosan did not remarkably alter the cellulose surface. This

indicates that the adsorption layer of chitosan is thin and tightly adhered to cellulose. The chitosan adsorption on cellulose was also analysed with SPR. Thickness of the adsorbed chitosan layer was founded to be 0.4 nm. By comparing the SPR and QCM-D data, it was estimated that the water content of the chitosan layer was 83 %. The observed adsorption phenomenon and minimal topographical changes correspond to earlier published findings (Myllytie, Salmi & Laine 2009)(Eronen et al. 2011a). Compared to the random coiled adsorption layer of CMC, chitosan creates a thin adsorption layer which has a rather flat conformation due to the presence of electrostatic interactions between chitosan and cellulose.

4.1.3 Carboxylation of cellulose by TEMPO-oxidation

The TEMPO-oxidation reaction was used in Papers III and IV to introduce carboxyl groups on cellulose nanofibrils. The TEMPO-oxidation reaction was originally utilized to produce cellulose nanofibrils from wood pulp (Saito, Isogai 2004), and this reaction has earlier been used in the modification of cellulose for conjugation of, e.g., PEG (Araki, Wada & Kuga 2001), PVAm (Pelton et al. 2011), and proteins (Arola et al. 2012). The use of TEMPO-mediated functionalization of cellulose for the conjugation of antibodies has not earlier been published. It is important to note here that TEMPO-mediated oxidation cannot be used with the amorphous cellulose surfaces, because it is known to disrupt the structure of amorphous cellulose (Hirota et al. 2010). In this work, the carboxylation of NFC with the alkaline TEMPO-mediated oxidation reaction (pH 10) was analyzed in QCM-D with NFC-model cellulose surfaces. A short, 2 min TEMPO-NaBr-NaOCl injection led to a significant drop in the frequency and increased dissipation (Figure 24a and b), which corresponds to an enhanced water uptake in the NFC-film due to the Donnan equilibrium (Osmotic pressure against the NFC-film). This strongly indicates the introduction of carboxyl groups on the surfaces of the NFC-fibrils. The oxidation reaction was stopped by ethanol addition, which quenches the oxidation reaction. MilliQ-water rinsing again led to significant swelling of the NFC-surface (a drastic negative frequency change) due to the removal of salt from the system. However, rinsing with a salt containing buffer solution recompresses the NFC-film, which is observed in the subsequent positive frequency change and negative dissipation change (the frequency change after buffer rinsing was approximately -90 Hz). The topographical changes on the NFC-surfaces after TEMPO-oxidation were investigated by AFM. The TEMPO-oxidation reaction did not alter the topography of the NFC-surfaces as can be seen from the AFM-images (Figure 24c and d). Compared to the CMC and chitosan adsorption methods, the effect of TEMPO-oxidation

was significant, since the change in the frequency curve corresponds only to water binding. A longer TEMPO-oxidation time (60 min) was also analyzed in Paper III. In this case, the frequency change after the oxidation and MilliQ-rinsing was about +170 Hz, which demonstrates significant peeling of carboxylated cellulose nanofibrils (Hirota et al. 2010). However, the carboxylated NFC-surface was also observed to be uniform after this longer oxidation period, as analysed by AFM (Paper III).

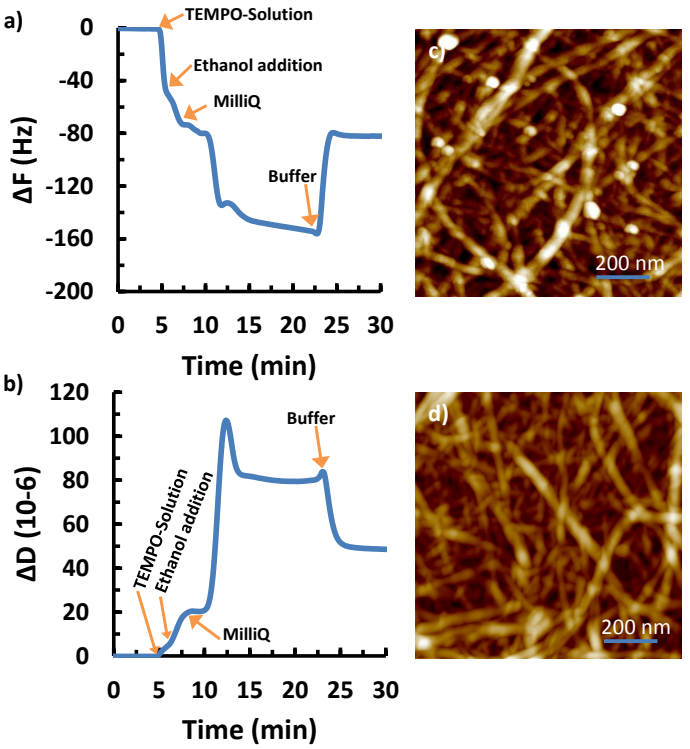

Figure 24. (a) Change in frequency (ΔF) and (b) change in dissipation (ΔD) for carboxylation of a NFC-surface by a TEMPO-NaBr-NaClO solution. The TEMPO-oxidation is stopped by an ethanol addition. AFM images of NFC-surface before (c) and after TEMPO-oxidation (d). The z-limit of the images was 30 nm. (Paper IV).

The alkaline TEMPO-mediated oxidation chemistry with wood fibers has earlier been analyzed in detail by (Saito, Isogai 2004)(Saito et al. 2007)(Isogai, Kato 1998)(Bragd, van Bekkum & Besemer 2004)(Saito et al. 2006)(Habibi, Chanzy & Vignon 2006). Compared to those reports, the reaction kinetics with NFC model films was faster compared to wood fibers due to the better accessibility of TEMPO-chemicals with the open NFC-surface. In

this work TEMPO-oxidation was also used on the topographical functionalization of NFC-films, and these results are discussed in more detail in a section of 4.5.

4.2 Adsorption of proteins on modified cellulose

The functionalization of cellulose with both polysaccharide adsorption and TEMPO-oxidation alters the charge properties of the cellulosic material. The effect of the surface functionalization strategies on the adsorption of proteins on cellulose was investigated (Figure 25). The main results are presented in this part, and more detailed results can be found in Papers I and III.

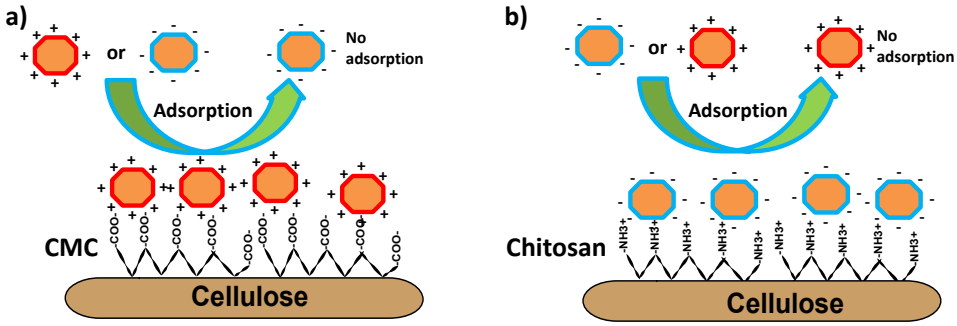

Figure 25. Schematic illustration of the electrostatic interactions driving protein adsorption on CMC (a) and chitosan (b) modified cellulose.

4.2.1 Adsorption of globular proteins on surface modified cellulose

Bovine Serum Albumin (BSA) is a globular protein that has widely been used as a protein standard for analyzing the adhesion of proteins to surfaces. The detailed properties of BSA can be found in papers of Böhme, Scheler (2007) and Vaiana et al. (2004). BSA adsorption on polysaccharide functionalized regenerated cellulose surfaces was analyzed by SPR (Paper I). Figure 26 shows the adsorption of BSA on unmodified, CMC-modified and chitosan-modified cellulose at pHs 4.0, 5.0, 6.2, and 7.4. The corresponding adsorbed amounts (calculated from the SPR data) are shown in Figure 27. BSA adsorbed effectively on all surfaces tested close to its isoelectric point (pI of BSA is 5.0). This adsorption phenomenon is typical for several proteins due to their reduced solvency at pI (Su et al. 1998).

The adsorption of BSA on unmodified cellulose at other tested pHs was relative constant, which demonstrates that the adsorption was driven mainly by non-electrostatic forces. The CMC-modification of cellulose remarkably increased the adsorption of BSA on cellulose at pH 4.0 due to the presence of electrostatic interactions. At pH 7.4, the adsorption of BSA on CMC-modified cellulose surface was limited mainly due to the presence of electrostatic repulsions. Earlier researchers have found that the adsorption of hard proteins, such as BSA, on hydrophilic surfaces is controlled mainly by electrostatic forces (Arai, Norde 1990)(Norde 1996). Two different types of adsorption phenomena was observed on the adsorption of BSA on chitosan modified cellulose. At pH 4, electrostatic repulsion limited the adsorption of BSA on chitosan modified cellulose. On the other hand, at pHs 6.2 and 7.4, the BSA adsorption was enhanced due to the lowered hydrophilicity and electrostatic interactions (pI of chitosan is about 6.5). This observed phenomenon is accordance with earlier findings of Prime, Whitesides (1991). The surface functionalization of cellulose by CMC and chitosan adsorption also altered the adsorption kinetics of BSA due to the different adsorption driving forces. The presence of electrostatic forces caused significantly faster adsorption of BSA on surface-functionalized cellulose. Whereas, with only non-electrostatic forces the adsorption of BSA was slow. These finding are in accordance with the earlier published data of Buijs, Hlady (1997).

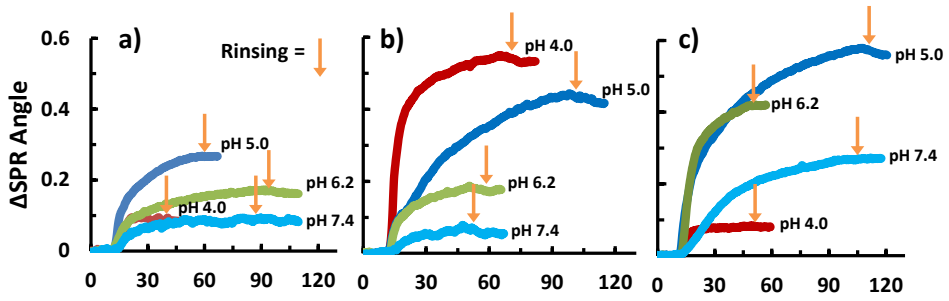

Figure 26. Adsorption of 0.1 mg/ml BSA on (a) pure, (b) CMC-modified, and (c) chitosan-modified cellulose at pHs 4.0, 5.0, 6.2, and 7.4 by SPR. (Paper I).

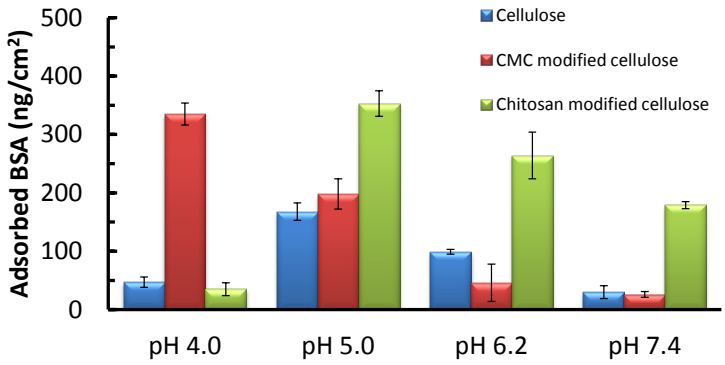

Figure 27. Adsorbed amounts of 0.1 mg/ml BSA on surface modified cellulose surfaces. The values are calculated using equation 3.3. (Paper I).

4.2.2 Adsorption of glycoproteins on surface modified cellulose

The adsorption of glycoproteins on surface modified cellulose was analyzed by QCM-D (Paper III). Glycoproteins are a group of proteins that have oligosaccharide chains present on their protein cores. Therefore, those proteins may have a different type of adhesion mechanism with cellulose than globular proteins. The glycoprotein analyzed was avidin, a quaternary biotin binding protein that has pI of 10.5, which was also utilized in immobilization of antibodies on cellulose (shown in chapter 4.4). A more detailed introduction to the properties of avidin can be found in articles of Green (1975), Green, Joynson (1970), and DeLange, Huang (1971). The effect of the oligosaccharide chains of avidin on the adsorption on cellulose was analyzed with neutravidin (pI of 6.3), which is a deglycosylated version of avidin (Bayer et al. 1995). The adsorption of avidin and neutravidin on cellulose surfaces have not earlier been analyzed with QCM-D or SPR. Figure 28 shows the adsorption of avidin and neutravidin on cellulose at pHs 5.0 and 7.4. The pH values were selected to change the net charge of neutravidin, which could give further highlight the adsorption mechanism of avidins. The corresponding adsorbed masses (calculated by equation 3.6) for avidin at pHs 5.0 and 7.4 were 114, 97, respectively and for neutravidin 369, and 245 ng/cm^2, respectively. Wolny, Spatz & Richter (2010) have presented that the frequency changes of -26 and -32 Hz correspond to the formation of a monolayer of avidin and neutravidin on biotinylated surfaces. These frequency changes correspond to the adsorbed masses of 460 and 566 ng/cm^2 (equation 3.4), respectively. This indicates that the adsorbed avidin or neutravidin on unmodified cellulose do not form a saturated monolayer.

However, the binding of avidin to cellulose via a biotin-link or physical adsorption may lead to several different conformations of adhering avidin molecules since the biotin-link may prevent the structural arrangements. Therefore it is possible that a lower amount of physically adsorbed avidin saturates the surface compared to the biotinylated surface. The irreversible adsorption of avidin on cellulose was rather similar at both analyzed pHs mainly due to the high isoelectric point of avidin. The neutravidin adsorbed much more on cellulose than avidin. This indicates that the deglycosylation alters the adsorption phenomenon of avidin. It is possible that the oligosaccharide chains stabilize the structure of avidin in water, which reduces its affinity for cellulose surfaces. Neutravidin adsorbed at pH 5 much more than at pH 7.4, which verifies the effect of the electrostatic interaction between the cationically charged protein and the slightly anionically charged cellulose. However, significant adsorption of neutravidin on cellulose above the pI suggests that non-electrostatic forces are the main driving force causing avidins to adhere on cellulose. When compared to the results of Wolny, Spatz & Richter (2010), where avidin was physically adsorbed on silica and gold, the amounts of avidins adsorbed on cellulose were lower. Dupont-Filliard et al. (2004) have been shown, with modified polypyrrole films, that a hydrophilic polymer substrate slightly decreases the adsorption of avidin compared to a hydrophobic polymer substrate.

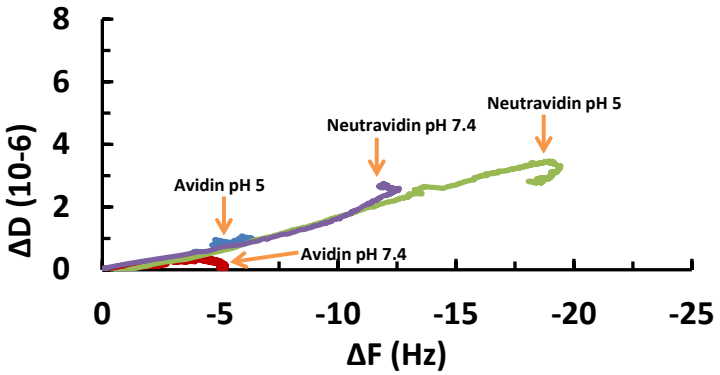

Figure 28. ΔD-ΔF plots of QCM-D for the adsorption of 0.1 mg/ml avidin and neutravidin on unmodified cellulose at pHs of 5.0 and 7.4. (Paper III).

The effect of the carboxylation of cellulose on the adsorption of avidin was analyzed by QCM-D. With CMC adsorbed on cellulose the adsorption of both avidin and neutravidin increased drastically (Figure 29). Avidin adsorbed on CMC-modified cellulose slightly more at pH 7.4 than at pH 5. This may be caused by the somewhat higher extent of dissociated carboxyl groups on CMC at pH 7.4 (pKa of CMC is about 4.5), which slightly increases the electrostatic interaction. The corresponding adsorbed masses (calculated by

equation 3.6) for avidin at pHs 5 and 7.4 were 1070 and 1245 ng/cm², respectively. Neutravidin adsorbed significantly more on CMC-modified cellulose than avidin, similarly as on unmodified cellulose. This suggests again that the deglycosylation of avidin enhances its binding to anionically charged cellulose surfaces. The corresponding adsorbed masses (calculated by equation 3.6) for neutravidin at pHs 5 and 7.4 were 2842 and 2589 ng/cm², respectively. Thus, neutravidin adsorbed on CMC-modified cellulose also at pH 7.4, which indicates again that non-electrostatic interactions are present in the adsorption of neutravidin on hydrophilic surfaces. The adsorption kinetics of avidin on CMC-modified cellulose was remarkably faster compared to that for neutravidin. The adsorbed values were in the same level than the reported values for the adsorption of neutravidin on modified gold surfaces (Boujday et al. 2008).

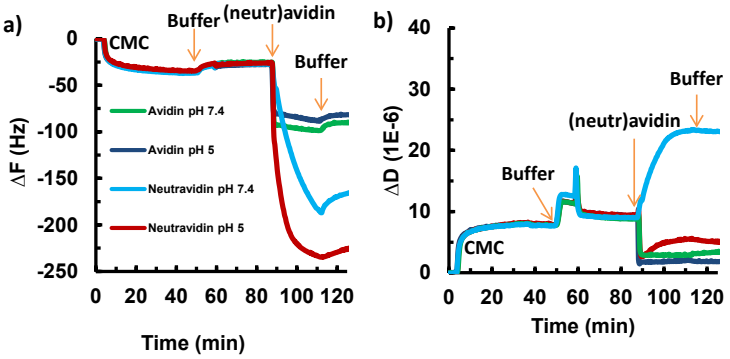

Figure 29. Change in frequency (Δf) (a) and change in dissipation (b) for the adsorption of 0.1 mg/ml avidin and neutravidin on CMC-modified cellulose at pHs 5.0 and 7.4. (Paper III).

Topographical changes of cellulose after avidin and neutravidin treatment and drying were imaged by AFM. Figure 30 shows the topographical changes on CMC-modified cellulose surfaces after adsorption of avidin and neutravidin. Both adsorbed avidin and neutravidin covered the CMC-modified cellulose surfaces with a granular type of adsorption layer. The granule heights on neutravidin coated surfaces were slightly higher compared to that on the avidin coated surfaces. The heights of the granules were greater when compared to the size of an avidin in water (5.6 x 5 x 4 nm (Green 1975)). This suggests the aggregation of avidin and neutravidin on CMC-modified cellulose. Similar observations have been reported by Wolny, Spatz & Richter (2010). A clear correlation between the adsorbed amounts of avidin measured by QCM-D at different pH values and the AFM images was observed. The AFM profiles reminded the earlier published result of Kim et al. (2004), who adsorbed streptavidin on smooth mica and gold surfaces.

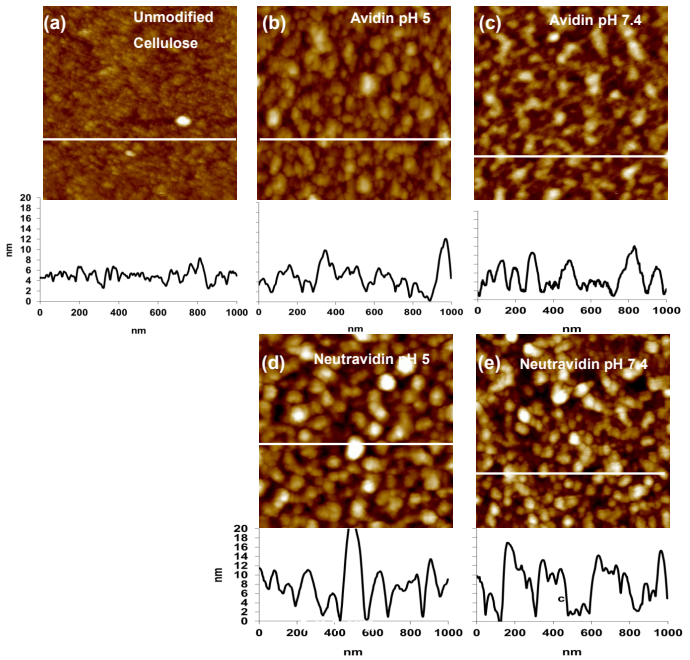

Figure 30. The AFM height images for adsorbed avidin (b and c) and neutravidin (d and e) on CMC-modified cellulose. The Z-range of the images is 20 nm. (Paper II).

4.2.3 Adsorption of antibodies on surface modified cellulose

The adsorption phenomenon of antibodies on surface modified cellulose was analyzed in this work by SPR with polyclonal human immunoglobulin G (hIgG) (Paper I). Figure 31 shows typical SPR sensograms for the adsorption of hIgG on unmodified (a), CMC-modified (b), and chitosan-modified cellulose (c). The corresponding adsorbed masses are shown in Figure 32. hIgG adsorbed on the unmodified cellulose surface mostly at pH 5 mainly due to its positive net charge (the isoelectric point of hIgG is between 6.8 and 7.4). This indicates that acidic conditions favor the adsorption of hIgG on unmodified cellulose due to the presence of attractive electrostatic interactions. The pre-adsorbed CMC-layer remarkably increased the adsorption of hIgG on cellulose at acidic conditions due to the increased attractive electrostatic forces between the negatively charged CMC-layer and the positively charged hIgG. At pH 7.4, the adsorbed mass of hIgG was found to be lower than that on the unmodified cellulose, due to the presence of repulsive electrostatic forces. In

general, the adsorption phenomenon of hIgG on the anionic cellulose surface was similar to that of BSA.

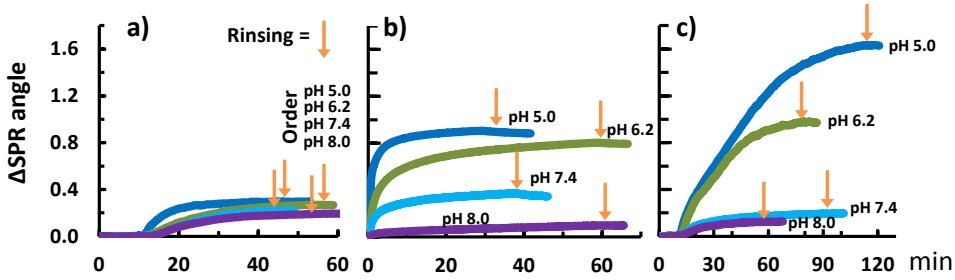

Figure 31. Adsorption of 0.1 mg/ml human immunoglobulin G on (a) pure, (b) CMC-modified, and (c) chitosan-modified cellulose at pHs of 4.0, 5.0, 6.2, and 7.4 by SPR. (Paper I).

Surprisingly, the adsorption of hIgG on chitosan modified cellulose was mainly driven by non-electrostatic forces as can be seen from the adsorption curves (Figure 31c). The presence of the pre-adsorbed chitosan layer dramatically increased the adsorption of hIgG at low pH (pH 5.0 and 6.2). At higher pHs (pH 7.4 and 8.0), the pre-adsorbed chitosan layer slightly reduced the adsorption of hIgG when compared to unmodified cellulose. Chitosan is positively charged in acidic conditions (pI of 6.5), and it becomes uncharged above the pI (lower solubility in water). At pH 5, the amount adsorbed was found to be more than five times larger compared to that on unmodified cellulose. On the other hand, the adsorbed amount of hIgG was reduced at higher pH (pH 7.4 and pH 8.0), indicating that the uncharged and more hydrophobic pre-adsorbed chitosan layer prevents adsorption of hIgG. The observed adsorption phenomenon that lower pH favors the adsorption of hIgG on chitosan is supported by the findings of Machado et al. (2006). The results presented here indicate that CMC-modified cellulose is more controllable platform for cellulose based biointerfaces than chitosan-modified cellulose. However, both chitosan- and CMC-modification techniques can be used to tune the adsorption of proteins on cellulosic materials.

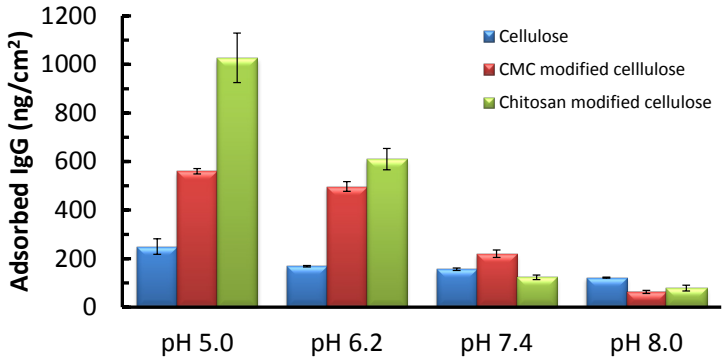

Figure 32. Adsorbed amounts of 0.1 mg/ml human immunoglobulin G on surface-modified cellulose surfaces. The values are calculated using equation 3.3. (Paper I).

4.3 Conjugation of antibodies on cellulose in random orientation

The covalent conjugation of antibodies on surface functionalized cellulose was analyzed by QCM-D and SPR. The platforms tested for antibody conjugation were CMC (Figure 33) and chitosan modified cellulose, and TEMPO-oxidized cellulose. In order to obtain an optimal antibody binding, antibodies have to contain a high number of accessible antigen binding sites (FAB-fragments). In this work EDC/NHS conjugation chemistry was used, which utilizes amine containing amino acids (lysine and argine) that can also be found in the FAB-fragments. However, EDC/NHS chemistry is not capable to form oriented antibody conformation on solid surfaces (referred to as random conjugation), and the biological activity of the immobilized antibody can be reduced due to the steric hindrances. The main observations are summarized here, and more detailed results can be found in Papers II and IV.

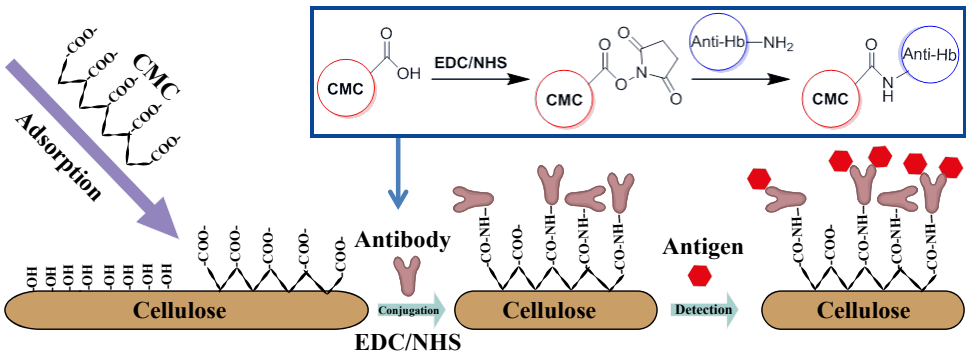

Figure 33. Schematic illustration of conjugation of antibodies on CMC-modified cellulose using carboxyl reactive EDC/NHS chemistry. Subsequent antigen detection of prepared biointerface is also shown.

4.3.1 Anti-hemoglobin conjugation on CMC functionalized cellulose

The conjugation of antibodies on CMC-modified cellulose was examined by QCM-D (paper II). The ultimate goal of this study was to prepare a specific bioactive cellulose surface for hemoglobin detection. Figure 34a illustrates the conjugation of anti-hemoglobin IgG on CMC-modified cellulose via EDC/NHS activation. The effect of EDC/NHS activation is evident since without EDC/NHS activation, anti-hemoglobin IgG did not adsorb on CMC-modified cellulose. The amount conjugated on CMC-modified cellulose was 548 ng/cm^2 (calculated from equation 3.4). The topographical changes on the cellulose surface were investigated by AFM. The adsorbed CMC-layer altered the topography of the unmodified cellulose surface only slightly (the RMS roughness was 0.45 and 0.43 nm for unmodified and CMC-modified cellulose, respectively). After conjugation of anti-hemoglobin, a clustered structure on the CMC-modified cellulose surface was observed (Figure 34c), and the surface roughness increased to 0.76 nm. It can be seen from Figure 34c that anti-hemoglobin was rather evenly distributed on the CMC-modified cellulose surface, and no empty regions was observed in AFM. The conjugated amount of anti-hemoglobin was in accordance with earlier published results on the conjugation of antibodies to CMC:PEI hydrogels (Carrigan, Scott & Tabrizian 2005b)(Carrigan, Tabrizian 2005). The effect of conjugation pH, 4.0 and 7.4, was also tested (unpublished data). At pH 7.4 the amount of anti-hemoglobin IgG conjugated on activated CMC-modified cellulose was low, which indicates that the presence of electrostatic interactions (pI of anti-hemoglobin is approximately pH 6) is important for the conjugation of antibodies on CMC-modified cellulose.

The observation is in accordance with reported data; the presence of electrostatic interactions has been demonstrated to enhance the conjugated amount of antibodies (Johnsson et al. 1995).

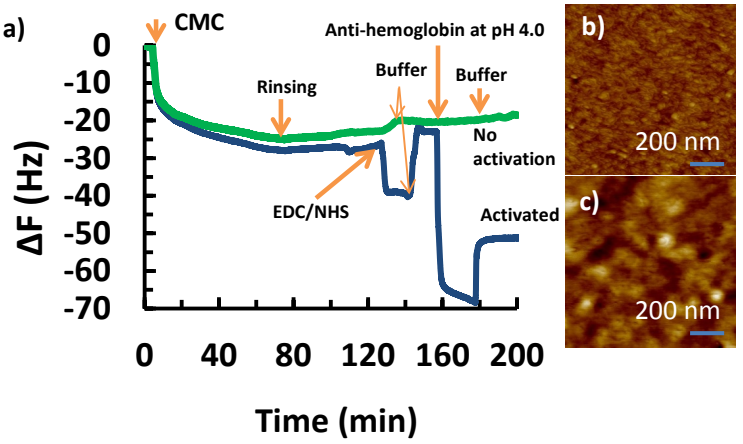

Figure 34. Change in frequency (Δf) for conjugation of 0.2 mg/ml anti-hemoglobin in 10 mM NaOAc buffer at pH 4.0 on CMC-modified cellulose via an activation with a mixture of 0.1 M EDC with 0.4 M NHS (a). The reference curve shows the non-specific adsorption of anti-hemoglobin on CMC-modified cellulose. The AFM height images for unmodified (b) and anti-hemoglobin treated CMC-modified cellulose (c). The z-limit of the images is 10 nm. (Paper II).

Figure 35 shows the effect of the adsorbed amount of CMC and conformation of the adsorbed CMC-layer on antibody conjugation. Surprisingly, irrespectively of the large differences in CMC sorption the conjugated mass of hemoglobin in all tested salt concentrations was almost constant. The adsorbed CMC-layer in a solution with zero salt has a more extended conformation, whereas the presence of salt leads to a more coiled conformation (Gondo et al. 2006). At high ionic strength, the carboxyl groups inside the coils are inaccessible to anti-hemoglobin conjugation, while at low ionic strength the carboxyl groups are oriented towards the solution due to the repulsion between the negative surface and CMC. Hence, they are accessible for the covalent linking.

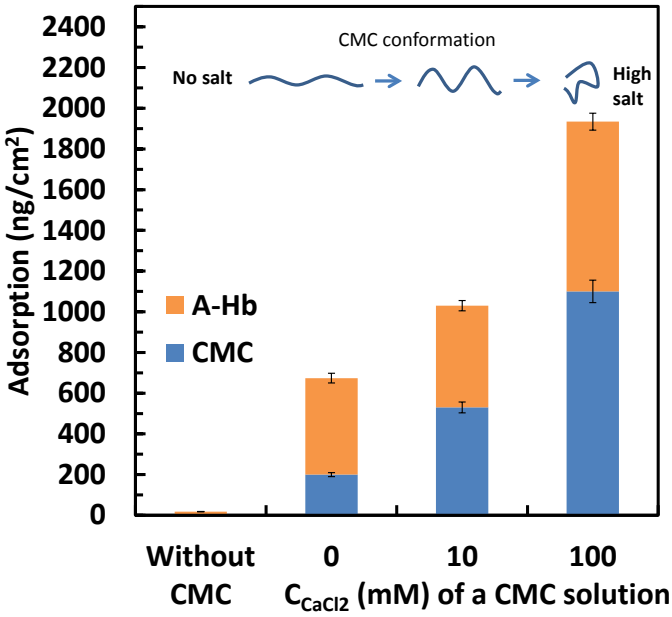

Figure 35. The effect of adsorbed amount of CMC and conformation of CMC-layer on conjugation of anti-hemoglobin to cellulose by QCM-D data. First 0.2 mg/ml CMC was adsorbed on cellulose at three different CaCl2 concentrations. Subsequently 0.2 mg/ml anti-hemoglobin was conjugated via EDC/NHS activation to CMC-modified cellulose surfaces. The reference test shows conjugated amount of anti-hemoglobin on cellulose without CMC-modification. (Paper II).

That random conjugation may reduce the activity of antibodies to bind antigens due to the steric hindrances (Lu et al. 1995)(Lin, Andrade & Chang 1989)(Turko, Yurkevich & Chashchin 1992). The hemoglobin binding on the anti-hemoglobin biointerface prepared on CMC-modified cellulose was analyzed by QCM-D and SPR (Paper II). Figure 36a shows the hemoglobin detection cycles on the anti-hemoglobin biointerface in SPR. After each detection cycle, the biointerface was regenerated with acid rinsing that desorbed the bound antigens. The corresponding adsorption profile is shown in Figure 36b. The adsorption of hemoglobin on the anti-hemoglobin biointerface increased as a function of antigen concentration, and the adsorption profile (SPR data) corresponded to Langmuir type adsorption. The biointerface was capable of detecting antigen after several regeneration cycles; this demonstrates that CMC-modified cellulose is stable substrate for biointerfaces. Similar detection performance has been reported earlier (Carrigan, Tabrizian 2005)(Carrigan, Scott & Tabrizian 2005a). The non-specific binding of hemoglobin on CMC-modified cellulose was negligible, demonstrating that the prepared anti-hemoglobin biointerface was highly specific. The observed negligible non-specific adsorption of anti-

gen is beneficial for enhancing the detection limit of the biointerface (Rusmini, Zhong & Feijen 2007). The sequential conjugation method, in which CMC is first adsorbed on cellulose and then antibodies are subsequently conjugated on functionalized cellulose, leads to an effective gathering of antibodies. Hence, the sequential methods create an active interface that provides a good accessibility of antigens to bind on conjugated antibodies.

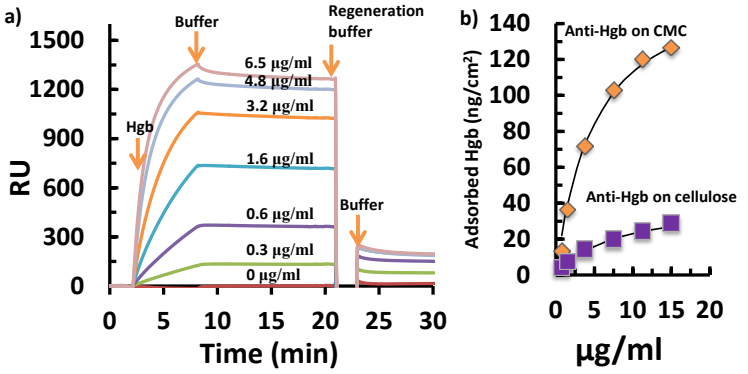

Figure 36. (a) The adsorption cycles for hemoglobin (Hgb) on anti-hemoglobin conjugated on CMC modified cellulose by SPR. The regeneration between cycles was performed with 0.1 M glycine-HCl at pH 2.7. (b) The adsorption profiles of hemoglobin on conjugated anti-hemoglobin on pure and CMC modified cellulose calculated by equation 3.1 from the SPR data. (Paper II).

4.3.2 hIgG conjugation on chitosan-functionalized cellulose

The use of chitosan-modified cellulose as a platform for antibody conjugation was analyzed by SPR (unpublished data). The conjugation of enzymes to chitosan with the EDC/NHS chemistry has earlier been demonstrated (Ghanem, Ghaly 2004). Conjugation of antibodies to chitosan-modified cellulose takes place between carboxyls of hIgG and amines of chitosan. A disadvantage of this approach is that all proteins contain both amine and carboxyl containing amino acids, and therefore the EDC/NHS chemistry may lead to crosslinking between proteins (Grabarek, Gergely 1990). Two different coupling agents was explored to characterize this approach: (a) NHS-PEG$_n$-NHS and (b) EDC with NHS (Figure 37).

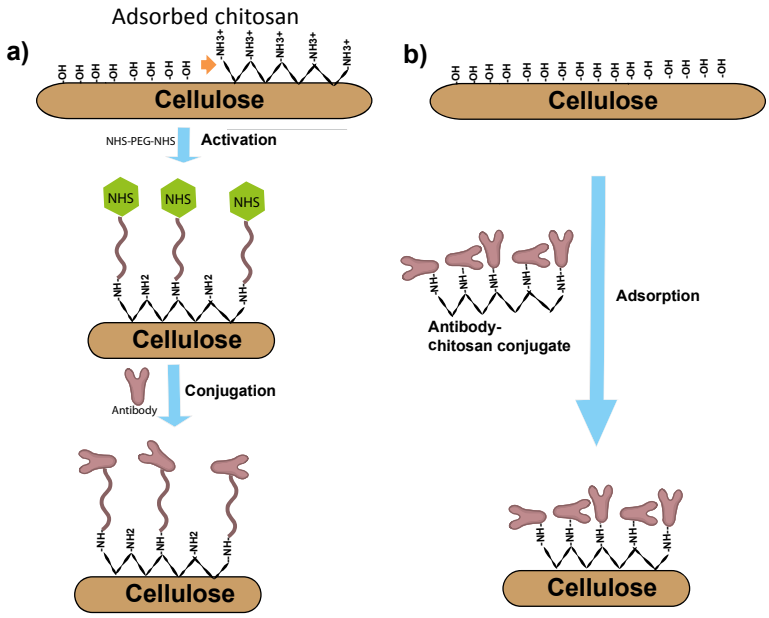

Figure 37. Schematic illustration of conjugation of antibodies on cellulose by (a) NHS-PEG$_5$-NHS activation with chitosan pre-adsorption and (b) adsorption of pre-conjugated chitosan-antibody conjugate.

In the first method, amine reactive PEG (NHS-PEG$_5$-PEG) was first adsorbed on chitosan-modified cellulose followed by the injection of hIgG. In this approach the self-crosslinking of proteins is not present. The NHS-PEG$_5$-PEG linker molecule binds irreversibly to chitosan-modified cellulose (Figure 38). The amount conjugated and layer thickness were calculated to be 686 ± 30 ng/cm² and 57 ± 3 Å, respectively (equation 3.2, modeling parameters; na_{PEG} 1.352, nO_{PEG} 1.2). The measured thickness was found to be more than double of the theoretical length of a NHS-PEG$_5$-PEG that suggests a bilayer type of adsorption. However, the amount of hIgG adsorbed on the NHS-PEG$_5$-PEG layer was negligible most likely due to the presence of only a few free NHS groups since most of them reacted with amine groups of chitosan. This demonstrates that the NHS-PEG-NHS linker is not suitable to conjugate antibodies on chitosan-modified cellulose. on the other hand, the negligible hIgG adsorption indicated that the bound PEG-layer prevented the further adsorption. These facts are in agreement with earlier findings related to the effect of hydrophilic, hydrated PEG layers that have been shown to effectively passivate protein adsorption (Hermanson 2008).

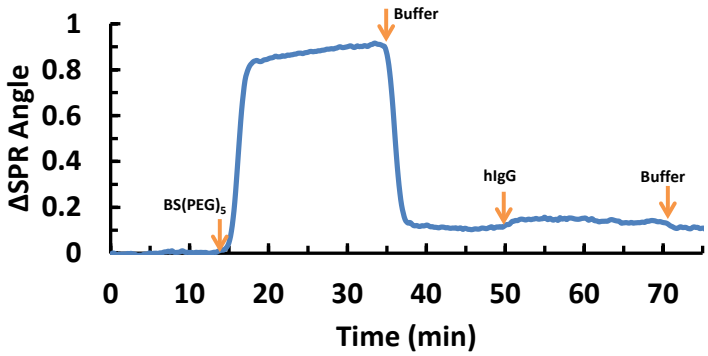

Figure 38. Conjugation of Human IgG (hIgG), Mw 532.50 with spacer arm of 21.7 Å, onto the chitosan-modified cellulose via Bis(PEG)5 activation at pH 7.4. 10 mM of Bis(PEG)5 was adsorbed onto the pre-adsorbed chitosan at pH 7.4 buffer followed by the buffer rinsing to remove the excess of Bis(PEG)5. 100 µg/ml of hIgG was adsorbed on activated surface at pH 7.4 Pb followed by the buffer rinsing at pH 7.4 Pb to remove the unbound hIgG. (Unpublished data).

In the second approach, hIgG was first activated with EDC and NHS to make it amine-reactive. Then, the activated hIgG was immediately adsorbed onto the chitosan-modified cellulose surface to reduce the reaction time for self-crosslinking of hIgG. Figure 39 shows the adsorption of activated hIgG on chitosan modified cellulose. The amount of activated hIgG attached to chitosan-modified cellulose was 410 ± 26 ng/cm^2. Rinsing with acidic buffer (pH 2) did not alter the amount immobilized; this demonstrates covalent bonding of the EDC/NHS-activated hIgG on chitosan-modified cellulose. However, the adsorption of activated hIgG on unmodified cellulose also increased (adsorbed amount of 237 ± 7 ng/cm^2). This observation indicates that in the presence of EDC/NHS activation chemicals, proteins are partially cross-linked together. The results are in accordance with earlier reported data (Ghanem, Ghaly 2004).

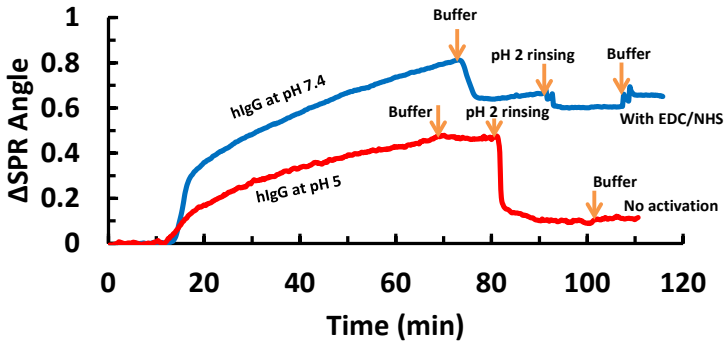

Figure 39. Conjugation of Human IgG (hIgG) on chitosan-modified cellulose via EDC/NHS activation. 0.1 mg/ml of hIgG was activated by adding 10 mM EDC with 40 mM NHS at pH 7.4. Activated Human IgG was adsorbed on chitosan modified cellulose at pH 7.4, followed by the buffer rinsing at pH 7.4 and pH 2. The reference test shows adsorption of 0.1 mg/ml hIgG on chitosan-modified cellulose at pH 5, followed by a pH 2 rinsing step. (Unpublished data).

4.3.3 Anti-hIgG conjugation on TEMPO-oxidized NFC

Conjugation of proteins and polymers on cellulose through TEMPO-oxidation with the EDC/NHS activation has been reported earlier by, e.g., Arola et al. (2012), Araki, Wada & Kuga (2001), and Filpponen, Argyropoulos (2010). In this work (Paper IV), the model cellulose approach was utilized to analyze the conjugation of antibodies on TEMPO-oxidized cellulose nanofibrils. Figure 40 shows the typical QCM-D curve for conjugation of anti-human IgG on an NFC-surface. The 2 min TEMPO-oxidation treatment caused an approximately -40 Hz change in frequency (value after buffer rinsing), which demonstrates a water uptake in the NFC-film by virtue of the formation of carboxyl groups. Subsequently performed EDC/NHS activation of TEMPO-oxidized NFC caused an approximately -95 Hz change in frequency (value after buffer rinsing). The EDC/NHS chemistry only plays with carboxyl groups (Staros, Wright & Swingle 1986), and therefore this result verifies that a short 2 min oxidation time was enough to enable the attachment of amine reactive NHS-esters on NFC. Earlier, rather high aldehyde contents in TEMPO-oxidized fibers have been reported when short oxidation times are used (Saito, Isogai 2004). However, the accessibility of TEMPO-oxidation chemicals in wood fibers is drastically lower compared to high surface area NFC. Therefore, it is likely that the aldehyde content of the NFC-surface was low. A significant amount of anti-hIgG adsorbed on the activated NFC-surface at pH 5 is due to electrostatic interactions. The ethanolamine treatment removed most of the uncon-

jugated antibodies. The amount conjugated after ethanolamine rinsing was -31 Hz; this corresponds to an adsorbed mass (calculated by equation 3.4) of 552 ng/cm^2. The pKa of anti-hIgG is approximately 6.8, which leads to an electrostatic interaction between anionic NFC and cationically charged anti-hIgG at a pH 5. The conjugated mass on NFC was equal to conjugated amount of anti-hemoglobin on CMC-modified cellulose, 548 ng/cm^2 (Paper II). However, it is likely that the NFC-cellulose surface has a higher specific surface area compared to the LS-cellulose surface. On the other hand, the CMC-modification technique gives more 3D structure that can leads to slightly higher conjugated amounts of IgGs on cellulosic materials. The anti-hIgG surface was finally treated with *superblock* to prevent the non-specific binding of charged antigens. HIgG adsorbed specifically on the anti-hIgG biointerface on NFC, and the amount adsorbed was approximately -5 Hz, which corresponds to an adsorbed mass of 88.5 ng/cm^2 (calculated by equation 3.4). The detection efficiency of an anti-hIgG biointerface on the NFC-surface was approximately 50 % lower compared to that of anti-hemoglobin interface prepared on the CMC-modified LS-cellulose surface (Paper II). This can partly be explained by the purity of the antibodies used. hIgG is a polyclonal antibody also containing unreactive species, whereas anti-hemoglobin is a monoclonal antibody. Without antibody, the amount of hIgG adsorbed on TEMPO-oxidized NFC was negligible.

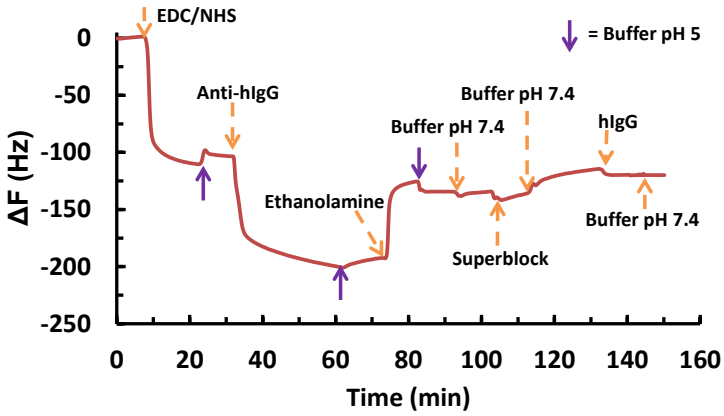

Figure 40. Conjugation of anti-human IgG (100 µg/ml in 10 mM NaOAc at pH 5 for 30 min) on the TEMPO-oxidized NFC-surface (0.013 mM TEMPO, 0.47 mM NaBr, and 0.57 mM NaClO at pH 10 for 2 min) through the EDC/NHS activation (0.1 M EDC plus 0.4 M NHS in 10 mM NaOAc buffer at pH 5 for 20 min). The activity of the conjugated antibody was tested by adsorbing 100 µg/ml hIgG in 10 mM phosphate buffer at pH 7.4 for 10 min on an activated NFC-surface with anti-human IgG. (Paper IV).

4.3.4 Attachment of proteins on cellulose via pre-conjugation with CMC

Printing and coating technologies have been utilized to transfer antibodies onto paper matrixes. In that case, antibodies are pre-conjugated to a linker molecule before transferring them to the matrix (Heikkinen et al. 2011)(Di Risio, Yan March 2010)(Delaney, Smith & Schubert 2009)(Hossain et al. 2009). In this work the pre-crosslinking approach (Figure 41) for the covalent conjugation of antibodies on cellulose was analyzed with anti-hemoglobin IgG and CMC by QCM-D (Paper II).

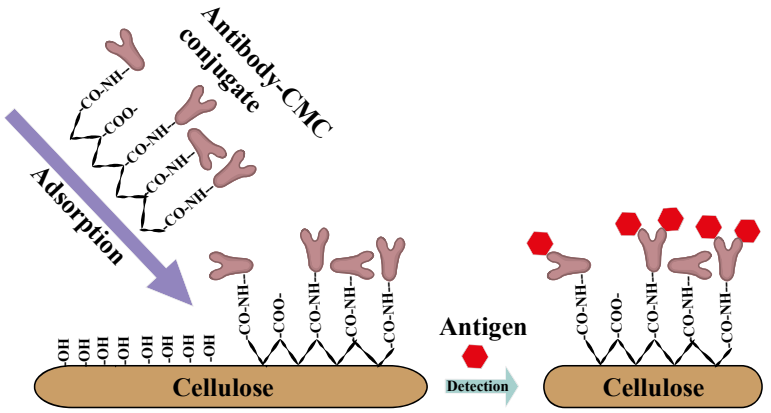

Figure 41. Schematic illustration of immobilization of antibody on cellulose by adsorption of pre-conjugated antibody-CMC conjugate.

Figure 42a shows the irreversible adsorption of pre-conjugated anti-hemoglobin IgG with CMC on unmodified cellulose. The amount attached was approximately -8 Hz, which corresponds to a mass uptake of 140 ng/cm² (calculated by equation 3.4). It can be seen that the conjugated amount of anti-hemoglobin, was in this case lower than that of the sequential conjugation method (Paper II). This demonstrates that pre-conjugation may alter the binding ability of CMC on cellulose. The figure also shows that pre-conjugated anti-hemoglobin specifically detected hemoglobin, which verifies that at least part of anti-hemoglobin IgGs were accessible to antigen binding. The attached amount was -4 Hz (0.4 µg/ml hemoglobin), which corresponds to the adsorbed mass of approximately 70 ng/cm².

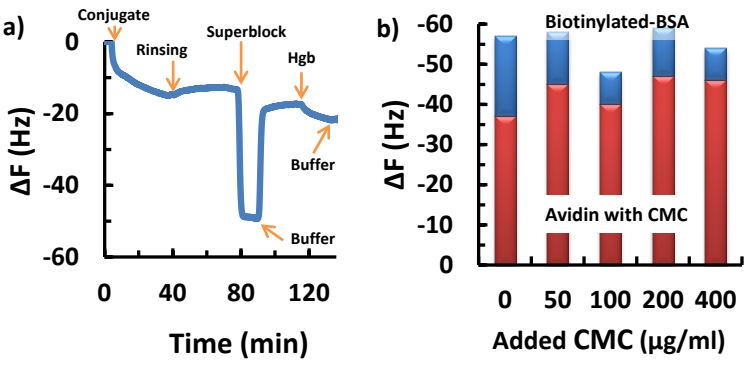

Figure 42. (a) adsorption of pre-conjugated anti-hgb IgG with CMC on cellulose (Paper II), and 0.4 µg/ml hemoglobin binding on the anti-hemoglobin biointerface. (b) adsorption of pre-complexed 0.1 mg/ml avidin with varying amounts of CMC on cellulose at pH 5 (unpublished data). Subsequently, the 10 µg/ml biotinylated-BSA was adsorbed at pH 7.4 on the avidin-CMC biointerfaces.

The ability of the pre-conjugated antigen complexes to sense the antigen was analyzed in more detail with CMC and avidin (unpublished data). Avidin was mixed with CMC, and then the positively charged complex was adsorbed at pH 5 on unmodified NFC-surfaces. The ability of avidin to detect its counterpart (biotin) was tested by adsorbing biotinylated-BSA on avidin-CMC biointerfaces at pH 7.4. As a reference, biotinylated-BSA did not adsorb on CMC modified cellulose without avidin. The biotinylated-BSA binding to the avidin biointerface was highest without CMC (Figure 42b). The added CMC lowered the amount of biotinylated-BSA adsorbed most likely due to the covering of the avidin molecules that blocks the adsorption sites. However, pre-complexation did not completely block the biotin binding ability of avidin. Therefore, the pre-conjugation method could be a suitable tool to immobilize antibodies on cellulose in specific applications.

4.4 Oriented attachment of antibodies on cellulose

Immunoglobulins always contain multiple conjugation sites which lead to the conjugation of antibodies on solid surfaces in random orientations. This may reduce their affinity to bind antigens due to the steric hindrance (Rao, Anderson & Bachas 1998). The avidin-biotin method is more expensive than the direct conjugation of sensing molecules to substrates. However, if controllable, non-toxic, and oriented immobilization chemistries are needed, the direct conjugation method cannot reach those requirements. A big advantage

of the avidin-biotin method is its stability in strong chemical environments; the antibodies and enzymes are denatured in those conditions before a breakage of an avidin-biotin linkage. Moreover, various biotinylated functional molecules are commercially available. In this work a method to gently orient the conformation of antibodies on a cellulose surface with the avidin-biotin linkage was analysed (Figure 43). The conjugation of proteins on cellulose via the avidin-biotin complex was analyzed with QCM-D and model cellulose films. The main results are summarized here, and more detailed results can be found in Paper III.

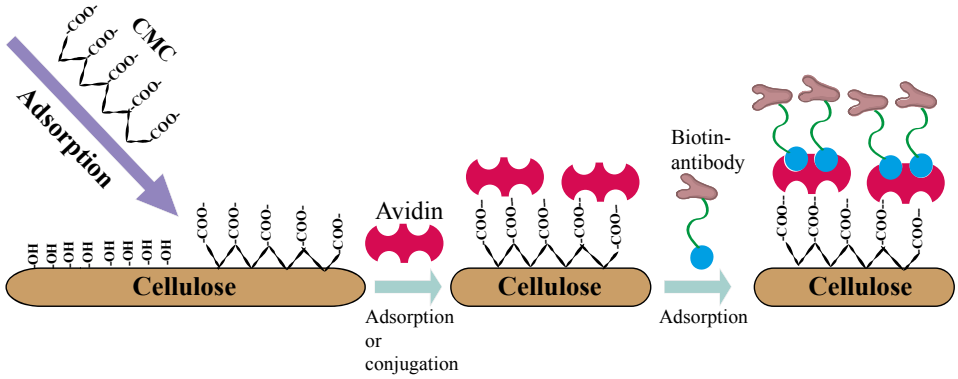

Figure 43. Schematic illustration of immobilization of biotinylated antibodies on avidin modified cellulose. The immobilization of avidin on cellulose is tuned by carboxylation of cellulose.

4.4.1 Immobilization of Avidin and neutravidin on surface modified cellulose

The adsorption phenomena of avidin and its deglycosylated form (neutravidin) on inactivated CMC-modified cellulose were discussed in chapter 4.2.2. The covalent conjugation of avidins on carboxylated cellulose was utilized since it has been reported that the direct adsorption of proteins may lead to unstable binding and reduced activity of the attached proteins (Rusmini, Zhong & Feijen 2007). Avidin conjugation on carboxyl-modified gold with EDC/NHS activation has earlier been reported by Caruso et al. (1997), where similar conjugation chemistry as in this thesis was used. Moreover, avidin linking to biotinylated-cellulose has been demonstrated by Goldstein et al. (1986). Avidin adsorption on biotinylated-CMC (Wenz, Liepold 2007) and avidin conjugation on chitosan (Nettles, Elder & Gilbert 2002) have been demonstrated in the literature. In this work, avidin conjugation on CMC-modified cellulose was examined with cellulose model surfaces by QCM-D. Figure 44

shows the EDC/NHS-conjugation curves for avidin and its deglycosylated form (neutravidin) on CMC-modified cellulose at pH 5 and pH 7.4 in QCM-D. The corresponding amounts attached were for avidin 1187 ng/cm^2 and 1485 ng/cm^2 and for neutravidin 3830 ng/cm^2 and 2808 ng/cm^2, respectively (calculated by equation 3.6). The conjugated masses were surprisingly similar to the adsorbed masses of avidins on CMC-modified cellulose without any activation steps (Figure 29). This indicates that the EDC/NHS activation does not remarkably alter the mass uptake. The conjugation kinetics of avidin on activated CMC-modified cellulose was much faster (and leveled off) compared to neutravidin. The observed curve profiles and conjugated amounts of avidin on CMC-modified cellulose were similar to that of reported for conjugation of avidin with EDC/NHS on carboxylated gold surfaces (Caruso et al. 1997). The avidin treated CMC-cellulose surfaces were further analyzed in dry state with AFM (Figure 44b-d). The AFM experiments indicated that more uniform surface distribution of the immobilized avidin is achieved by using EDC/NHS activation when compared to that of the adsorption method. The heights of spots on the AFM images suggest that the conjugated layer was thicker than a monolayer due to the dimensions of avidin molecules (5.6 x 5 x 2 nm (Green, Joynson 1970)). The observed AFM results were accordance with earlier reported data of (Wolny, Spatz & Richter 2010). The effect of EDC/NHS activation on the stability of avidin biointerfaces to CMC-modified cellulose was analyzed by XPS. The nitrogen peak was used to demonstrate the attachment of avidin on CMC-modified cellulose, since cellulose does not contain any nitrogen containing groups. The covalent conjugation method produced a more even distribution of attached avidin compared to the adsorption method, shown by the lower scattering of nitrogen content. Based on the AFM and XPS data one can postulate that the avidin aggregates observed on the surfaces of CMC-modified cellulose, where avidin was adsorbed without EDC/NHS activation, were formed during the drying the surface. However, the EDC/NHS chemistry permanently binds avidin molecules to the surface causing a more even distribution of avidin molecules, which does not alter while the water is removed from the biointerface.

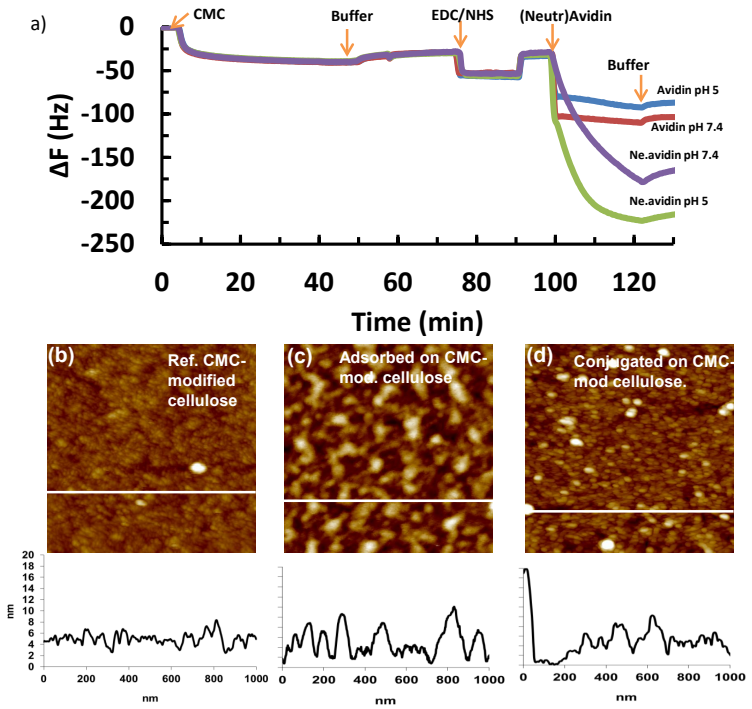

Figure 44. Change in frequency on conjugation of 100 µg/ml avidin and neutravidin on CMC modified cellulose through the EDC/NHS activation (a). AFM height images for adsorbed (c) and conjugated avidin (d) at pH 7.4 on CMC modified cellulose. (Paper III).

The conjugation of neutravidin on TEMPO-oxidized NFC was also analyzed in QCM-D (paper III). Figure 45 shows the conjugation curve of neutravidin on NFC activated with EDC/NHS. The amount conjugated was very high approximately – 180 Hz, which corresponds to an adsorbed mass of 3730 ng/cm² (calculated by equation 3.6). When comparing to the amount of neutravidin conjugated on CMC-modified cellulose, the conjugated value was slightly higher. Neutravidin adsorption on unmodified NFC was approximately -10 Hz that corresponds to the mass adsorption of 200 ng/cm². After neutravidin conjugation, AFM images demonstrated the remarkably topography change on the NFC surface (Figure 45b-c). The cellulose nanofibrils were covered with a thick protein layer that verified the attachment of neutravidin to NFC.

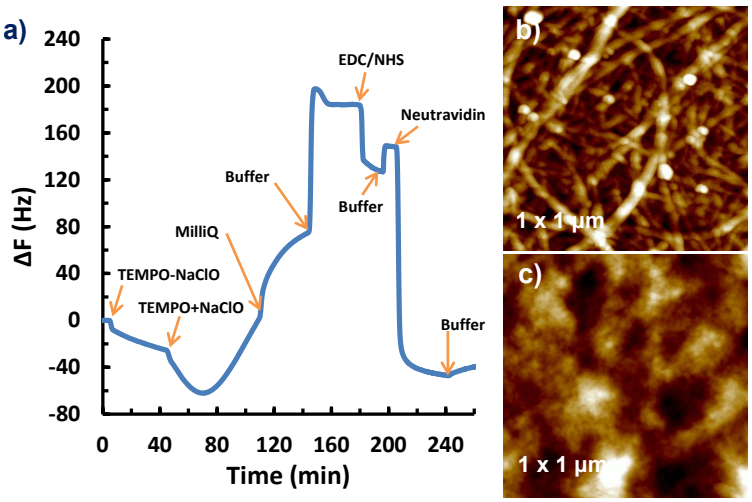

Figure 45. (a) conjugation of neutravidin on NFC with TEMPO and EDC/NHS chemistries in QCM-D. The NFC-surface was first TEMPO-oxidized (0.013 mM TEMPO, 0.47 mM NaBr, and 0.57 mM NaClO at pH 8.5) and then 100 µg/ml neutravidin at pH 5 was conjugated on activated (0.1 M EDC with 0.4 M NHS at pH 5) NFC. AFM height images for ref NFC (b) and conjugated neutravidin on NFC (c). (Paper III).

4.4.2 Effect of the oriented immobilization strategy on antigen binding of antibodies

The adsorption of biotinylated functionalities to immobilized avidin on CMC-modified cellulose were analyzed by QCM-D (Paper III). The binding of biotin-BSA on (neutr)avidin biointerfaces on CMC-modified cellulose took place rapidly, and the binding was complete within minutes, which demonstrates the high affinity of biotin to bind to avidins. The profiles of adsorbed biotin-BSA on avidin biointerfaces were similar to those reported for adsorption of biotinylated-DNA on avidin that was conjugated on carboxyl-modified gold (Caruso et al. 1997). In Figure 46 the adsorbed amounts of biotinylated-BSA on the avidin and neutravidin biointerfaces on unmodified and the two CMC-modified celluloses are compared. Avidin on unmodified and the two CMC-modified celluloses detected biotin-BSA, indicating that avidin was not denatured during the attachment processes. However, the amounts of biotin-BSA adsorbed on avidin biointerfaces with the CMC-modified celluloses were higher due to the higher avidin contents on carboxylated cellulose. As a reference, without avidin no adsorption of biotinylated-BSA on unmodified or CMC-modified cellulose was observed. The covalent conjugation of avidin on CMC-modified cellulose reduced the adsorption of biotinylated BSA. On the other hand, the covalent conjugation

did not alter the amount of biotin-BSA bound to neutravidin. The bound amounts of biotin-BSA on the avidin biointerfaces were higher compared to hemoglobin binding on monoclonal anti-hemoglobin biointerfaces on CMC-modified celluloses (Paper II). This is most likely due to the quaternary structure of avidin, which leads to better accessibility for biotinylated proteins to reach avidin. The amount of biotin-BSA adsorbed on the conjugated avidin biointerface was similar compared to the earlier published data for biotinylated-DNA on the avidin biointerface attached on top of carboxylated gold (Caruso et al. 1997).

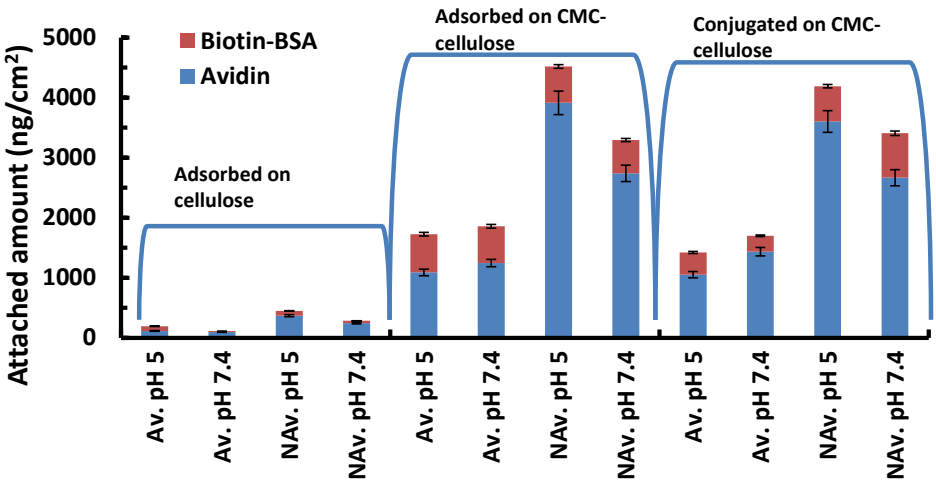

Figure 46. Adsorption of 10 µg/ml biotinylated bovine serum albumin at pH 7.4 on avidin (Av) and neutravidin (NAv) surfaces on cellulose prepared by either adsorption or conjugation methods on CMC-modified cellulose. (Paper III).

The effect of avidin-linkage on the detection of antigens was analyzed with TEMPO-oxidized NFC-surfaces by QCM-D. The avidin-biotin method was compared to the random conjugation technique. The anti-hIgG antibody was conjugated on TEMPO-oxidized NFC-surfaces using both direct EDC/NHS attachment and avidin-biotin linked conjugation. The amounts of anti-human IgG on EDC/NHS treated NFC and biotinylated anti-human IgG on avidin treated NFC were -32 and -20 Hz, respectively. The corresponding masses were 566 and 354 ng/cm² (calculated by equation 3.4), respectively. The direct conjugation method led to a slightly higher conjugated amount compared to the avidin-biotin method. In addition, anti-hIgG or hIgG (cationically charged molecules at pH 7.4) did not adsorb on superblock treated NFC, which verifies the specific attachment. Finally, 10 µg/ml hIgG at pH 7.4 was adsorbed on both biointerfaces. The adsorbed masses on random orientated (direct conjugation) and avidin linked biointerfaces were -5 and -10 Hz,

respectively. The corresponding masses were 89 and 177 ng/cm² (calculated by equation 3.4), respectively. The orient anti-hIgG biointerface binds over two-fold more hIgG compared to the random orient anti-hIgG biointerface. This difference is accordance with earlier published data of Lu et al. (1995), Kang et al. (2007) and Pei, Yang & Wang (2001), where they found over two-fold better binding ability for whole antibodies when orient immobilization chemistries were used. In addition, the antigen binding ability of orientated conjugated individual FAB fragments has been reported to be over six-fold better compared to random orientated antibodies (Peluso et al. 2003).

4.5 Preparation of a biointerface on NFC-films

Preparation of an antibody biointerface on a nanofibrillar cellulose (NFC) film using immobilization chemistries examined in the previous sections is represented in this chapter. Rather water resistant and smooth NFC films are ideal materials for several applications. In this work NFC-films were used as a support for biointerfaces by using topographical surface activation chemistry (Figure 47). The detailed results can be found in Paper IV.

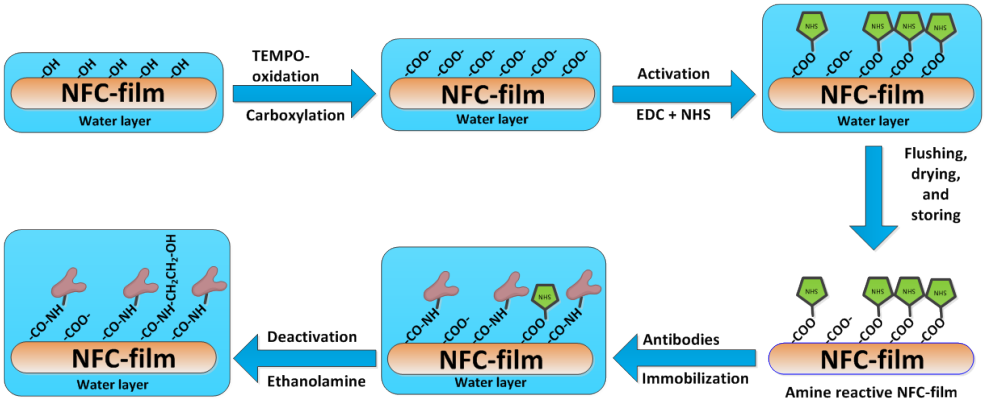

Figure 47. Schematic illustration of the immobilization of antibodies on topographically modified NFC-films. NFC-films are carboxylated by TEMPO-mediated oxidation, and transferred to amine reactive form by EDC/NHS activation. Attachment of antibodies can be carried out using non-contact inkjet printing or adsorption techniques.

Low charged NFC-film has a rather low water uptake due to the lack of macro pores and high compatibility of cellulose nanofibrils together (Spence et al. 2010)(Nogi et al. 2009). However, the lack of functional conjugation sites on unmodified cellulose nanofibrils leads to the demand to find a surface functionalization strategy that does not break the structure

of the NFC-film. In this work TEMPO-oxidation was selected to introduce conjugation sites on the NFC-films. Figure 48a shows the effect of TEMPO-oxidation on the contact angle and charge of the oxidized NFC-film. The contact angle decreased to below 10° after a 30 sec TEMPO-oxidation period. The oxidation kinetics on NFC-surfaces seem to be extremely fast, most likely due to the high accessibility. The highest charge after a 300 sec oxidation time was approximately 235 μeq/g, which is probably close to the maximum value that can be obtained without breaking the NFC-film. The aldehydes are not measured in conductometric titration, and therefore the observed increase corresponds to the introduction of carboxyls on a NFC-film. Compared to fully oxidized cellulose nanofibrils (charge approximately 1200 μeq/g (Saito et al. 2006)), the charge of the carboxylated NFC-films was low, which suggests that the short TEMPO-oxidation treatment only modifies the surfaces of the NFC-film.

The dried TEMPO-oxidized NFC-films were imaged with AFM (Figure 48b and c). Compared to the reference sample, only small topographical changes were observed after TEMPO-oxidation. The most important finding was observed with the phase images of AFM where significant softening of the surfaces of the NFC-film was observed after carboxylation. This was expected to be caused by water binding from the room atmosphere to the hydrophilic NFC-film. The carboxylation of the surfaces of the NFC-films was characterized also with XPS. Table 3 shows the XPS data for TEMPO-oxidized NFC-films. A small increase in the C=O and C-C bonds was observed on a TEMPO-oxidized NFC-film. However, in the literature it has been proposed that carboxyl formation in an OH of C6 carbon of cellulose cannot be observed in XPS data (DiFlavio et al. 2007).

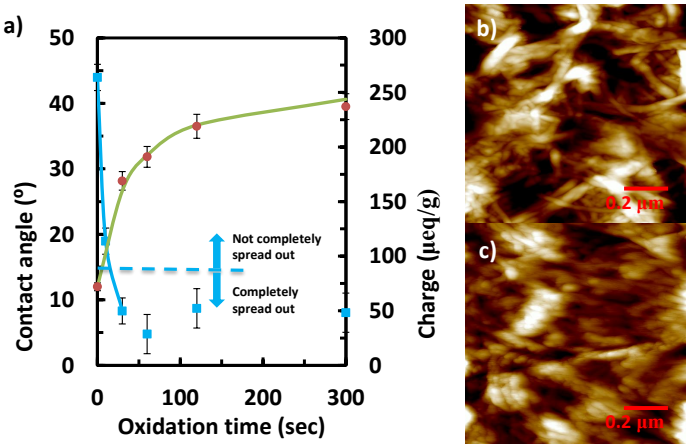

Figure 48. Changes in charge and contact angle during alkaline TEMPO-oxidation (pH 10) of NFC-films with varying oxidation times (a). AFM images of NFC-film before (a) and after 120 sec TEMPO-oxidation. (Paper IV).

Table 3. XPS data for TEMPO-oxidized NFC films before and after EDC/NHS activation. (Paper IV).

	TEMPO-oxidation time (sec.)	O 1s (at. %)	C 1s (at. %)	C 1s components (%) C(C-C) (%)	C(C-O) (%)	C(C=O) (%)	C(COO) (%)	N 1s (at. %)
TEMPO-oxidized NFC-films	0	40.0	60.0	5.8	42.2	10.7	1.3	0.0
	30	39.7	60.1	7.5	40.8	10.8	1.0	0.2
	60	38.5	60.9	8.9	39.2	11.8	1.1	0.1
	120	39.4	59.7	7.9	39.6	11.0	1.1	0.1
	300	38.6	60.3	9.5	38.9	10.8	1.1	0.2
TEMPO-oxidized plus EDC/NHS activated NFC-films	30	38.9	60.5	7.2	41.5	10.7	1.1	0.6
	60	38.9	60.4	7.7	41.1	10.5	1.1	0.7
	300	39.9	57.9	7.2	38.9	10.4	1.4	2.2
Human IgG adsorbed on activated NFC-films	300	31.8	62.3	14.3	34.9	12.1	1.0	5.8

After TEMPO-oxidation, the carboxylated NFC-films were treated with an EDC/NHS solution, where the amine reactive NHS-esters were linked to the carboxylated NFC-films (mechanism is shown in Figure 12). The attachment of NHS on carboxylated NFC-films was analyzed with XPS, where the nitrogen signal was followed (only NHS contains nitrogen). The nitrogen content increased linearly as a function of oxidation time, which demonstrate the presence of NHS-groups, and a subsequent increase in the amount of carboxyls. However, the increase was not fully linear with the charge of the NFC-film measured with conductometric titration that may verify the higher carboxyl content compared to aldehydes when longer oxidation times are used. In the initial state, the TEMPO-oxidation reaction has been observed to produce almost an equal amount of aldehydes and carboxyls on surfaces of cellulose nanofibrils, but in the later stage the content of carboxyls is more dominating (Saito, Isogai 2004). The stability of the attached NHS-groups on NFC-surfaces after a drying period was examined with QCM-D with NFC-model cellulose surfaces. BSA coupling to the activated NFC-surface was observed after a one day storage period, demonstrating that the NHS-groups were present on the dried carboxylated NFC-surfaces.

Inkjet printing and simple adsorption techniques were employed to demonstrate the attachment of antibodies on topographically activated NFC-films. Inkjet printing is a non-contact deposition method that is widely used for depositing antibodies and other proteins on various substrates (Bruzewicz, Reches & Whitesides 2008)(Abe, Suzuki & Citterio 2008)(Di Risio, Yan March 2010)(Delaney, Smith & Schubert 2009)(Hossain et al. 2009). Figure 49a shows a fluorescence image of a dansyl-stained anti-hIgG biointerface that was prepared by inkjet printing on an activated NFC-film. The NFC-film had a rather high auto-fluorescence that can be seen as the white color at the unprinted regions. However, the visible print “Aa” verifies the region where the dansylated-antibody was printed. The

inkjet printing of fluorescein stained anti-human IgG on activated NFC-films was also tested. Figure 49b shows the CLSM fluorescence intensity image for a border of the texture of printed antibody. Due to the small image dimensions of the CLSM technique, only a small section of the printed antibody texture can be seen. The adsorption of FITC-stained anti-hIgG on activated NFC-films was analyzed with CLSM. Figure 49c-d verified the formation of covalent bonds between anti-hIgG and activated NFC-films. The fluorescence intensity was ten-fold higher when topographical activation chemistry was used, which demonstrates the formation of covalent linkages between antibodies and the NFC-film. This finding is accordance with an earlier report — the NHS ester group linked to a carboxyl is rather stable, and its half-time in water (neutral pH) is hours (Hermanson 2008). The attachment was further investigated by a XPS, and significant increase in the nitrogen content (nitrogen content of 2.2 % vs. 5.8 % after NHS-activation) was observed that verified the covalent attachment of anti-hIgG on an activated NFC-film (Table 3). Topographically activated NFC-films could be useful in immunodiagnostics (mainly ELISA testing) and filtration applications.

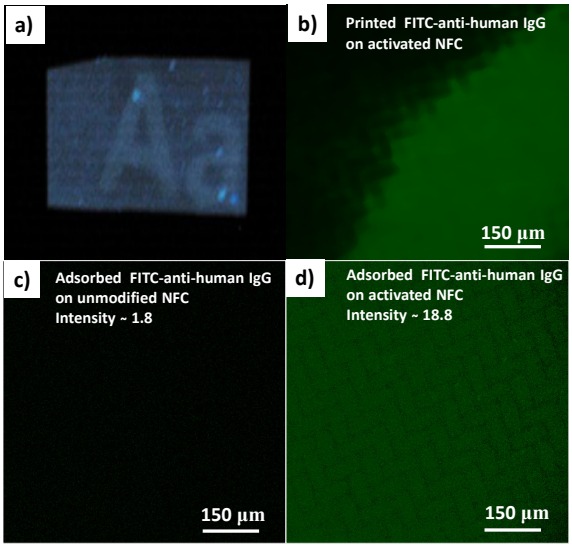

Figure 49. Printed dansylated anti-human IgG (1 mg/ml in 10 mM phosphate buffer at pH 7.4) on an activated NFC-film under UV-light (366 nm) (a). CLSM-intensity image for printed FITC-stained anti-human IgG (1 mg/ml in 10 mM phosphate buffer at pH 7.4) on an activated NFC-film (b). CLSM intensity images for adsorbed FITC-stained anti-human IgG (0.1 mg/ml in 10 mM phosphate buffer at pH 7.4) on an unmodified (c) and an activated NFC-film (d). Both surfaces were rinsed with 10 mM NaCl at pH 10 to remove electrostatically bound antibodies. CLSM images are recorded using 848 V laser power with constant imaging conditions. (Paper IV).

5 Concluding remarks

The immobilization of proteins on solid supports is the initial step in the development of immunodiagnostic tests. In this thesis different methods to immobilize antibodies on cellulosic supports were investigated. The first part relates to the interactions of proteins with cellulose, and how protein adsorption can be controlled by using surface modification chemistries. In the second part, immobilization strategies to covalently attach antibodies on cellulose surfaces were developed. The third part of this thesis deals with the use of the immobilization strategies developed to prepare an antibody biointerface on NFC-films.

First, surface plasmon resonance (SPR) studies were exploited in order to examine the adsorption of proteins on modified cellulose surfaces. The findings suggest that the adsorption of proteins on unmodified cellulose is driven mainly by non-electrostatic forces, and adsorption is largely irreversible. On low charged cellulose surfaces, all proteins tested adsorbed mostly at their isoelectric points (pI) due to their reduced solubility in water. The increased surface charge that promotes the electrostatic interaction of globular proteins lead to increased adsorption on the cellulose surface. The electrostatic interaction introduced enhanced the absorption on cellulose surfaces for all tested proteins. The adsorption phenomenon of glycoproteins is more complicated compared to globular proteins since the adsorption is promoted by combinations of non-electrostatic and electrostatic interactions. Moreover, the oligosaccharide chains of avidin were found to reduce the adsorption of glycoproteins on cellulose surfaces.

In order to introduce functional groups on cellulosic surfaces for enabling covalent conjugation of antibodies on cellulose, CMC-adsorption, chitosan-adsorption, and TEMPO-oxidation methods were explored by QCM-D. The studies showed that both CMC and chitosan adsorbed irreversibly on cellulose surfaces but their adsorption phenomena varied slightly. The adsorbed chitosan layer on cellulose has a less extended conformation compared to the adsorbed CMC layer due to the presence of electrostatic attractive interactions. Both polysaccharide layers had a hydrogel like structure and they coupled significant amounts of water. The chemical modification method, TEMPO-oxidation created carboxyl groups on cellulose that was observed to cause significant water uptake in the cellulose film. The TEMPO-oxidation reaction was extremely fast, and seems to be a usable tool to functionalize cellulosic materials. However, the possible irreversible structural changes it causes in the cellulosic material must be considered.

All tested functionalization strategies enabled covalent conjugation of antibodies to cellulose. The CMC and TEMPO-oxidation methods were more usable compared to chitosan modification due to the lack of self-crosslinking in antibodies. The CMC-modification method is also a gentle method that does not alter the substructure of a cellulosic matrix. Both the CMC-modification and the TEMPO-oxidation methods led to similar surface coverages for immobilized antibodies. The biological activity of conjugated antibodies on CMC-modified and TEMPO-oxidized cellulose surfaces were verified with specific counter parts. The specific detection of antigens with high detection efficiency was found that suggest the usability of the developed immobilization routes towards the development of immunodiagnostic applications.

The avidin-biotin chemistry was used to orient the conformation of antibodies on cellulose surfaces for enhancing the detection sensitivity of the cellulose based biointerface. The attachment of avidin on cellulose can be significantly enhanced by increasing the anionic charge on cellulosic surfaces by CMC-adsorption and by TEMPO-oxidation. The immobilized avidins bind biotinylated proteins specifically, which verifies the negligible changes in their biological activity. The avidin-biotin system was compared to traditional EDC/NHS conjugation, and an over two-fold better antigen detection was found compared to the traditional conjugation chemistry.

Finally, NFC-films were utilized to act as a support for biointerfaces. The NFC-films were first activated with TEMPO-oxidation. The studies shown that only a short TEMPO-oxidation treatment was needed to create a high carboxyl content on the surfaces of a NFC-film without remarkable damage to the substructure or water resistivity of the NFC-film. The surface sensitive carboxylated NFC-films were transferred to amine reactive form by EDC/NHS activation. The amine reactivity of the activated NFC-film was demonstrated after a drying period, which showed that the reactivity of the film remains at least short periods. The conjugation of antibodies on activated NFC-films was carried out using both inkjet and adsorption methods. The covalent linking reaction was observed only when the activation chemistry was utilized.

Taken together, understanding of the adsorption of proteins and their conjugation phenomena on cellulosic materials give us valuable information on how cellulosic materials can be utilized in advanced immunodiagnostic applications.

6 References

Abe, K., Suzuki, K. & Citterio, D. 2008, "Inkjet-printed microfluidic multianalyte chemical sensing paper", *Analytical Chemistry,* vol. 80, no. 18, pp. 6928-6934.

Agnihotri, V. & Giles, C. 1972, "The cellulose-dye adsorption process. A study by the monolayer method", *Journal of the Chemical Society,* vol. 2, no. 15, pp. 2241-2246.

Ahola, S., Myllytie, P., Österberg, M., Teerinen, T. & Laine, J. 2008a, "Effect of polymer adsorption on cellulose nanofibril water binding capacity and aggregation", *Bioresources,* vol. 3, no. 4, pp. 1315-1328.

Ahola, S., Salmi, J., Johansson, L.-., Laine, J. & Österberg, M. 2008b, "Model Films from Native Cellulose Nanofibrils. Preparation, Swelling, and Surface Interactions", *Biomacromolecules,* vol. 9, no. 4, pp. 1273-1282.

Ahola, S., Turon, X., Österberg, M., Laine, J. & Rojas, O.J. 2008c, "Enzymatic Hydrolysis of Native Cellulose Nanofibrils and Other Cellulose Model Films: Effect of Surface Structure", *Langmuir,* vol. 24, no. 20, pp. 11592-11599.

Allen, S., Chen, X., Davies, J., Davies, M.C., Dawkes, A.C., Edwards, J.C., Roberts, C.J., Sefton, J., Tendler, S.J.B. & Williams, P.M. 1997, "Detection of Antigen-Antibody Binding Events with the Atomic Force Microscopy ", *Biochemistry,* vol. 36, no. 24, pp. 7457-7463.

Amit, A., Mariuzza, R., Phillips, S. & Poljak, R. 1986, "Three-dimensional structure of an antigen-antibody complex at 2.8 A resolution", *Science,* vol. 233, no. 4765, pp. 747-753.

Arai, T. & Norde, W. 1990, "The behavior of some model proteins at solid-liquid interfaces 1. Adsorption from single protein solutions", *Colloids and Surfaces,* vol. 51, no. 0, pp. 1-15.

Arakawa, T. & Timasheff, S.N. 1984, "Mechanism of protein salting in and salting out by divalent cation salts: balance between hydration and salt binding", *Biochemistry,* vol. 23, no. 25, pp. 5912-5923.

Araki, J., Wada, M. & Kuga, S. 2001, "Steric Stabilization of a Cellulose Microcrystal Suspension by Poly(ethylene glycol) Grafting", *Langmuir,* vol. 17, no. 1, pp. 21-27.

Arola, S., Tammelin, T., Setälä, H., Tullila, A. & Linder, M. 2012, "Immobilization-stabilization of proteins on nanofibrillated cellulose derivatives and their bioactive film formation", *Biomacromolecules,* vol. 13, no. 3, pp. 594-603.

Aslan, F.M., Yu, Y., Mohr, S.C. & Cantor, C.R. 2005, "Engineered single-chain dimeric streptavidins with an unexpected strong preference for biotin-4-fluorescein", *Proceedings of the National Academy of Sciences of the United States of America,* vol. 102, no. 24, pp. 8507-8512.

Atalla, R.H. & Vanderhart, D.L. 1984, "Native Cellulose: A Composite of Two Distinct Crystalline Forms", *Science,* vol. 223, no. 4633, pp. 283-285.

Atalla, R.H., Hackney, J.M., Uhlin, I. & Thompson, N.S. 1993, "Hemicelluloses as structure regulators in the aggregation of native cellulose", *International journal of biological macromolecules,* vol. 15, no. 2, pp. 109-112.

Aulin, C., Ahola, S., Josefsson, P., Nishino, T., Hirose, Y., Österberg, M. & Wagberg, L. 2009, "Nanoscale Cellulose Films with Different Crystallinities and Mesostructures-Their Surface Properties and Interaction with Water", *Langmuir,* vol. 25, no. 13, pp. 7675-7685.

Aulin, C., Gällstedt, M. & Lindström, T. 2010, "Oxygen and oil barrier properties of microfibrillated cellulose films and coatings", *Cellulose,* vol. 17, no. 3, pp. 559-574.

Bayer, E., De Meester, F., Kulik, T. & Wilchek, M. 1995, "Preparation of deglycosylated egg white avidin", *Applied Biochemistry and Biotechnology,* vol. 53, no. 1, pp. 1-9.

Bhattacharya, A. & Misra, B.N. 2004, "Grafting: a versatile means to modify polymers: Techniques, factors and applications", *Progress in Polymer Science,* vol. 29, no. 8, pp. 767-814.

Binnig, G., Quate, C. & Gerber, C. 1986, "Atomic force microscope", *Physical Review Letters,* , no. 56, pp. 930-934.

Blodgett, K.B. 1935, "Films Built by Depositing Successive Monomolecular Layers on a Solid Surface", *Journal of the American Chemical Society,* vol. 57, no. 6, pp. 1007-1022.

Boerjan, W., Ralp, J. & Baucher, M. 2003, "Lignin biosynthesis", *Annual Review of Plant Biology,* vol. 54, pp. 519-546.

Böhme, U. & Scheler, U. 2007, "Effective charge of bovine serum albumin determined by electrophoresis NMR", *Chemical Physics Letters,* vol. 435, no. 4-6, pp. 342-345.

Bordo, D. & Argos, P. 1991, "Suggestions for “safe” residue substitutions in site-directed mutagenesis", *Journal of Molecular Biology,* vol. 217, no. 4, pp. 721-729.

Boujday, S., Bantegnie, A., Briand, E., Marnet, P., Salmain, M. & Pradier, C. 2008, "In-Depth Investigation of Protein Adsorption on Gold Surfaces: Correlating the Structure and Density to the Efficiency of the Sensing Layer", *The Journal of Physical Chemistry B,* vol. 112, no. 21, pp. 6708-6715.

Braden, B. & Poljak, R. 1995, "Structural features of the reactions between antibodies and protein antigens", *The FASEB Journal,* vol. 9, no. 1, pp. 9-16.

Bragd, P.L., van Bekkum, H. & Besemer, A.C. 2004, "TEMPO-Mediated Oxidation of Polysaccharides: Survey of Methods and Applications", *Topics in Catalysis,* vol. 27, no. 1, pp. 49-66.

Branden, C. & Tooze, J. cop. 1999, *Introduction to protein structure,* 2. ed. edn, Garland Publ, New York (N.Y.).

Bruzewicz, D.A., Reches, M. & Whitesides, G.M. 2008, "Low-Cost Printing of Poly(dimethylsiloxane) Barriers To Define Microchannels in Paper", *Analytical Chemistry,* vol. 80, no. 9, pp. 3387-3392.

Buijs, J. & Hlady, V. 1997, "Adsorption Kinetics, Conformation, and Mobility of the Growth Hormone and Lysozyme on Solid Surfaces, Studied with TIRF", *Journal of colloid and interface science,* vol. 190, no. 1, pp. 171-181.

Canfield, S.M. & Morrison, S.L. 1991, "The binding affinity of human IgG for its high affinity Fc receptor is determined by multiple amino acids in the CH2 domain and is modulated by the hinge region.", *The Journal of experimental medicine,* vol. 173, no. 6, pp. 1483-1491.

Carrigan, S.D., Scott, G. & Tabrizian, M. 2005a, "Rapid three-dimensional biointerfaces for real-time immunoassay using hIL-18BPa as a model antigen", *Biomaterials,* vol. 26, no. 35, pp. 7514-7523.

Carrigan, S.D., Scott, G. & Tabrizian, M. 2005b, "Real-Time QCM-D Immunoassay through Oriented Antibody Immobilization Using Cross-Linked Hydrogel Biointerfaces", *Langmuir,* vol. 21, no. 13, pp. 5966-5973.

Carrigan, S.D. & Tabrizian, M. 2005, "Reducing Nonspecific Adhesion on Cross-Linked Hydrogel Platforms for Real-Time Immunoassay in Serum", *Biochemical Methods,* vol. 21, no. 26, pp. 12320-12326.

Caruso, F., Rodda, E., Furlong, D.N., Niikura, K. & Okahata, Y. 1997, "Quartz Crystal Microbalance Study of DNA Immobilization and Hybridization for Nucleic Acid Sensor Development", *Analytical Chemistry,* vol. 69, no. 11, pp. 2043-2049.

Cheng, C., Martinez, A., Gong, J., Mace, C., Phillips, S., Carrilho, E., Mirica, K. & Whitesides, G. 2010, "Paper-Based ELISA", *Angewandte Chemie International Edition,* vol. 49, no. 28, pp. 4771-4774.

Cooper, G.K., Sandberg, K.R. & Hinck, J.F. 1981, "Trimethylsilyl cellulose as precursor to regenerated cellulose fiber", *Journal of Applied Polymer Science,* vol. 26, no. 11, pp. 3827-3836.

Cooper, M.A. 2002, "Optical biosensors in drug discovery", *Nat Rev Drug Discov,* vol. 1, no. 7, pp. 515-528.

Cosgrove, D.J. 2005, "Growth of the plant cell wall", *Nature reviews. Molecular cell biology,* vol. 6, no. 11, pp. 850-861.

Davies, D.R., Sheriff, S. & Padlan, E.A. 1988, "Antibody-antigen complexes.", *Journal of Biological Chemistry,* vol. 263, no. 22, pp. 10541-10544.

Dawsey, T.R. & McCormick, C.L. 1990, "The lithium chloride/dimethylacetamide solvent for cellulose: a literature review", *Journal of Macromolecular Science, Part C: Polymer Reviews,* vol. 30, no. 3-4, pp. 405-440.

De Nooy, A., Besemer, A.C. & Van Bekkum, H. 1995, "Highly selective nitroxyl radical-mediated oxidation of primary alcohol groups in water-soluble glucans", *Carbohydrate research,* vol. 269, no. 1, pp. 89-98.

Delaney, J.T., Smith, P.J. & Schubert, U.S. 2009, "Inkjet printing of proteins", *Soft Matter,* vol. 5, no. 24, pp. 4866-4877.

DeLange, R.J. & Huang, T. 1971, "Egg White Avidin", *Journal of Biological Chemistry,* vol. 246, no. 3, pp. 698-709.

Deville, W., Yzermans, J., van Duijn, N., Bezemer, P.D., van der Windt, D. & Bouter, L. 2004, "The urine dipstick test useful to rule out infections. A meta-analysis of the accuracy", *BMC Urology,* vol. 4, no. 4, pp. 1-14.

Di Risio, S. & Yan, N. March 2010, "Bioactive Paper Through Inkjet Printing", *Journal of Adhesion Science and Technology,* vol. 24, pp. 661-684.

DiFlavio, J., Pelton, R., Leduc, M., Champ, S., Essig, M. & Frechen, T. 2007, "The role of mild TEMPO–NaBr–NaClO oxidation on the wet adhesion of regenerated cellulose membranes with polyvinylamine", *Cellulose,* vol. 14, no. 3, pp. 257-268.

Duchesne, I. & Daniel, G. 2000, "Changes in surface ultrastructure of norway spruce fibres during kraft pulping - visualisation by field emission sem.", *Nordic Pulp Pap.Res.J.,* , no. 15, pp. 54-61.

Duchesne, I., Hult, E., Molin, U., Daniel, G., Iversen, T. & Lennholm, H. 2001, "The influence of hemicellulose on fibril aggregation of kraft pulp fibres as revealed by FE-SEM and CP/MAS 13C-NMR", *Cellulose,* vol. 8, no. 2, pp. 103-111.

Dupont-Filliard, A., Billon, M., Bidan, G. & Guillerez, S. 2004, "Investigation by QCM of the Specific and Nonspecific Avidin Interaction onto a Biotinylated Polypyrrole Film", *Electroanalysis,* vol. 16, no. 8, pp. 667-673.

Elias, K. 2000, "Affinity membranes: a 10-year review", *Journal of Membrane Science,* vol. 179, no. 1–2, pp. 1-27.

Engvall, E. & Perlmann, P. 1971, "Enzyme-linked immunosorbent assay (ELISA) quantitative assay of immunoglobulin G", *Immunochemistry,* vol. 8, no. 9, pp. 871-874.

Eronen, P., Junka, K., Laine, J. & Österberg, M. 2011a, "Interaction between water-soluble polysaccharides and native nanofibrillar cellulose thin films", *BioResources,* , no. 6, pp. 4200-4217.

Eronen, P., Österberg, M., Heikkinen, S., Tenkanen, M. & Laine, J. 2011b, "Interactions of structurally different hemicelluloses with nanofibrillar cellulose", *Carbohydrate Polymers,* vol. 86, no. 3, pp. 1281-1290.

Fahlen, J. & Salmen, L. 2005, "Pore and Matrix Distribution in the Fiber Wall Revealed by Atomic Force Microscopy and Image Analysis", *Biomacromolecules,* vol. 6, no. 1, pp. 433-438.

Fall, A.B., Lindstrom, S.B., Sundman, O., Oldberg, L. & Wågberg, L. 2011, "Colloidal Stability of Aqueous Nanofibrillated Cellulose Dispersions", *Langmuir,* vol. 27, no. 18, pp. 11332-11338.

Fenton, E.M., Mascarenas, M.R., López, G.P. & Sibbett, S.S. 2009, "Multiplex Lateral-Flow Test Strips Fabricated by Two-Dimensional Shaping", - *ACS Applied Materials & Interfaces,* , no. 1, pp. 124-129.

Fernandez-Lafuente, R., Rosell, C.M., Rodriguez, V., Santana, C., Soler, G., Bastida, A. & Guisán, J.M. 1993, "Preparation of activated supports containing low pK amino groups. A new tool for protein immobilization via the carboxyl coupling method", *Enzyme and microbial technology,* vol. 15, no. 7, pp. 546-550.

Filpponen, I. & Argyropoulos, D.S. 2010, "Regular Linking of Cellulose Nanocrystals via Click Chemistry: Synthesis and Formation of Cellulose Nanoplatelet Gels", *Biomacromolecules,* vol. 11, no. 4, pp. 1060-1066.

Fink, H. & Philipp, B. 1985, "Models of cellulose physical structure from the viewpoint of the cellulose I ? II transition", *Journal of Applied Polymer Science,* vol. 30, no. 9, pp. 3779-3790.

Forsgren, A. & Sjöquist, J. 1966, ""Protein A" from S. Aureus", *The Journal of Immunology,* vol. 97, no. 6, pp. 822-827.

Free, A.H., Adams, E.C., Kercher, M.L., Free, H.M. & Cook, M.H. 1957, "Simple Specific Test for Urine Glucose", *Clinical chemistry,* vol. 3, no. 3, pp. 163-168.

Friguet, B., Chaffotte, A.F., Djavadi-Ohaniance, L. & Goldberg, M.E. 1985, "Measurements of the true affinity constant in solution of antigen-antibody complexes by enzyme-linked immunosorbent assay", *Journal of immunological methods,* vol. 77, no. 2, pp. 305-319.

Fujisawa, S., Okita, Y., Fukuzumi, H., Saito, T. & Isogai, A. 2011, "Preparation and characterization of TEMPO-oxidized cellulose nanofibril films with free carboxyl groups", *Carbohydrate Polymers,* vol. 84, no. 1, pp. 579-583.

Geffroy, C., Labeau, M.P., Wong, K., Cabane, B. & Cohen Stuart, M.A. 2000, "Kinetics of adsorption of polyvinylamine onto cellulose", *Colloids and Surfaces A: Physicochemical and Engineering Aspects,* vol. 172, no. 1-3, pp. 47-56.

Gersten, D.M. & Marchalonis, J.J. 1978, "A rapid, novel method for the solid-phase derivatization of IgG antibodies for immune-affinity chromatography", *Journal of immunological methods,* vol. 24, no. 3-4, pp. 305-309.

Ghanem, A. & Ghaly, A. 2004, "Immobilization of glucose oxidase in chitosan gel beads", *Journal of Applied Polymer Science,* vol. 91, no. 2, pp. 861-866.

Gilles, M.A., Hudson, A.Q. & Borders Jr., C.L. 1990, "Stability of water-soluble carbodiimides in aqueous solution", *Analytical Biochemistry,* vol. 184, no. 2, pp. 244-248.

Goldstein, L., Yankofsky, S.A., Cohen, G. & Frank Chytil and Donald, B.M. 1986, "[13] Solid-phase assay for d-biotin and avidin on cellulose disks", *Methods in Enzymology,* vol. 122, pp. 72-82.

Gondo, T., Watanabe, M., Soma, H., Kitao, O., Yanagisawa, M. & Isogai, A. 2006, "SEC-MALS study on carboxymethyl cellulose (CMC): Relationship between conformation of CMC molecules and their adsorption behavior onto pulp fibers", *Nordic Pulp & Paper Research Journal,* vol. 21, no. 5, pp. 591-597.

Grabarek, Z. & Gergely, J. 1990, "Zero-length crosslinking procedure with the use of active esters", *Analytical Biochemistry,* vol. 185, no. 1, pp. 131-135.

Greber, G. & Paschinger, O. 1981, "Silylderivate der cellulose", *Papier,* , no. 35, pp. 547-554.

Green, N.M. 1975, "Avidin", *Advances in protein chemistry,* vol. Volume 29, no. 29, pp. 85-133.

Green, N.M. & Joynson, M.A. 1970, "A preliminary crystallographic investigation of avidin", *Biochemical Journal,* vol. 118, no. 1, pp. 71-72.

Guesdon, J.L., Ternynck, T. & Avrameas, S. 1979, "The use of avidin-biotin interaction in immunoenzymatic techniques.", *Journal of Histochemistry & Cytochemistry,* vol. 27, no. 8, pp. 1131-1139.

Habibi, Y., Chanzy, H. & Vignon, M. 2006, "TEMPO-mediated surface oxidation of cellulose whiskers", *Cellulose,* vol. 13, no. 6, pp. 679-687.

Hage, D.S. 1999, "Affinity Chromatography: A Review of Clinical Applications", *Clinical chemistry,* vol. 45, no. 5, pp. 593-615.

Hall, D.B., Underhill, P. & Torkelson, J.M. 1998, "Spin coating of thin and ultrathin polymer films", *Polymer Engineering & Science,* vol. 38, no. 12, pp. 2039-2045.

Hamilton, R. 1987, "Human IgG subclass measurements in the clinical laboratory.", *Clin Chem,* , no. 33, pp. 1070-1075.

Hawkes, R., Niday, E. & Gordon, J. 1982, "A dot-immunobinding assay for monoclonal and other antibodies", *Analytical Biochemistry,* vol. 119, no. 1, pp. 142-147.

Haynes, C.A. & Norde, W. 1994, "Globular proteins at solid/liquid interfaces", *Colloids and Surfaces B: Biointerfaces,* vol. 2, no. 6, pp. 517-566.

Hearle, J.W.S. 1958, "A fringed fibril theory of structure in crystalline polymers", *Journal of Polymer Science,* vol. 28, no. 117, pp. 432-435.

Heikkinen, J.J., Kivimäki, L., Määttä, J.A.E., Mäkelä, I., Hakalahti, L., Takkinen, K., Kulomaa, M.S., Hytönen, V.P. & Hormi, O.E.O. 2011, "Versatile bio-ink for covalent immobilization of chimeric avidin on sol–gel substrates", *Colloids and Surfaces B: Biointerfaces,* vol. 87, no. 2, pp. 409-414.

Heinze, T. & Koschella, A. 2005, "Carboxymethyl Ethers of Cellulose and Starch. A Review", *Macromolecular Symposia,* vol. 223, no. 1, pp. 13-40.

Henriksson, M., Berglund, L.A., Isaksson, P., LindstroÌˆm, T. & Nishino, T. 2008, "Cellulose Nanopaper Structures of High Toughness", *Biomacromolecules,* vol. 9, no. 6, pp. 1579-1585.

Hermanson, G.T. 2008, *Bioconjugate techniques,* Academic Press, San Diego (CA).

Herrick, F., Casebier, R., Hamilton, J. & Sandberg, K. 1983, "Microfibrillated cellulose: Morphology and accessibility.", *J. Appl. Polym. Sci.: Appl. Polym. Symp.,* vol. 2, no. 37, pp. 797-813.

Hiller, Y., Gershoni, J.M., Bayer, E.A. & Wilchek, M. 1987, "Biotin binding to avidin. Oligosaccharide side chain not required for ligand association", *Biochem. J.,* vol. 248, no. 1, pp. 167-171.

Hirota, M., Furihata, K., Saito, T., Kawada, T. & Isogai, A. 2010, "Glucose/Glucuronic Acid Alternating Co-polysaccharides Prepared from TEMPO-Oxidized Native Celluloses by Surface Peeling", *Angewandte Chemie,* vol. 122, no. 42, pp. 7836-7838.

Homola, J., Yee, S.S. & Gauglitz, G. 1999, "Surface plasmon resonance sensors: review", *Sensors and Actuators B: Chemical,* vol. 54, no. 1-2, pp. 3-15.

Höök, F., Rodahl, M., Brzezinski, P. & Kasemo, B. 1998, "Energy dissipation kinetics for protein and antibody-antigen adsorption under shear oscillation on a quartz crystal microbalance", *Langmuir,* vol. 14, no. 4, pp. 729-734.

Hossain, S.M., Luckham, R.E., Smith, A.M., Lebert, J.M., Davies, L.M., Pelton, R.H., Filipe, C.D. & Brennan, J.D. 2009, "Development of a bioactive paper sensor for detection of neurotoxins using piezoelectric inkjet printing of sol-gel-derived bioinks", *Analytical Chemistry,* vol. 81, no. 13, pp. 5474-5483.

Ishimaru, Y. & Lindström, T. 1984, "Adsorption of water-soluble, nonionic polymers onto cellulosic fibers", *Journal of Applied Polymer Science,* vol. 29, no. 5, pp. 1675-1691.

Isogai, A. & Kato, Y. 1998, "Preparation of polyuronic acid from cellulose by TEMPO-mediated oxidation.", *Cellulose,* vol. 5, no. 5, pp. 153-164.

Jameson, D.M. & Wong, S.S. 2009, *Chemistry of Protein Conjugation and Cross-Linking, Second Edition,* Taylor and Francis.

Jefferis, R. 2009, "Glycosylation as a strategy to improve antibody-based therapeutics", *Nat Rev Drug Discov,* vol. 8, no. 3, pp. 226-234.

Johannsmann, D., Mathauer, K., Wegner, G. & Knoll, W. 1992, "Viscoelastic properties of thin films probed with a quartz-crystal resonator", *Phys.Rev.B,* vol. 46, no. 12, pp. 7808-7815.

Johansson, L. & Campbell, J.M. 2004, "Reproducible XPS on biopolymers: cellulose studies", *Surface and Interface Analysis,* vol. 36, no. 8, pp. 1018-1022.

Johnsson, B., Löfås, S., Lindquist, G., Edström, Å., Hillgren, R.M. & Hansson, A. 1995, "Comparison of methods for immobilization to carboxymethyl dextran sensor surfaces by analysis of the specific activity of monoclonal antibodies", *Journal of Molecular Recognition,* vol. 8, no. 1-2, pp. 125-131.

Jung, L.S., Campbell, C.T., Chinowsky, T.M., Mar, M.N. & Yee, S.S. 1998, "Quantitative Interpretation of the Response of Surface Plasmon Resonance Sensors to Adsorbed Films", *Langmuir,* vol. 14, no. 19, pp. 5636-5648.

Kang, J.H., Choi, H.J., Hwang, S.Y., Han, S.H., Jeon, J.Y. & Lee, E.K. 2007, "Improving immunobinding using oriented immobilization of an oxidized antibody", *Journal of Chromatography A,* vol. 1161, no. 1–2, pp. 9-14.

Kästner, U., Hoffmann, H., Dönges, R. & Hilbig, J. 1997, "Structure and solution properties of sodium carboxymethyl cellulose", *Colloids and Surfaces A: Physicochemical and Engineering Aspects,* vol. 123-124, no. 0, pp. 307-328.

Kenna, J.G., Major, G.N. & Williams, R.S. 1985, "Methods for reducing non-specific antibody binding in enzyme-linked immunosorbent assays", *Journal of immunological methods,* vol. 85, no. 2, pp. 409-419.

Kim, J., Yamasaki, R., Park, J., Jung, H., Lee, H. & KawaiI, T. 2004, "Highly Dense Protein Layers Confirmed by Atomic Force Microscopy and Quartz Crystal Microbalance", *Journal of bioscience and bioengineering.,* vol. 97, no. 2, pp. 138-140.

Klemm, D. 1998, *Comprehensive cellulose chemistry. Volume 1, Fundamentals and analytical methods,* Wiley-VCH, Weinheim.

Klemm, D., Heinze, T., Philipp, B. & Wagenknecht, W. 1997, "New approaches to advanced polymers by selective cellulose functionalization", *Acta Polymerica,* vol. 48, no. 8, pp. 277-297.

Klemm, D., Philipp, B. & Heinze, T. 1998., *Comprehensive cellulose chemistry. Volume 2, Functionalization of cellulose,* VCH, Weinheim.

Kontturi, E., Tammelin, T. & Österberg, M. 2006, "Cellulose-model films and the fundamental approach", *Chemical Society Reviews,* vol. 35, no. 12, pp. 1287-1304.

Kontturi, E., Thune, P.C. & Niemantsverdriet, J.W. 2003, "Cellulose Model Surfaces: Simplified Preparation by Spin Coating and Characterization by X-ray Photoelectron Spectroscopy, Infrared Spectroscopy, and Atomic Force Microscopy", *Langmuir,* vol. 19, no. 14, pp. 5735-5741.

Krapp, S., Mimura, Y., Jefferis, R., Huber, R. & Sondermann, P. 2003, "Structural Analysis of Human IgG-Fc Glycoforms Reveals a Correlation Between Glycosylation and Structural Integrity", *Journal of Molecular Biology,* vol. 325, no. 5, pp. 979-989.

Krässig, H.A. 1993., *Cellulose : structure, accessibility and reactivity,* Gordon & Breach, Lausanne.

Kretchmann, E. & Reather, H. 1968, "Radiative decay of non radiative surface plasmons excited by light (Surface plasma waves excitation by light and decay into photons applied to nonradiative modes) ", *Naturforsch., Teil A, ,* no. 23, pp. 2135-2136.

Krska, R. & Molinelli, A. 2009, "Rapid test strips for analysis of mycotoxins in food and feed", *Analytical and Bioanalytical Chemistry,* vol. 393, no. 1, pp. 67-71.

Kwok, D.Y. & Neumann, A.W. 1999, "Contact angle measurement and contact angle interpretation", *Advances in Colloid and Interface Science,* vol. 81, no. 3, pp. 167-249.

Laine, J., Lindstrom, T., Nordmark, G.G. & Risinger, G. 2000, "Studies on topochemical modification of cellulosic fibers. Part 1. Chemical conditions for the attachment of

carboxymethyl cellulose onto fibers", *Nordic Pulp Pap.Res.J.,* vol. 15, no. 5, pp. 520-526.

Laine, J., Stenius, P. 1994, "Surface characterization of unbleached kraft pulps by means of ESCA", *Cellulose*, Vol 1, no. 2, pp. 145-160.

Laitinen, O.H., Nordlund, H.R., Hytönen, V.P., Uotila, S.T.H., Marttila, A.T., Savolainen, J., Airenne, K.J., Livnah, O., Bayer, E.A., Wilchek, M. & Kulomaa, M.S. 2003, "Rational Design of an Active Avidin Monomer", *Journal of Biological Chemistry,* vol. 278, no. 6, pp. 4010-4014.

Langmuir, I. 1917, "The constitution and fundamental properties of solids and liquids. II liquids.", *Journal of the American Chemical Society,* vol. 39, no. 9, pp. 1848-1906.

Langmuir, I. & Schaefer, V.J. 1938, "Activities of Urease and Pepsin Monolayers", *Journal of the American Chemical Society,* vol. 60, no. 6, pp. 1351-1360.

Lappalainen, T., Teerinen, T., Vento, P., Hakalahti, L. & Erho, T. 2010, "Cellulose as a novel substrate for laminar flow assays.", *Nordic Pulp & Paper Research Journal,* vol. 25, no. 4, pp. 529-543.

Lee, R.G. & Kim, S.W. 1974, "Adsorption of proteins onto hydrophobic polymer surfaces: Adsorption isotherms and kinetics", *Journal of Biomedical Materials Research,* vol. 8, no. 5, pp. 251-259.

Leppiniemi, J., Maatta, J.A.E., Hammaren, H., Soikkeli, M., Laitaoja, M., Janis, J., Kulomaa, M.S. & Hytonen, V.P. 2011, "Bifunctional Avidin with Covalently Modifiable Ligand Binding Site", *PLoS ONE,* vol. 6, no. 1, pp. e16576.

Lequin, R.M. 2005, "Enzyme Immunoassay (EIA)/Enzyme-Linked Immunosorbent Assay (ELISA)", *Clinical chemistry,* vol. 51, no. 12, pp. 2415-2418.

Lin, J.N., Andrade, J.D. & Chang, I.-. 1989, "The influence of adsorption of native and modified antibodies on their activity", *Journal of immunological methods,* vol. 125, no. 1–2, pp. 67-77.

Lindstrom, T. & Wågberg, L. 1983, "Effect of pH and electrolyte concentration on the adsorption of cationic polyacrylamides on cellulose", *Tappi,* , no. 6, pp. 83-85.

Liu, Z., Choi, H., Gatenholm, P. & Esker, A.R. 2011, "Quartz Crystal Microbalance with Dissipation Monitoring and Surface Plasmon Resonance Studies of Carboxymethyl Cellulose Adsorption onto Regenerated Cellulose Surfaces", *Langmuir,* vol. 27, no. 14, pp. 8718-8728.

Lu, B., Smyth, M. & O'Kennedy, R. 1996, "Tutorial review. Oriented immobilization of antibodies and its applications in immunoassays and immunosensors", *Analyst,* vol. 121, no. 3, pp. 29R-32R.

Lu, B., Xie, J., Lu, C., Wu, C. & Wei, Y. 1995, "Oriented Immobilization of Fab' Fragments on Silica Surfaces", *Analytical Chemistry,* vol. 67, no. 1, pp. 83-87.

M V Voinova, e.a. 1999, *Viscoelastic Acoustic Response of Layered Polymer Films at Fluid-Solid Interfaces: Continuum Mechanics Approach.*

Machado, R.L., de Arruda, E.J., Santana, C.C. & Bueno, S.M.A. 2006, "Evaluation of a chitosan membrane for removal of endotoxin from human IgG solutions", *Process Biochemistry,* vol. 41, no. 11, pp. 2252-2257.

Madigan, M.T., Martinko, J.M. & Brock, T.D. 2009, *Brock biology of microorganisms,* Pearson Prentice Hall, Upper Saddle River, NJ :.

Magonov, S.N., Elings, V. & Whangbo, M.-. 1997, "Phase imaging and stiffness in tapping-mode atomic force microscopy", *Surface Science,* vol. 375, no. 2–3, pp. L385-L391.

Majeti N.V, R.K. 2000, "A review of chitin and chitosan applications", *Reactive and Functional Polymers,* vol. 46, no. 1, pp. 1-27.

Maloney, T. & Paulapuro, H. 1999, "The formation of pores in the cell wall. ", *Journal of pulp and paper science,* vol. 25, pp. 430-436.

Manavalan, P. & Ponnuswamy, P. 1978, "Hydrophobic character of amino acid residues in globular proteins", *Nature,* vol. 275, no. 5681, pp. 673-674.

Martinez, A.W., Phillips, S.T., Whitesides, G.M. & Carrilho, E. 2010, "Diagnostics for the Developing World: Microfluidic Paper-Based Analytical Devices", *Analytical Chemistry,* vol. 82, no. 1, pp. 3-10.

Meyer, E. 1992, "Atomic force microscopy", *Progress in Surface Science,* vol. 41, no. 1, pp. 3-49.

Mishima, T., Hisamatsu, M., York, W.S., Teranishi, K. & Yamada, T. 1998, "Adhesion of [beta]--glucans to cellulose", *Carbohydrate Research,* vol. 308, no. 3-4, pp. 389-395.

Mizuochi, T., Taniguchi, T., Shimizu, A. & Kobata, A. 1982, "Structural and numerical variations of the carbohydrate moiety of immunoglobulin G", *The Journal of Immunology,* vol. 129, no. 5, pp. 2016-2020.

Motchmann, H. & Stamm, M. 1991, *Adsorption kinetics of block copolymers from a good solvent: a two-stage process*, American Chemical Society.

Moulder, J.F. & Chastain, J. 1992, *Handbook of x-ray photoelectron spectroscopy : a reference book of standard spectra for identification and interpretation of XPS data,* Physical Electronics Division, Perkin-Elmer Corp., Eden Prairie, Minn.

Müller, M., Czihak, C., Schober, H., Nishiyama, Y. & Vogl, G. 2000, "All Disordered Regions of Native Cellulose Show Common Low-Frequency Dynamics", *Macromolecules,* vol. 33, no. 5, pp. 1834-1840.

Myllytie, P., Salmi, J. & Laine, J. 2009, "The influence of PH on the adsorption and interaction of chitosan with cellulose", *Bioresources,* vol. 4, no. 4, pp. 1647-1662.

Nakajima, N. & Ikada, Y. 1995, "Mechanism of Amide Formation by Carbodiimide for Bioconjugation in Aqueous Media", *Bioconjugate chemistry,* vol. 6, no. 1, pp. 123-130.

Nakanishi, K., Sakiyama, T. & Imamura, K. 2001, "On the Adsorption of Proteins on Solid Surfaces, a Common but Very Complicated Phenomenon", *The Society for Biotechnology, Japan,* vol. 91, no. 3, pp. 233-244.

Nehls, I., Wagenknecht, W., Philipp, B. & Stscherbina, D. 1994, "Characterization of cellulose and cellulose derivatives in solution by high resolution 13C-NMR spectroscopy", *Progress in Polymer Science,* vol. 19, no. 1, pp. 29-78.

Nettles, D., Elder, S. & Gilbert, J. 2002, "Potential use of chitosan as a cell scaffold material for cartilage tissue engineering.", *Tissue engineering,* vol. 8, no. 6, pp. 1009-1016.

Nogi, M., Iwamoto, S., Nakagaito, A.N. & Yano, H. 2009, "Optically Transparent Nanofiber Paper", *Advanced Materials,* vol. 21, no. 16, pp. 1595-1598.

Norde, W. 1996, "Driving forces for protein adsorption at solid surfaces", *Macromolecular Symposia,* vol. 103, no. 1, pp. 5-18.

Norde, W. & Zoungrana, T. 1998, "Surface-induced changes in the structure and activity of enzymes physically immobilized at solid/liquid interfaces", *Biotechnology and applied biochemistry,* vol. 28, no. 2, pp. 133-143.

Nordgren, N., Eronen, P., Österberg, M., Laine, J. & Rutland, M.W. 2009, "Mediation of the Nanotribological Properties of Cellulose by Chitosan Adsorption", *Biomacromolecules,* vol. 10, no. 3, pp. 645-650.

Nordlund, H.R., Laitinen, O.H., Hytönen, V.P., Uotila, S.T.H., Porkka, E. & Kulomaa, M.S. 2004, "Construction of a Dual Chain Pseudotetrameric Chicken Avidin by Combining Two Circularly Permuted Avidins", *Journal of Biological Chemistry,* vol. 279, no. 35, pp. 36715-36719.

Nordlund, H.R., Laitinen, O.H., Uotila, S.T.H., Nyholm, T., Hytönen, V.P., Slotte, J.P. & Kulomaa, M.S. 2003, "Enhancing the Thermal Stability of Avidin", *Journal of Biological Chemistry,* vol. 278, no. 4, pp. 2479-2483.

Osborn, J.L., Lutz, B., Fu, E., Kauffman, P., Stevens, D.Y. & Yager, P. 2010, "Microfluidics without pumps: reinventing the T-sensor and H-filter in paper networks", *Lab on a Chip,* vol. 10, no. 20, pp. 2659-2665.

Österberg, M. 2000, "The effect of a cationic polyelectrolyte on the forces between two cellulose surfaces and between on cellulose and one mineral surface", *Journal of Colloid and Interfacial Science*, vol. 229, no. 2, pp. 1-8.

O'Shannessy, D.J. & Hoffman, W.L. 1987, *Site-directed immobilization of glycoproteins on hydrazide-containing solid supports*.

O'Sullivan, A. 1997, "Cellulose: the structure slowly unravels", *Cellulose,* vol. 4, no. 3, pp. 173-207.

Pääkkö, M., Ankerfors, M., Kosonen, H., Nykänen, A., Ahola, S., Österberg, M., Ruokolainen, J., Laine, J., Larsson, P.T., Ikkala, O. & Lindström, T. 2007, "Enzymatic Hydrolysis Combined with Mechanical Shearing and High-Pressure Homogenization for Nanoscale Cellulose Fibrils and Strong Gels", *Biomacromolecules,* vol. 8, no. 6, pp. 1934-1941.

Paddock, S. 1999, "Confocal laser scanning microscopy", *BioTechniques,* , no. 27, pp. 992-1004.

Patrickios, C.S. & Yamasaki, E.N. 1995, "Polypeptide Amino Acid Composition and Isoelectric Point II. Comparison between Experiment and Theory", *Analytical Biochemistry,* vol. 231, no. 1, pp. 82-91.

Pattnaik, P. 2005, "Surface plasmon resonance", *Applied Biochemistry and Biotechnology,* vol. 126, no. 2, pp. 79-92.

Payen, A. & Persoz, J.F. 1833, "Memoire sur la diastase, les principaux prodults de ses reactions et leur applications aux arts industries.", *Ann. Chim. Phys.,* , no. 53, pp. 73-92.

Peakman, M., Vergani, D., Pyne, D.J. & Woodward, M. 2009, *Basic and clinical immunology,* Elsevier/Churchill Livingstone, Edinburgh; New York.

Pei, R., Yang, X. & Wang, E. 2001, "Enhanced surface plasmon resonance immunosensing using a streptavidin-biotinylated protein complex", *Analyst,* vol. 126, no. 1, pp. 4-6.

Pelton, R. 2009, "Bioactive paper provides a low-cost platform for diagnostics", *TrAC Trends in Analytical Chemistry,* vol. 28, no. 8, pp. 925-942.

Pelton, R., Ren, P., Liu, J. & Mijolovic, D. 2011, "Polyvinylamine-graft-TEMPO Adsorbs onto, Oxidizes, and Covalently Bonds to Wet Cellulose", *Biomacromolecules,* vol. 12, no. 4, pp. 942-948.

Peluso, P., Wilson, D.S., Do, D., Tran, H., Venkatasubbaiah, M., Quincy, D., Heidecker, B., Poindexter, K., Tolani, N., Phelan, M., Witte, K., Jung, L.S., Wagner, P. & Nock, S. 2003, "Optimizing antibody immobilization strategies for the construction of protein microarrays", *Analytical Biochemistry,* vol. 312, no. 2, pp. 113-124.

Peterson, E.A. & Sober, H.A. 1956, "Chromatography of Proteins. I. Cellulose Ion-exchange Adsorbents", *Journal of the American Chemical Society,* vol. 78, no. 4, pp. 751-755.

Postek, M., Vladár, A., Dagata, J., Farkas, N., Ming. B., Wagner, R., Raman, A., Moon, R.J., Sabo, R., Wegner, T. & Beecher, J. 2011, "Development of the metrology and imaging of cellulose nanocrystals", *Measurement Science and Technology,* vol. 22, no. 2, pp. 024005.

Posthuma-Trumpie, G., Korf, J. & van Amerongen, A. 2009, "Lateral flow (immuno)assay: its strengths, weaknesses, opportunities and threats. A literature survey", *Analytical and Bioanalytical Chemistry,* vol. 393, no. 2, pp. 569-582.

Prime, K.L. & Whitesides, G.M. 1993, "Adsorption of proteins onto surfaces containing end-attached oligo(ethylene oxide): a model system using self-assembled monolayers", *Journal of the American Chemical Society,* vol. 115, no. 23, pp. 10714-10721.

Prime, K. & Whitesides, G. 1991, "Self-assembled organic monolayers: model systems for studying adsorption of proteins at surfaces", *Science,* vol. 252, no. 5010, pp. 1164-1167.

Rao, S.V., Anderson, K.W. & Bachas, L.G. 1998, "Oriented immobilization of proteins", *Microchimica Acta,* vol. 128, no. 3, pp. 127-143.

Ricka, J. & Tanaka, T. 1984, "Swelling of ionic gels: quantitative performance of the Donnan theory", *Macromolecules,* vol. 17, no. 12, pp. 2916-2921.

Riihimaki, T., Kukkurainen, S., Varjonen, S., Harha, J., Nyholm, T., Kulomaa, M. & Hytönen, V. 2011, "Construction of Chimeric Dual-Chain Avidin by Tandem Fusion of the Related Avidins", *PLoS ONE,* vol. 6, no. 5, pp. e20535.

Risén, J., Hultén, A.H. & Paulsson, M. 2004, "Surface Characterization of Softwood and Hardwood Kraft Pulp Fibers from Different Stages in a Bleaching Sequence", *Journal of Wood Chemistry and Technology,* vol. 24, no. 4, pp. 307-321.

Ritchie, C.D. 1972, "Nucleophilic reactivities toward cations", *Accounts of Chemical Research,* vol. 5, no. 10, pp. 348-354.

Rodahl, M., Hook, F., Krozer, A., Brzezinski, P. & Kasemo, B. 1995, "Quartz crystal microbalance setup for frequency and Q-factor measurements in gaseous and liquid environments", *Rev. Sci. Instrum.,* vol. 66, no. 7, pp. 3924-3931.

Rojas, R. & Apodaca, G. 2002, "Immunoglobulin transport across polarized epithelial cells", *Nature reviews. Molecular cell biology,* vol. 3, no. 12, pp. 944-956.

Rosenau, T., Potthast, A., Sixta, H. & Kosma, P. 2001, "The chemistry of side reactions and byproduct formation in the system NMMO/cellulose (Lyocell process)", *Progress in Polymer Science,* vol. 26, no. 9, pp. 1763-1837.

Roy, D., Semsarilar, M., Guthrie, J.T. & Perrier, S. 2009, "Cellulose modification by polymer grafting: a review", *Chemical Society Reviews,* vol. 38, no. 7, pp. 2046-2064.

Rugar, D. & Hansma, P. 1990, "Atomic Force Microscopy", *Physics Today,* vol. 43, no. 10, pp. 23-30.

Rusmini, F., Zhong, Z. & Feijen, J. 2007, "Protein Immobilization Strategies for Protein Biochips", *Biomacromolecules,* vol. 8, no. 6, pp. 1775-1789.

Saarinen, T., Orelma, H., Grönqvist, S., Andberg, M., Holappa, S. & Laine, J. 2009, "Adsorption of differenct laccases on cellulose and ligning surfaces.", *BioResources,* , no. 4, pp. 94-110.

Saito, T., Okita, Y., Nge, T.T., Sugiyama, J. & Isogai, A. 2006, "TEMPO-mediated oxidation of native cellulose: Microscopic analysis of fibrous fractions in the oxidized products", *Carbohydrate Polymers,* vol. 65, no. 4, pp. 435-440.

Saito, T. & Isogai, A. 2004, "TEMPO-Mediated Oxidation of Native Cellulose. The Effect of Oxidation Conditions on Chemical and Crystal Structures of the Water-Insoluble Fractions", *Biomacromolecules,* vol. 5, no. 5, pp. 1983-1989.

Saito, T., Kimura, S., Nishiyama, Y. & Isogai, A. 2007, "Cellulose Nanofibers Prepared by TEMPO-Mediated Oxidation of Native Cellulose", *Biomacromolecules,* vol. 8, no. 8, pp. 2485-2491.

Saito, T., Nishiyama, Y., Putaux, J., Vignon, M. & Isogai, A. 2006, "Homogeneous Suspensions of Individualized Microfibrils from TEMPO-Catalyzed Oxidation of Native Cellulose", *Biomacromolecules,* vol. 7, no. 6, pp. 1687-1691.

Sauerbrey 1959, "Verwendung von Schwingquarzen zur Wägung dünner Schichten und zur Mikrowägung ", *Zeitschrift fur Physik. C, Particles and fields,* vol. 155, no. 2, pp. 206.

Schasfoort, R.B.M., Tudos, A.J. & Gedig, E.T. (eds) 2008, *Handbook of Surface Plasmon Resonance*, The Royal Society of Chemistry, Cambridge, UK.

Schaub, M., Wenz, G., Wegner, G., Stein, A. & Klemm, D. 1993, "Ultrathin films of cellulose on silicon wafers", *Advanced Materials,* vol. 5, no. 12, pp. 919-922.

Scheutjens, J.M.H.M. & Fleer, G.J. 1980, "Statistical theory of the adsorption of interacting chain molecules. 2. Train, loop, and tail size distribution", *The Journal of physical chemistry,* vol. 84, no. 2, pp. 178-190.

Sethuraman, A. & Belfort, G. 2005, "Protein Structural Perturbation and Aggregation on Homogeneous Surfaces", *Biophysical journal,* vol. 88, no. 2, pp. 1322-1333.

Siró, I. & Plackett, D. 2010, "Microfibrillated cellulose and new nanocomposite materials: a review", *Cellulose,* vol. 17, no. 3, pp. 459-494.

Sjöström, E. 1993., *Wood chemistry : fundamentals and applications,* 2nd, rev. ed. edn, Academic Press, San Diego (CA).

Smith, C.K., Withka, J.M. & Regan, L. 1994, "A Thermodynamic Scale for the .beta.-Sheet Forming Tendencies of the Amino Acids", *Biochemistry,* vol. 33, no. 18, pp. 5510-5517.

Smits, H.L., Eapen, C.K., Sugathan, S., Kuriakose, M., Gasem, M.H., Yersin, C., Sasaki, D., Pujianto, B., Vestering, M., Abdoel, T.H. & Gussenhoven, G.C. 2001, "Lateral-Flow Assay for Rapid Serodiagnosis of Human Leptospirosis", *Clinical and diagnostic laboratory immunology,* vol. 8, no. 1, pp. 166-169.

Spence, K., Venditti, R., Rojas, O., Habibi, Y. & Pawlak, J. 2010, "The effect of chemical composition on microfibrillar cellulose films from wood pulps: water interactions and physical properties for packaging applications", *Cellulose,* vol. 17, no. 4, pp. 835-848.

Spinola, S.M. & Cannon, J.G. 1985, "Different blocking agents cause variation in the immunologic detection of proteins transferred to nitrocellulose membranes", *Journal of immunological methods,* vol. 81, no. 1, pp. 161-165.

Staros, J.V., Wright, R.W. & Swingle, D.M. 1986, "Enhancement by N-hydroxysulfosuccinimide of water-soluble carbodiimide-mediated coupling reactions", *Analytical Biochemistry,* vol. 156, no. 1, pp. 220-222.

Stenberg, E., Persson, B., Roos, H. & Urbaniczky, C. 1991, "Quantitative determination of surface concentration of protein with surface plasmon resonance using radiolabeled proteins", *Journal of Colloid and Interface Science,* vol. 143, no. 2, pp. 513-526.

Stöllner, D., Scheller, F.W. & Warsinke, A. 2002, "Activation of Cellulose Membranes with 1,1′-Carbonyldiimidazole or 1-Cyano-4-dimethylaminopyridinium tetrafluoroborate as a Basis for the Development of Immunosensors", *Analytical Biochemistry,* vol. 304, no. 2, pp. 157-165.

Su, T.J., Lu, Thomas, R.K., Cui, Z.F. & Penfold, J. 1998, "The Conformational Structure of Bovine Serum Albumin Layers Adsorbed at the Silicaâˆ'Water Interface", *The Journal of Physical Chemistry B,* vol. 102, no. 41, pp. 8100-8108.

Sverre-Henning, B. 1997, "Bovine serum albumin (BSA) as a reagent against non-specific immunogold labeling on LR-White and epoxy resin", *Micron,* vol. 28, no. 3, pp. 189-195.

Swerin, A., Ödberg, L. & lindström, T. 1990, "Deswelling of hardwood kraft pulp fibers by cationic polymers: the effect on wet pressing and sheet properties.", *Nordic Pulp Pap.Res.J.,* , no. 5, pp. 188-196.

Syverud, K. & Stenius, P. 2009, "Strength and barrier properties of MFC films", *Cellulose,* vol. 16, no. 1, pp. 75-85.

Taipale, T., Österberg, M., Nykänen, A., Ruokolainen, J. & Laine, J. 2010, "Effect of microfibrillated cellulose and fines on the drainage of kraft pulp suspension and paper strength", *Cellulose,* vol. 17, no. 5, pp. 1005-1020.

Tammelin, T., Saarinen, T., Oesterberg, M. & Laine, J. 2006, "Preparation of Langmuir/Blodgett-cellulose Surfaces by Using Horizontal Dipping Procedure. Application for Polyelectrolyte Adsorption Studies Performed with QCM-D", *Section Title: Cellulose, Lignin, Paper, and Other Wood Products,* vol. 13, no. 5, pp. 519-535.

Thanki, N., Thornton, J.M. & Goodfellow, J.M. 1988, "Distributions of water around amino acid residues in proteins", *Journal of Molecular Biology,* vol. 202, no. 3, pp. 637-657.

Turbak, A., Snyder, F. & Sandberg, K. 1983, "Microfibrillated cellulose, a new cellulose product: properties, uses, and commercial potential.", *J Appl Polym Sci Appl Polym Symp,* vol. 37, no. 37, pp. 815-827.

Turko, I.V., Yurkevich, I.S. & Chashchin, V.L. 1992, "Oriented immunoglobulin G layer onto the Langmuir-Blodgett films of protein A", *Thin Solid Films,* vol. 210–211, Part 2, no. 0, pp. 710-712.

Turon, X., Rojas, O.J. & Deinhammer, R.S. 2008, "Enzymatic Kinetics of Cellulose Hydrolysis: A QCM-D Study", *Langmuir,* vol. 24, no. 8, pp. 3880-3887.

Uy, R. & Wold, F. 1977, "1,4-Butanediol diglycidyl ether coupling of carbohydrates to sepharose: Affinity adsorbents for lectins and glycosidases", *Analytical Biochemistry,* vol. 81, no. 1, pp. 98-107.

Vaiana, S.M., Emanuele, A., Palma-Vittorelli, M.B. & Palma, M.U. 2004, "Irreversible formation of intermediate BSA oligomers requires and induces conformational changes", *Proteins: Structure, Function, and Bioinformatics,* vol. 55, no. 4, pp. 1053-1062.

Van Hardeveld, R.M., Gunter, P.L.J., van IJzendoorn, L.J., Wieldraaijer, W., Kuipers, E.W. & Niemantsverdriet, J.W. 1995, "Deposition of inorganic salts from solution on flat substrates by spin-coating: theory, quantification and application to model catalysts", *Applied Surface Science,* vol. 84, no. 4, pp. 339-346.

Van Leemputies, E. & Horisberger, M. 1974, "Immobilization of trypsin on partially oxidized cellulose", *Biotechnology and bioengineering,* vol. 16, no. 7, pp. 997-1003.

Wågberg, L. 2000, "Polyelectrolyte adsorption onto celluse fibries - A review", *Nordic Pulp Pap.Res.J.,* , no. 5, pp. 586-597.

Wagberg, L., Decher, G., Norgren, M., Lindstrom, T., Ankerfors, M. & Axnas, K. 2008, "The Build-Up of Polyelectrolyte Multilayers of Microfibrillated Cellulose and Cationic Polyelectrolytes", *Langmuir,* vol. 24, no. 3, pp. 784-795.

Walecka, J. A. 1956, "An investigation of low degree of substitution of carboxymethylcelluloses", Tappi journal, vol. 39, no. 7, pp. 458-463.

Wenz, G. & Liepold, P. 2007, "Self-assembly of biotin and thio-functionalized carboxymethyl celluloses on gold and molecular recognition of streptavidin detected by surface plasmon resonance", *Cellulose,* vol. 14, no. 2, pp. 89-98.

Wolny, P.M., Spatz, J.P. & Richter, R.P. 2010, "On the Adsorption Behavior of Biotin-Binding Proteins on Gold and Silica", *Langmuir,* vol. 26, no. 2, pp. 1029-1034.

Wood, R.W. 1902, "On a remarkable case of uneven distribution of light in a diffraction grating spectrum", *Philosophical Magazine Series 6,* vol. 4, no. 21, pp. 396-402.

Wu, S. & Wong, S. 2005, "Engineering Soluble Monomeric Streptavidin with Reversible Biotin Binding Capability", *Journal of Biological Chemistry,* vol. 280, no. 24, pp. 23225-23231.

Yager, P., Edwards, T., Fu, E., Helton, K., Nelson, K., Tam, M.R. & Weigl, B.H. 2006, "Microfluidic diagnostic technologies for global public health", *Nature,* vol. 442, no. 7101, pp. 412-418.

Yalow, R.S. & Berson, S.A. 1959, "Assay of Plasma Insulin in Human Subjects by Immunological Methods", *Nature,* vol. 184, no. 4699, pp. 1648-1649.

You, H.X., Lin, S. & Lowe, C.R. 1995, "A scanning tunnelling microscopic study of site-specifically immobilized immunoglobulin G on gold", *Micron,* vol. 26, no. 4, pp. 311-315.

Zuk, R.F., Ginsberg, V.K., Houts, T., Rabbie, J., Merrick, H., Ullman, E.F., Fischer, M.M., Sizto, C.C., Stiso, S.N. & Litman, D.J. 1985, "Enzyme immunochromatography--a quantitative immunoassay requiring no instrumentation.", *Clinical chemistry,* vol. 31, no. 7, pp. 1144-1150.

Aalto-DD 138/2012

ISBN 978-952-60-4835-2
ISBN 978-952-60-4836-9 (pdf)
ISSN-L 1799-4934
ISSN 1799-4934
ISSN 1799-4942 (pdf)

Aalto University
School of Chemical Technology
Department of Forest Products Technology
www.aalto.fi

BUSINESS +
ECONOMY

ART +
DESIGN +
ARCHITECTURE

SCIENCE +
TECHNOLOGY

CROSSOVER

**DOCTORAL
DISSERTATIONS**